Breaking Down the Mortality and Social Cost of Carbon [JMP]

R. Daniel Bressler*

January 21, 2025

Updated frequently; click here for the latest version

The social cost of carbon (SCC) is arguably the most important concept in climate economics. Until recently, climate-mortality damages were either negligible or excluded in SCC models. Now, they constitute the majority of damages in latest-generation models, which also project damages at much higher spatial resolution. Previously, discounting (how to value the future) was considered the most consequential choice in determining the SCC. Here, I demonstrate that valuing lives in poorer versus richer countries is now the most consequential choice. I provide the first estimate of the mortality cost of carbon (MCC)—the number of deaths from emitting an additional tonne of CO₂—in a latest-generation climate-economy-mortality model broken down by country. 83% of the deaths in the MCC occur in low and lower-middle-income countries. I then calculate the SCC by monetizing these deaths and adding other damage categories. The highly unequal distribution of deaths makes the SCC extremely sensitive to how lives are valued in poor versus rich countries. I calculate the SCC across four approaches to valuing lives and livelihoods with support in the literature. Among approaches sanctioned in U.S. policymaking, the 2025 SCC varies from \$237 (U.S. EPA's current approach) to \$3,567 (U.S. income weighting). These results empower decision-makers to choose their preferred approach while understanding sensitivity to alternative approaches. Applying these estimates, the Inflation Reduction Act saves an estimated 2.8M lives through GHG reductions, with monetary benefits ranging from \$4.7T-\$74T, depending on the approach.

Keywords: Inequality, Climate, Health, Integrated Assessment Modelling, Welfare Theory, Inflation Reduction Act

JEL: D61, I14, I31, J17, Q54, Q58

^{*}Columbia University: rdb2148@columbia.edu. I thank Scott Barrett, Geoffrey Heal, Jeffrey Shrader, and Gernot Wagner for their invaluable continued support, guidance, and feedback. Yvon Lu, Baptiste Saez, Naomi Shimberg, Sky Sun, and Michelle Zhou provided excellent research assistance. I thank Floriane Cohen, Caroline Flammer, Robert Metcalfe, and Andrew Wilson for helpful comments that have improved the paper. All errors are my own. I gratefully acknowledge funding from BERI and the Open Philanthropy Project.

1 Introduction

A New Generation of Social Cost of Carbon Models

What happens when a pulse of CO₂ is added to the atmosphere? What results from, e.g., producing an extra tonne of steel, an extra batch of cement, or adding a new flight route? The answer to this simple question is at the heart of climate economics and policy. The social cost of carbon (SCC)—the monetized social cost of emitting one tonne of CO₂—has been called "the most important single economic concept in the economics of climate change" (Nordhaus, 2017). The SCC has been used extensively by many institutions, including governments, private companies, and philanthropies. When these institutions make a decision that adds CO₂ into the atmosphere (e.g., building new coal power plants) or reduces CO₂ (e.g., replacing coal power plants with solar farms), the SCC tells them the social cost of adding, or the social benefit of reducing, those emissions. In the U.S., federal regulations with benefits totaling trillions of dollars have used the SCC as part of their required benefit-cost analysis.

The SCC is estimated in models that determine the social cost of adding a pulse of CO₂ to the atmosphere. These models capture that an emissions pulse slightly increases the future concentration of CO₂. This slightly increases future temperatures around the world for hundreds of years. Slightly higher temperatures cause slightly more net damages, impacting the number of people who die, the number of future crops damaged, damages to coastlines, the amount of energy used by households, among other impacts. The modeler must summarize all of those future impacts into a single SCC number—representing the social cost resulting from that pulse of emissions—by monetizing and discounting all of the projected damages from the pulse.

In 2017, the National Academies of Sciences released a report stating that the existing SCC models were not updated to the best available science (NASEM, 2017). Since then, multiple studies have updated SCC models closer to the frontier of the scientific literature. This included the U.S. Government's comprehensive update to the SCC in 2023 (EPA, 2023a). One critical area of improvement is the representation of damages. Previous generation models either did not clearly specify how much, if any, of their damages came from mortality or projected little damage from mortality based on outdated studies. In the latest generation models, mortality now represents 50%-80% of climate damages using EPA's monetization approach (EPA, 2023a). In addition, climate damages are now projected at much higher levels of spatial resolution. The previous generation models were either not able to estimate the spatial distribution of damages or projected damages in a small number of regions. Now, damages can be projected at the country (Rennert et al., 2022) or even sub-country level (Carleton et al., 2022). In addition, the National Academies emphasized that incremental

and total damages should be shown in natural physical units in addition to monetized units because "natural-unit measures are more straightforward to compare to the impact literature and require fewer intermediate assumptions to estimate than their monetized counterparts" (NASEM, 2017). Bressler (2021) took a step in addressing the National Academies concerns by introducing a new metric: the mortality cost of carbon (MCC). The MCC is the number of deaths caused by adding a one-tonne pulse of emissions at some point in time. Said another way using the language of the National Academies: the MCC is the mortality-specific incremental damage caused by emitting a tonne of CO₂ represented in the physical units of mortality (deaths).

This Study's Contributions and Results

In these latest-generation models that calculate the SCC, mortality damages now represent a majority of the damages, and climate impacts are estimated at a much higher spatial resolution. This gives newfound importance to the modeler's choice of social welfare function (SWF), which determines how to value lives and livelihoods around the world. It has long been recognized in the climate economics literature that the SCC is sensitive to ethical choices, in particular around choosing discount rate parameters that determine how much value to place on the future relative to the present (Nordhaus, 2007; Stern, 2006). Despite the limited spatial resolution, all previous-generation models clearly projected climate damages across time, so naturally, the choice of discount rate parameters was a major focus. Now that deaths caused by climate change are clearly specified, substantial, and broken down spatially into countries with very different income levels, modelers must make an explicit choice on how to value those deaths.¹ Indeed, as I will show, this is now the most consequential choice in determining the value of the SCC in latest-generation models.

In this study, I use a climate-economy-mortality SCC model updated to the best available science. This model integrates a climate model (Smith et al., 2018), socioeconomic projections (Rennert et al., 2021), and market damage functions for agriculture (Moore et al., 2017), energy (Clarke et al., 2018), and sea level rise (Diaz, 2016) that are updated to the best available science and responsive to the National Academy's 2017 suggestions. These model components represent a significant improvement from the previous generation of SCC models, but they are not novel contributions of this study because other recent studies have also used these same components (Bressler et al., nd; EPA, 2023a; Rennert et al., 2022). I will briefly state the four novel contributions of this study here and then elaborate on them in the following paragraphs.

¹In their 2023 update to the U.S. government's SCC, the U.S. Environmental Protection Agency (EPA) chose to value the deaths from a pulse of emissions proportionally to the country's income where the death took place, a choice which has since generated some controversy (Broome, 2024; Hersher et al., 2023).

The first novel contribution of this study is integrating a country-level mortality damage function that accounts for the benefit of future income growth in reducing vulnerability to heat (Bressler et al., 2021) into my climate-economy model to estimate the physical mortality cost (the number of deaths) from adding a pulse of CO₂, i.e., the mortality cost of carbon (MCC). This is the first estimate of the MCC in a latest-generation climate-economy-mortality model responsive to the National Academies' 2017 suggestions.² The second novel contribution is leveraging this model to provide the first estimate of the MCC broken down by the country where the deaths are projected to occur.³ I find that the deaths from a pulse of emissions are overwhelmingly concentrated in lower-income countries in the global south. I then calculate the social cost of carbon (SCC)—the full monetized cost from adding a pulse of CO₂—by monetizing mortality damages from emitting an additional tonne of CO₂ (captured in the MCC) along with damages in the other sectors. The third novel contribution is calculating the SCC across four major monetization approaches—i.e., approaches to valuing lives and livelihoods—that have support in the literature. Because deaths in the MCC are substantial and overwhelmingly concentrated in poorer countries, I find that the SCC is extremely sensitive to how the modeler chooses to value the livelihoods and especially the lives of the poor versus the rich. To my knowledge, this is the most comprehensive exploration of the SCC's sensitivity to the choice of valuing lives and livelihoods in the literature.⁴ This choice has newfound importance now that climate damages are projected at a much higher level of spatial resolution and mortality damages are significant. The fourth novel contribution is that I provide evidence showing that the choice of valuing lives is now the most consequential choice in determining the value of the SCC.

First, I provide the first estimate of the MCC in a latest-generation climate-economy-mortality model responsive to the National Academies' 2017 suggestions. I find that the 2025 mortality cost of carbon (MCC) is 1.37×10^{-4} deaths per tonne CO_2 , which implies that adding 7,309 tonnes of CO_2 —equivalent to the lifetime emissions of 5.7 average Americans—causes one premature death globally in expectation from 2025-2300. To provide further resolution

²While Bressler (2021) calculated the MCC, it did so by extending the older generation DICE model (Nordhaus, 2017), which has many of the deficiencies highlighted by the National Academy of Sciences in 2017 (discussed in more detail in the main text).

³Bressler (2021) estimated the MCC in an extended DICE model, which has only a single global region. Here, I break down the MCC into the 184 different countries that make up my model.

⁴Other studies compare two approaches: e.g., Bressler et al. (nd) and Prest et al. (2024) compare the EPA 2023 approach with income weighting and Adler et al. (2017) compare a utilitarian approach that values everyone's wellbeing equally with a prioritarian approach that places higher weight on the wellbeing of the poor compared to the rich. Here, I take a comprehensive approach to the question of valuing lives and livelihoods by showing SCC values across four major approaches that have support in the literature, discussed in more detail below.

into the MCC, I break down the deaths caused by a pulse of emissions across time, and I find that half of the deaths occur within 100 years of the pulse. Importantly, these findings project that future populations will be less vulnerable to heat as they become richer in the future. If future populations remain as vulnerable to heat as current ones, however, I find that adding just 2,542 tonnes of CO₂—equivalent to the lifetime emissions of 2.0 average Americans—causes one premature death globally in expectation from 2025-2300. While other studies in the literature have projected the total physical mortality impact from climate change caused by all the world's emissions across time (e.g., Carleton et al. (2022); Gasparrini et al. (2017); Hales et al. (2014))⁵—this projection is less relevant for decision-making because the emissions decisions of any individual person, organization, or even country are marginal compared to all global emissions across time.⁶ Indeed, the MCC is the relevant metric for quantifying the number of deaths caused by a decision-maker increasing emissions or the number of lives saved by a decision-maker reducing emissions. Accordingly, I use MCC estimates from this study to estimate that the 2022 Inflation Reduction Act's emissions reductions are projected to save 2.8 million lives.⁷

Second, I provide the first estimate of the MCC broken down by the country where those deaths are projected to occur. I find that these deaths from a pulse of emissions are projected to occur overwhelmingly in poorer countries in the global south. 83% of these deaths are in low and lower-middle-income countries, and 75% are in Southern Asia and Sub-Saharan Africa. Meanwhile, only 2% of the deaths are in Europe, and only 2% are in the Western Hemisphere.

Third, I calculate the SCC across four major monetization approaches that have support in the literature. I find that the SCC is extremely sensitive to how the modeler chooses to value livelihoods and especially lives. The MCC findings in the previous paragraph provide some intuition for why this is the case. The first of the four approaches I consider to valuing lives and livelihoods is the approach that EPA took in its 2023 update to the SCC. In this approach, lives are valued proportionally to the per capita income of the country where the

⁵In addition to estimating the total physical mortality impact of climate change, Carleton et al. (2022) also provide an estimate of the marginal monetized mortality impact of climate change, i.e., the mortality partial SCC. However, they do not provide an estimate of the marginal physical mortality impact of climate change, i.e. the MCC, because monetization decisions were made upstream of the study's damage function, which is used to estimate the marginal impact from a pulse of emissions.

⁶While this study's novel contributions include estimating the marginal mortality impacts resulting from an emissions pulse, I also estimate the total mortality impacts from climate change. See, e.g., Figures A.1 and A.2.

⁷Using the MCC that accounts for reduced vulnerability to heat as populations become richer in the future. If we assume that future populations will be just as vulnerable to heat as current ones, then the Inflation Reduction Act is expected to save 8.6 million lives. See section 4 for details.

death is projected to take place. Crucially, the places where EPA's monetization approach values lives the least are also the places where most deaths are expected to occur: 83% of the deaths in the MCC occur in low and lower-middle-income countries. EPA's approach is informed by the Kaldor-Hicks approach to benefit-cost analysis (BCA), in which a dollar of damages to the very rich is counted the same as a dollar of damages to the very poor. Mortality damages are monetized based on the estimated willingness to pay to avoid mortality risks, which is estimated to scale proportionally to income. This results in valuing the lives of the rich more than the lives of the poor (this paragraph provides only a very brief summary on the approaches; see main text for details). I find that the 2025 SCC using EPA's approach is \$237.9

The second of the four approaches I consider with support in the literature and practice is the U.S. Status Quo approach (Bressler and Heal, 2022; Hemel, 2022; Meyer and Cooper, 1995; Sunstein, 2004, 2023). This approach takes the same approach as EPA for all non-mortality market damages (which in this study's model include agriculture, energy, and sea level rise), but instead of valuing lives as a function of income, all lives are valued the same at the average willingness to pay to avoid mortality risk across the population considered in the scope of the analysis. In the case of the SCC, this means that all lives are valued the same at the global average willingness to pay. The 2025 SCC using this approach is \$380.

The third of the four approaches was just officially sanctioned for use in U.S. benefit-cost analysis in 2023 (OMB, 2023a): income-weighting. Income-weighting quantifies the SCC in units of money that are adjusted for diminishing marginal utility, i.e., capturing that an additional dollar has more value to poorer individuals than richer individuals. Income weighting uses a utility function to determine the effect of damages on well-being based on an individual's income. All else equal, the more that climate damages fall on the poor relative to the rich, the higher the wellbeing loss. The 2025 income-weighted SCC using U.S. average income as the reference point is \$3,567. This implies that adding a tonne of CO₂ to the atmosphere causes the same wellbeing loss as taking away \$3,567 from an average American.

The fourth of the four approaches is prioritarian-weighting. Like income-weighting, prioritarian-weighting uses a utility function to estimate the effect of damages on wellbeing. But while income-weighting values everyone's wellbeing the same, prioritarian-weighting places extra weight on the wellbeing of the worse off (i.e., those with lower incomes). Prioritarian-weighting has support in the academic literature (Adler et al., 2017; Adler and Treich, 2015;

⁸The estimated willingess to pay to avoid a specific mortality risk is captured in an economic concept called the Value of Statistical Life (VSL). In section 3, I discuss this concept and its relationship to benfit-cost anlaysis in detail.

⁹My results here are similar to the central SCC values from EPA's 2023 update: their 2030 SCC ranged from \$219-\$238 depending on the damages module. See EPA (2023a) table 3.1.4.

Ferranna and Fleurbaey, 2020), but it is not yet used as far as I am aware in benefit-cost analysis for government policymaking in the U.S. or other countries. Prioritarian-weighting yields a much higher SCC since the wellbeing of the global poor—who are most impacted by climate damages—is given extra weight. The 2025 prioritarian-weighted SCC using U.S. average income as the reference level is \$11,839.

Importantly, the physical climate damages are the exact same across each of these four approaches. E.g., the same number of people in the same countries are projected to die from a pulse of emissions. Model parameters, including the pure rate of time preference and utility curvature, are held constant across all of these calculations.¹⁰ The only difference is how these approaches value the lives of people in poorer versus richer countries and how they value a dollar of market damages to people in poorer versus richer countries. Indeed, as these results show, the value of the SCC varies by a factor of 50 simply by making different choices around valuing lives and livelihoods.

Fourth, I find that the choice of valuing lives is now the most consequential choice in determining the value of the SCC. I consider the past debates in the climate economics literature around discounting, which has been considered the most consequential choice in determining the SCC. For instance, in the notable Stern-Nordhaus debate around discounting (Nordhaus, 2007; Stern, 2006), Nicholas Stern argued for a lower discount rate, which included a pure rate of time preference of 0.1% and utility curvature of 1. Whereas William Nordhaus argued for a higher discount rate, which included a pure rate of time preference of 1.5% and utility curvature of 2. When running the model to only consider the impact of these parameters on the Ramsey discount rate, I find that Stern's preferred discounting approach increases the SCC by a factor of 4 compared to Nordhaus's, much less than the factor of 50 that results from making different choices around valuing lives and livelihoods.

Finally, it is important to emphasize that this study is not normative; it does not argue for a particular approach to valuing lives and livelihoods around the world, either writ large or within the context of climate change. Previous work has examined the question of which of these approaches are more or less compelling within the specific context of climate change (Bressler and Heal, 2022). That is not the focus of this study. Instead, I seek to enrich the literature by providing formal expressions and estimates for the SCC across four monetization approaches that have received support in the literature and practice in a latest-generation model. This departs from the common practice of only showing SCC results in one or two

¹⁰The first two approaches use utility curvature to inform the Ramsey discount factor, while the latter two use utility curvature to estimate the impact of damages on wellbeing. See the main text for detailed explanation.

SWF approaches. In the context of discounting, it has become standard practice to present SCC results using multiple discount rates (e.g., Barrage and Nordhaus (2024); EPA (2023a); Nordhaus (2017); IWG (2016, 2021)). Perhaps this is in part because it is recognized that reasonable, knowledgeable experts can and have disagreed on the discount rate that should be used to calculate the SCC (Heal, 2017; Kelleher, 2024; NASEM, 2017; Nordhaus, 2007; Pindyck, 2013; Stern, 2006). Perhaps this is also because it is recognized that it is useful to provide information about the SCC's sensitivity to the choice of discount rate. Given the importance of the choice around valuing lives and livelihoods in the latest generation of models, this study takes this same approach with respect to this critical choice. This empowers decision-makers to have the information they need to choose their preferred approach to valuing lives and livelihoods while also understanding the SCC's sensitivity to alternative approaches.¹¹

¹¹In addition to policy, SCC values have been used to inform internal carbon prices used by companies and philanthropies. These organizations may have their own perspective on the way that they would prefer to value lives and livelihoods when they derive their own SCC that differs from the perspectives of governments or other organizations. E.g., I previously did consulting work to help a philanthropy figure out the internal SCC that they prefer to use given their preferred approaches to valuing lives and livelihoods around the world (Oehlsen, 2024).

2 The Distributional Mortality Cost of Carbon

2.1 Deriving the Mortality Cost of Carbon and the Distributional Mortality Cost of Carbon

The social cost of carbon (SCC) quantifies the *monetized* cost of emitting one extra tonne of CO₂ at a certain point in time (or, equivalently, the monetized benefit of reducing one extra tonne of CO₂ at a certain point in time). The SCC is widely used in benefit-cost analysis (BCA) because it provides valuable information on the monetized social cost of different policies with different levels of emissions. The SCC can be used to assess the social climate cost of such policies since emissions differences from policy changes are usually marginal in comparison to all global emissions across all countries across time.¹²

Because climate damages occur over long timescales, it has long been recognized in the climate economics literature that the SCC is highly sensitive to the modeler's choice of discount rate, which determines the rate at which future damages are converted into present value. Reasonable, knowledgeable experts can and have disagreed on the discount rate that should be used to calculate the SCC (Heal, 2017; NASEM, 2017; Nordhaus, 2007; Pindyck, 2013; Stern, 2006). Furthermore, while the SCC is often presented only as a single number, it is a function of a wide variety of factors in addition to the discount rate. E.g., the specific sectors/categories of damages that the modelers included (and the sectors/categories of damages that the modelers did not include). For these reasons, among others, the National Academies of Sciences emphasized in their 2017 report on improving the scientific basis for the SCC that greater care should be taken to increase the transparency with which SCC estimates are presented. In particular, they emphasized that in addition to the final SCC number, damages should be reported on a sector-by-sector basis in physical units—e.g., crop yield damages in the case of agriculture, deaths in the case of mortality—since damages represented in physical units are more straightforward and require fewer intermediary assumptions to estimate than their monetary counterparts. Furthermore, the National Academies emphasized that intermediate and disaggregated damage projections for both incremental and total damages should be made available along with the final SCC value (NASEM, 2017).

Bressler (2021) took a step in addressing the National Academies concerns by introducing a new metric that was responsive to the call for greater transparency in calculating the SCC: the mortality cost of carbon (MCC). The MCC is the number of deaths caused by emitting a tonne of CO₂ at some point in time. Said another way using the language of the National

¹²Although models producing the SCC can also be used to estimate the latter object as well: in this study, I use the climate-economy-mortality integrated assessment model to calculate both the marginal impacts from adding emissions as well as total impacts resulting from climate change, shown in the figures below.

Academies: it is the mortality-specific incremental damage caused by emitting a tonne of CO₂ represented in the physical units of mortality (deaths). It is an intermediate output that is produced on the way to the full SCC estimate; it is always implicit in any SCC estimate that includes climate mortality impacts, although it was never previously shown.¹³ To summarize the differences between the MCC and the SCC: (1) The SCC is intended to include all market and non-market damages from marginal emissions whereas the MCC only measures the mortality impact (2) The SCC monetizes all climate damages into a single value whereas the MCC does not monetize damages because it is in units of excess deaths (3) The SCC converts future damages to present value through discounting whereas the MCC is simply the number of excess deaths aggregated over some future period. To further increase transparency, the MCC can be broken down over time, as was done in Bressler (2021) and as I do here in figure 3 below. The MCC can also be broken down over space; I will label this object the distributional mortality cost of carbon (D-MCC).

Formally, the MCC resulting from a pulse of CO_2 emitted at time period t_0 can be represented by the following equation:

$$MCC_{t_0} = \sum_{t=t_0}^{t=T} \sum_{c=1}^{c=C} (\text{excess deaths with pulse}_{t_0,t,c} - \text{baseline excess deaths}_{t_0,t,c})$$
 (1)

Where the (excess deaths_{t_0,t,c}) term represents the temperature-related excess deaths caused by climate change, which is derived formally in equation 51 in the appendix. Semantically, this equation represents the number of additional excess deaths caused by a pulse of CO₂ in time t_0 aggregated from $t = t_0$ until t = T across the C countries available in the model. My model includes 184 countries, so C = 184 in my case.

The D-MCC resulting from a pulse of CO_2 emissions in time t_0 , D-MCC_{t_0}, can be represented as a Cx1 vector with each row represented by the term D-MCC_{t_0,c}:

$$D-MCC_{t_0,c} = \sum_{t=t_0}^{t=T} (\text{excess deaths with pulse}_{t_0,t,c} - \text{baseline excess deaths}_{t_0,t,c})$$
 (2)

Where D-MCC_{t_0,c} represents the number of excess deaths in country $c \in C$ caused by a pulse of CO₂ in time t_0 aggregated from $t = t_0$ until t = T.

A simplified schematic that provides intuition into how the climate-economy-mortality

¹³And, as mentioned above, the MCC would be less relevant in previous generation models that either did not clearly specify how much, if any, of their damages came from mortality or projected little damage from mortality.

2.2 A Climate-Economy-Mortality Integrated Assessment Model

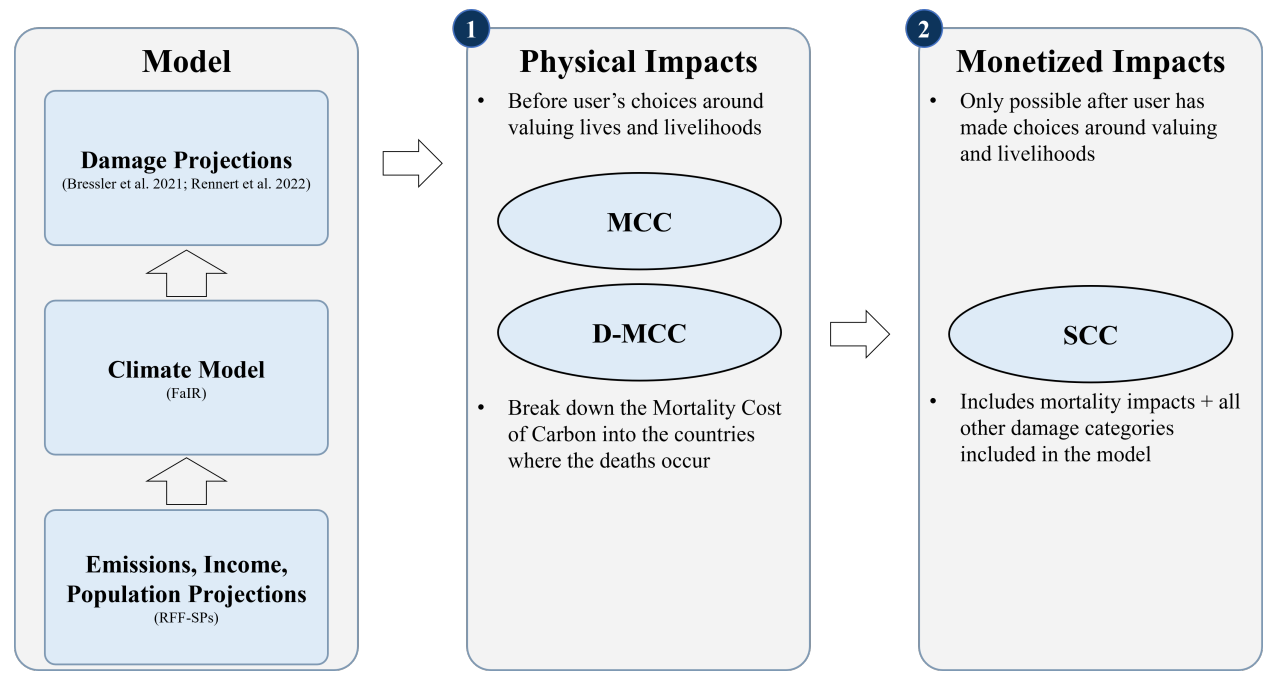


Figure 1 | Model Summary The figure is a simplified schematic to provide intuition for the more detailed information described in the text.

I leverage a climate-economy-mortality integrated assessment model to estimate both the D-MCC in this section as well as SCC estimates in the following section. This model has global probabilistic socioeconomic and emissions projections (Rennert et al., 2021), a climate model (Millar et al., 2017; Smith et al., 2018), and sector-specific market damage functions (Rennert et al., 2022) all updated to the latest science and responsive to the National Academies of Sciences' recommendations for improving the scientific basis for estimating the SCC (NASEM, 2017). These elements of the model are the same as in the U.S. Government's 2023 SCC update (EPA, 2023a) and in the 2022 version of the RFF-Berkeley Greenhouse Gas Impact Value Estimator (GIVE) model (Rennert et al., 2022) and in Bressler et al. (nd). I combine these elements with global mortality damage functions with country-level spatial resolution that explicitly account for changes in cold- and heat-related mortality and income-based adaptation (Bressler et al., 2021). I run 10,000 Monte Carlo simulations that capture uncertainty in emissions, population, economic growth, the response of the climate

system, and damages.¹⁴

Although climate change is projected to cause a significant increase in heat-related deaths, two factors will counteract this trend: (1) decreasing cold-related deaths, and (2) a reduced vulnerability to heat as populations become richer in the future (Bressler, 2021; Carleton et al., 2022; Deschênes and Greenstone, 2011; Gasparrini et al., 2017; Hajat et al., 2014; Houser et al., 2015; Kim et al., 2016; Lee and Kim, 2016). The climate-economy-mortality integrated assessment model here accounts for all of these factors: increasing heat-related mortality, decreasing cold-related mortality, and future vulnerability reduction to heat as incomes rise.

I use the Resources for the Future Socioeconomic Projections (RFF-SPs) to make probabilistic emissions, economic growth, and population projections (Rennert et al., 2022, 2021), which were also used in the US Government's 2023 update to the SCC (EPA, 2023a). The RFF-SP's median 21st-century emissions trajectory is most similar to Representative Concentration Pathway (RCP) 4.5. Economic projections in the RFF-SPs are represented in purchasing power parity (PPP) adjusted dollars, which adjusts market prices to account for the ability of money in different places to purchase fixed bundles of goods and services. See EPA (2023a); Rennert et al. (2022, 2021) for more details.

I represent the global climate system and carbon cycle dynamics with the Finite Amplitude Impulse Response (FaIR) version 1.6.2, which accounts for climate system uncertainty (see Rennert et al. (2022) for further details). Because the mortality damage function used in this study requires country-level temperature projections, I apply the temperature pattern scaling methodology discussed in appendix section A.4.

Rising incomes can reduce vulnerability to heat through multiple pathways, including by enabling increased adoption of air conditioning (Barreca et al., 2016), increasing the ability to relocate labor hours away from occupations and times of day most exposed to the heat (Kjellström et al., 2019), and increasing the ability to live in locations less susceptible to the urban heat island effect (Hsu et al., 2021). Not accounting for future income growth—i.e., assuming that more affluent future populations will be just as vulnerable to heat as historically observed populations by assuming that historical levels of adaptation are simply preserved in the future—will over-estimate future mortality impacts if future higher-income populations

¹⁴Another working paper Bressler et al. (nd) also uses the Bressler et al. (2021) mortality damage function and it compared the EPA (2023a) and income weighting approaches to monetization. However, the model considered in this study includes components for calculating the mortality cost of carbon (fig. 2), the mortality cost of carbon broken down across space (fig. 4), none of which are included in the Bressler et al. (nd) model. In addition, the model considered here included components for calculating all four of the major monetization approaches identified from the literature, including the EPA (2023a) approach, income weighting, U.S. Status Quo, and prioritarian weighting, whereas the Bressler et al. (nd) model included components only for the first two of these approaches.

end up being better at protecting themselves from heat compared to current populations.

The mortality damage function used in this study is based on Bressler et al. (2021), which extends Gasparrini et al. (2017). Here, I focus on the implementation of these damage functions into the GIVE model; see the original paper for detailed information on the damage functions themselves.

Bressler et al. (2021) produces country-level temperature-related mortality damage functions. It estimates the impact of climate change both on increasing heat-related mortality and decreasing cold-related mortality.¹⁵ It can make projections that account for income-based adaptation in different parts of the world, i.e., the benefit of future income growth in reducing vulnerability to heat-related mortality. It can also make projections assuming that the current vulnerability to temperature-related mortality remains the same in the future, i.e., that no additional adaptation from future income growth will occur. Here, I use the preferred models from Bressler et al. 2021 for both heat (model 4) and cold (model 3). A detailed description of the damage function implementation is given in section A.5.

2.2.1 A Note on Dry-Bulb Versus Wet-Bulb Temperature

Like much of the epidemiology and economics literature (Bressler, 2021; Carleton et al., 2022; Cromar et al., 2022; Deschênes and Greenstone, 2011; Gasparrini et al., 2017; Hales et al., 2014; Honda et al., 2014), I estimate mortality impacts in the climate-economy-mortality model based on dry-bulb temperature and not wet-bulb temperature. Dry-bulb temperature is simply the basic ambient air temperature metric that is most commonly reported and used. Wet-bulb temperature utilizes information, including dry-bulb temperature and the air's moisture content, to determine the temperature after accounting for the cooling effect of evaporation. Wet-bulb temperature has been identified in the scientific literature as an important metric for understanding the impact of heat on human health because it accounts for the critical role of sweat evaporation—the primary mechanism by which the human body cools itself—in maintaining homeostasis under heat exposure (Baldwin et al., 2023; Buzan and Huber, 2020). The higher the humidity, the less effective sweating is at cooling the body (Havenith and Fiala, 2011; Parsons, 2014; Steadman, 1979). 35°C wet bulb temperature represents the theoretical physiological limit at which humans are no longer able to dissipate

¹⁵It is important to note that the Bressler et al. (2021) mortality damage function as well as other mortality damage functions available in the literature (e.g., Bressler (2021); Carleton et al. (2022); Cromar et al. (2022)) only capture the impact of climate change on temperature-related mortality. It leaves out potentially important climate-mortality pathways such as the effect of climate change on infectious disease, civil and interstate war, food supply, and flooding. While it would be beneficial to be able to include those other climate-mortality pathways, the ability to make credible projections for those other climate mortality pathways remains challenged—see Bressler (2021) and Bressler et al. (2021) for more discussion on this point.

heat into the environment, and are thus physically incapable of survival when exposed for a sufficient length of time (Mora et al., 2017; Raymond et al., 2020; Sherwood and Huber, 2010). When this theoretical limit has been tested in the lab, it has been found to in practice actually be significantly lower: 31°C or lower (Vanos et al., 2023; Vecellio et al., 2022). Under high emissions scenarios, increasing humid heat stress is projected to cause some regions to reach these limits and become uninhabitable for parts of the year without artificial cooling (Powis et al., 2023; Sherwood and Huber, 2010). Despite the importance of both heat and humidity for human thermoregulation, most empirical studies on temperature-related mortality have focused on dry-bulb temperature, which does not account for humidity.

There are multiple reasons why I use dry-bulb temperature and not wet-bulb temperature in the climate-economy-mortality model. First, to my knowledge, the climate modules in all currently available models determine the temperature response to an emissions pulse in units of dry-bulb temperature and not wet-bulb temperature. To operationalize mortality damage functions that use wet-bulb temperature, the climate module would have to quantify the climatic response to an emissions pulse in units of wet-bulb temperature and not dry-bulb temperature. Second, very few empirical studies on temperature-related mortality have assessed the impact of wet-bulb temperature (Armstrong et al., 2019; Baldwin et al., 2023), despite the theoretical and physiological importance of wet-bulb temperature discussed in the previous paragraph. Notable exceptions to this include Geruso and Spears (2018) as well as my previous coauthored work that determine the age-specific temperature-related mortality impact using wet-bulb temperature in Mexico (Wilson* et al., 2024). In section A.6 below, I further add to this growing empirical literature that uses wet-bulb temperature by assessing the occupational-specific temperature-related mortality impact in Mexico. In that section I assess impacts using both wet-bulb and dry-bulb temperature.

2.3 Results

2.3.1 The Mortality Cost of Carbon: How Many Deaths Are Caused by a Pulse of Emissions when Aggregated Across the Whole World?

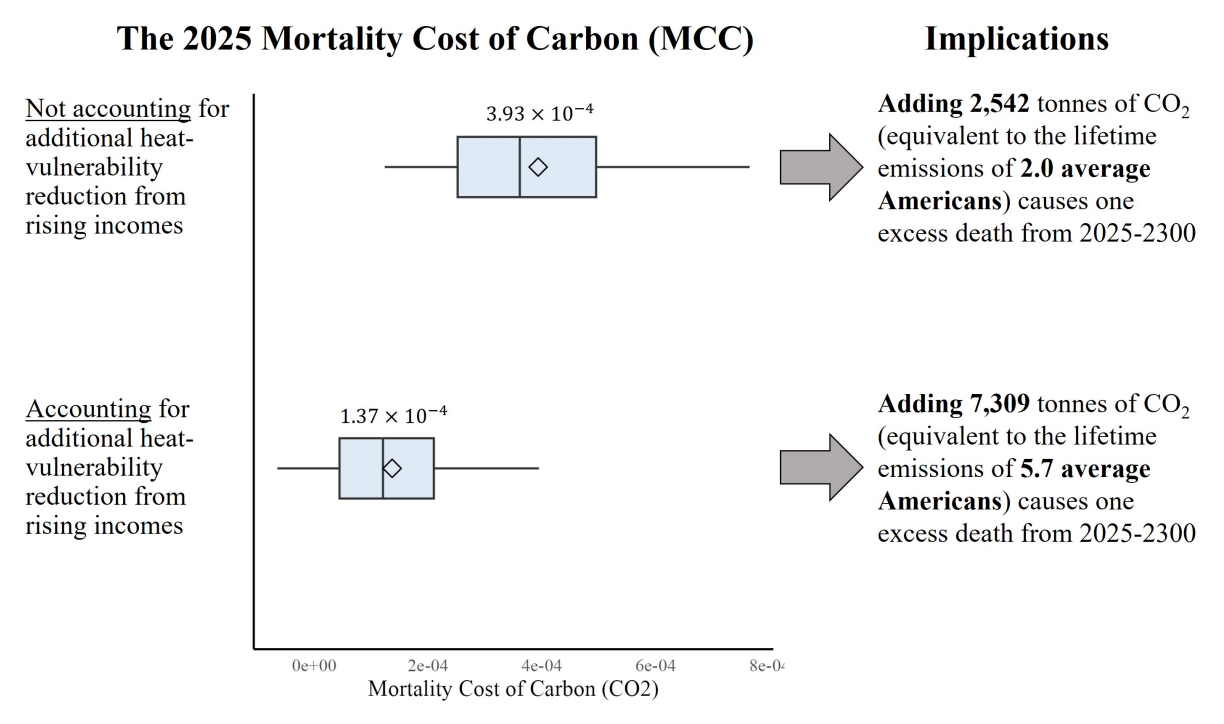


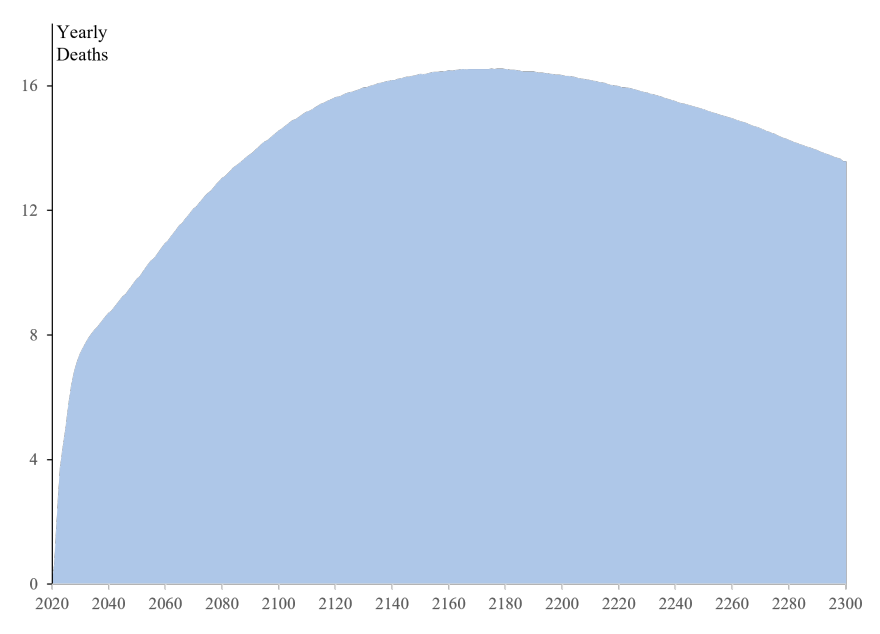
Figure 2 | The Mortality Cost of Carbon (MCC) Boxplots show median (center black line), mean (diamond), 25%–75% quantile range (box width), and 5%–95% quantile range (horizontal lines) MCC values caused by a pulse of 2025 emissions when the MCC aggregates deaths from 2025 to the end of the model in 2300. Mean, median, and quantile values are determined by 10,000 draws in a Monte Carlo simulation, which captures uncertainty in socioeconomic and emissions scenarios (RFF-SPs), uncertainty in climate (FaIR v1.6.2), and mortality damage function uncertainty. The labeled numbers are the mean value.

Figure 2 shows the MCC resulting from a one tonne pulse of CO_2 in 2025 aggregated to the end of the model in 2300.¹⁶ The top part of the figure shows the MCC not accounting for additional heat-vulnerability reduction from rising incomes, i.e., assuming that future populations will remain just as vulnerable to heat as current populations. In that case, I find that the MCC is 3.93×10^{-4} , which implies that adding 2,542 tonnes of CO_2 —equivalent

¹⁶Following the suggestions of the National Academies (NASEM, 2017), it has become standard in the SCC literature to project damages to 2300 (e.g., Carleton et al. (2022); EPA (2023a); Rennert et al. (2022)). Some prior-generation models, e.g. DICE-2016, projected damages out further to 2510. Figure 3 shows how the MCC broken out based on which year the death from marginal emissions takes place; if a user prefers to consider an MCC value that is summed over some period ending before 2300, they can use the underlying data from that figure to aggregate deaths over any time period that they prefer.

to the lifetime emissions of 2.0 average Americans—causes one excess death in expectation from 2025-2300. The bottom part of the figure shows the MCC accounting for additional heat-vulnerability reduction from rising incomes, i.e., accounting for future richer populations becoming less vulnerable to heat than current populations. I find that accounting for this vulnerability reduction significantly reduces the MCC. In this case, the MCC is 1.37×10^{-4} , which implies that adding 7,309 tonnes of CO_2 —equivalent to the lifetime emissions of 5.7 average Americans—causes one excess death from 2025-2300.

(a) Not accounting for additional heat-vulnerability reduction from rising incomes



(b) Accounting for additional heat-vulnerability reduction from rising incomes

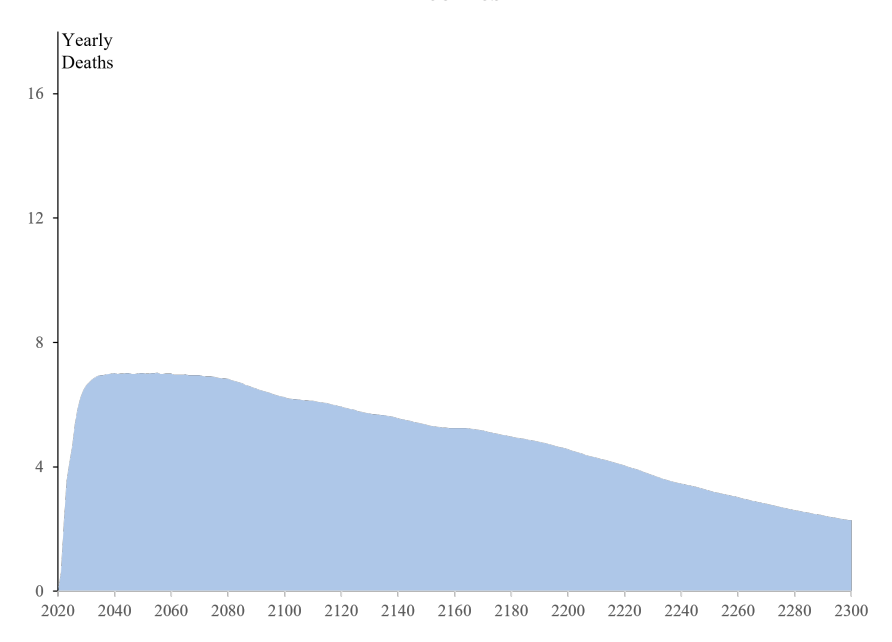


Figure 3 | Deaths over time from a pulse of emissions Figures show the number of deaths in each year resulting from a 10 million tonne pulse of CO₂ in 2025. Each year is represented with a bar corresponding to the number of deaths in that year that result from the 2025 emissions pulse. Deaths in each year are mean values across 10,000 draws in a Monte Carlo simulation, which captures uncertainty in socioeconomic and emissions scenarios (RFF-SPs), uncertainty in climate (FaIR v1.6.2), and mortality damage function uncertainty. (a) Shows the number of deaths without accounting for additional heat-vulnerability reduction from rising incomes. I.e., assuming that the current vulnerability to heat-related mortality remains the same in the future. (b) Shows the number of deaths accounting for additional heat-vulnerability reduction from rising incomes. I.e., populations will be less vulnerable to heat as they become richer in the future.

Figure 3 breaks down the MCC by when deaths from a pulse of emissions today will occur in the future. It shows the impacts of a 10 million tonne 2025 CO₂ pulse, which is equivalent to the yearly emissions of 2.5 average coal-fired power plants in the U.S (EPA, 2019). Importantly, accounting for the role of rising incomes in reducing vulnerability to heat significantly changes the dynamics of the MCC. When assuming that future populations are just as vulnerable to heat as current populations (panel a), future deaths caused by adding 10 million tonnes of CO₂ emissions today increase every year until peaking in 2166 at 17 deaths. Under this assumption, aggregating across all of the years from 2025-2300 in panel (a) shows that adding 10 million tonnes of CO₂ in 2025 causes 3,930 deaths, which is equal to 10 million multiplied by the one-tonne MCC not accounting for additional heat-vulnerability reduction shown in figure 2.

When accounting for future income-based vulnerability reduction (panel b), however, future deaths caused by adding 10 million tonnes of CO₂ emissions today peak in the relatively near future in 2041 at 7 deaths before declining to the end of the model period in 2300. Likewise, aggregating across all of the years from 2025-2300 in panel (b) yields 1,370 deaths, which is equal to 10 million multiplied by the one-tonne MCC accounting for additional heat-vulnerability reduction shown in figure 2.

In total, when accounting for additional heat-vulnerability reduction from rising incomes in panel b, half of the deaths from a current pulse of emissions occur over the next 100 years. Both panels (a) and (b) have the same underlying climate dynamics determined by the underlying FaIR climate model: a pulse of 2020 emissions incrementally increases temperatures in all future periods by the same amount in both panels. In both panels, this incrementally decreases cold-related mortality while incrementally increasing heat-related mortality in countries around the world, and in both panels, the net mortality impact of less cold-related mortality and more heat-related mortality is a net increase in premature deaths in each year when aggregating across all countries. The difference is that in panel (a), future populations are just as vulnerable to heat as current populations, so the incremental increase in future temperatures from an emissions pulse today continues to be quite damaging to them into the 22nd and 23rd centuries. Whereas in panel (b), future populations become less vulnerable to heat as their incomes grow. So while the incremental increase in future temperatures from an emissions pulse today continues to cause harm through the end of the model period, it causes progressively less harm over time as future richer populations become progressively better adapted to heat-related mortality over time.

2.3.2 The Distributional Mortality Cost of Carbon: How Many Deaths in Each Country Are Caused by a Pulse of Emissions?

The full 184x1 vector for the D-MCC for a pulse of 2025 emissions is given in the appendix in table A.1. The D-MCC that accounts for heat-vulnerability reduction from rising incomes is given in column 2 and the D-MCC that holds temperature vulnerability constant at current levels is given in column 6. As that table shows, deaths are overwhelmingly concentrated in hotter, poorer countries: Southern Asia and Sub-Saharan Africa account for 75% of deaths in the D-MCC in column 2. 83% of the deaths are in low and lower-middle-income countries. When accounting for future income-based vulnerability reduction, some colder and higher-income countries see a slight decrease in premature mortality. In these cases in these countries, the benefit of fewer cold-related deaths outweighs the cost of more heat-related deaths. For lower-income and hotter countries, however, less exposure to cold temperatures does not overcome the burden of exposure to higher temperatures. The mortality benefits accruing to some richer and colder countries is dwarfed by excess deaths in hotter and colder countries. It takes 713K tonnes of emissions—equivalent to the lifetime emissions of 559 average Americans— to save one life in richer and colder countries that have a negative D-MCC component value in column 2 of table A.1, while those same emissions are expected to cause 99 deaths in the hotter and poorer countries that have a positive D-MCC component value.

Figure 4 shows a choropleth cartogram visualization of the D-MCC results. Country size is determined by the country share of deaths in the D-MCC, shown in table A.1 column 3 (the cartogram part of the figure). Said another way, this figure represents what the world would look like if land area was determined by how many people are expected to die in that country in the future by adding emissions today. This figure shows how disproportionally these deaths are distributed across the globe. The whole western hemisphere almost disappears, since only 2% of the expected deaths are there. Europe also nearly disappears, representing only 2% of expected deaths. Whereas Sub-Saharan Africa, representing 42% of the deaths, is greatly magnified as is South Asia, representing 33% of the deaths. The country color is determined by how disproportionally countries are impacted relative to their population size (the chloropleth part of the figure). A darker color implies that the country is more disproportionally impacted. Somalia and Niger are the most disproportionally impacted countries in the world: they represent 4% and 3% of the deaths despite having just 0.3% and 0.2% of the world's population respectively.

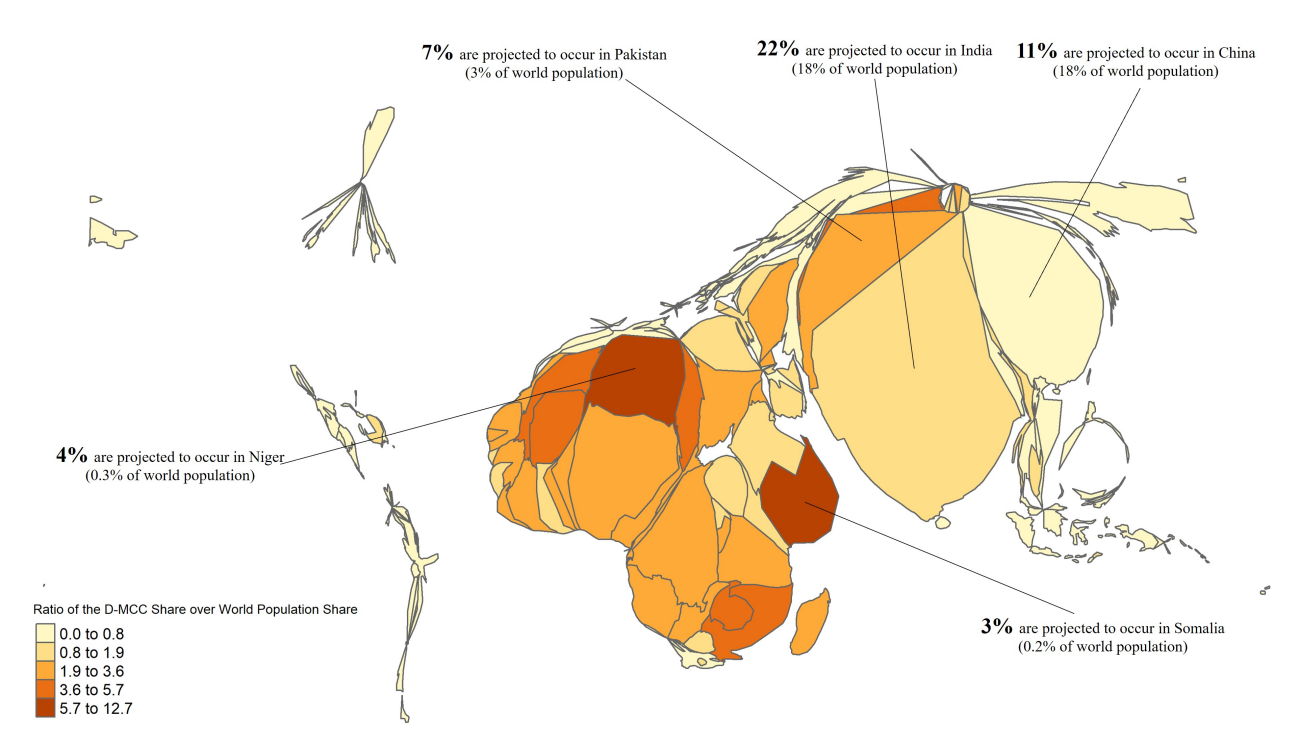


Figure 4 | Chloropleth Cartogram of the Distributional Mortality Cost of Carbon (D-MCC) Country size is proportional to country share of death assuming that future richer populations will be less vulnerable to heat (column 3 of table A.1). India is the largest country in the figure because it has the largest share of deaths. Country color represents how disproportionally countries are impacted relative to their population size. The chart was produced in R version 4.4.3 using the rubber sheet distortion algorithm (Dougenik et al., 1985) in the cartogram package (Jeworutzki, 2016).

2.4 Comparison to Previous Work

In this section, I produced the first estimate of the mortality cost of carbon in a latest-generation climate-economy-mortality model broken down by country. However, I also produced outputs that are more directly comparable with outputs from other papers in the literature. For instance, other studies in the literature also have projected the total impact of climate change on premature mortality. The spatial distribution of the impact of climate change on premature mortality in 2100 shown in figure A.1 is quite similar to the spatial distribution of impacts found by the Climate Impact Lab in Carleton et al. (2022) figure 4. These spatial findings here and in Carleton et al. (2022) are consistent with a large swath of the climate-mortality literature that has found that hotter and poorer locations are projected to be more adversely impacted than colder and richer locations (Bressler, 2021; Ebi et al., 2021; Gasparrini et al., 2017; Mora et al., 2017).

Comparing the total aggregated global mortality impact of climate change requires using

a comparable emissions scenario, as this output is very sensitive to underlying emissions assumptions. Mortality impacts in higher emissions scenarios tend to be significantly higher than in lower emissions scenarios (Bressler, 2021; Carleton et al., 2022; Gasparrini et al., 2017). In this study, I use the probablistic RFF-SPs (Rennert et al., 2021). However, the RFF-SPs are fairly new and most past studies in this literature have instead made projections in the deterministic Representative Concentration Pathways (RCPs). Figure 9 green line in Carleton et al. (2020) shows the Climate Impact Lab's total mortality impacts in the deterministic high RCP 8.5 emissions scenario at the end of the century, finding a 5.1% increase in the global mortality rate in 2100.¹⁷ Bressler et al. (2021), whose mortality damage function I leverage in this study, also provides mortality projections in the deterministic RCP emissions scenarios and finds a 4.4% increase in the global mortality rate in the RCP 8.5 emissions scenario.

The only other study in the literature that has projected the MCC is the Bressler (2021) study that introduced the concept, discussed above. That study extended the DICE-2016 model (Nordhaus, 2017) to create the DICE-EMR model, which calculated the MCC. This study makes a number of methodological improvements over that previous study, most of which involve improving the underlying components from DICE-2016. To highlight some of the major improvements: first, the DICE-2016 model is completely deterministic. Emissions trajectories, socioeconomics projections, the climate model, damages, and all other aspects of the model did not have any uncertainty. The mortality damage function that was added in DICE-EMR did include low central and high mortality projections, but besides that, there was no other characterization of uncertainty. This study, by contrast, accounts for uncertainty in emissions, socioeconomic projections, the climate model, and damages and each of the results I show here result from running 10,000 Monte Carlos simulations so that uncertainty can be characterized along with central estimates. Second, the FaIR v1.6.2 climate model used in this study that estimates the climatic impact of a pulse of CO₂ is a significant improvement that better reflects the current understanding of climate dynamics compared to the DICE-2016 climate model. Multiple studies have shown that the DICE-2016 climate model underestimates the short-term warming impact and overestimates the long-run warming impact of CO₂ emissions (Dietz et al., 2021; Folini et al., 2024). Third, DICE-2016 uses a deterministic baseline emissions scenario that results in 4.1°C warming over preindustrial levels in 2100, which is now considered by many experts to be quite pessimistic. This is due in part to DICE-2016's climate model, which tends to overestimate the long-run warming impact of a given emissions trajectory, but it also results from a more pessimistic emissions trajectory than many experts now assume. This study, by contrast, uses the probabilistic RFF-SPs that

¹⁷See Bressler (2021) for conversion from deaths per 100,000 to increase in the mortality rate.

used expert elicitation and other methods to make socioeconomic and emissions projections (see Rennert et al. (2021) for details). The median warming scenario in the RFF-SPs is considerably more optimistic than the DICE-2016 baseline emissions scenario. It involves just over 2°C warming over preindustrial levels in 2100. The deterministic DICE-2016 4.1°C 2100 warming scenario, by contrast, is outside of the 95th percentile warming scenario in the RFF-SPs. Fourth, the mortality damage function in Bressler (2021) was constructed in a similar way to the underlying DICE-2016 economic damage function (Nordhaus and Moffat, 2017). 18 Importantly, like the underlying DICE-2016 damage function, the DICE-EMR mortality damage function is only a function of global average temperature¹⁹. Furthermore, because none of the underlying studies used to construct the mortality damage function made projections beyond 2100 and a richer representation of the relationship between mortality and other model variables besides global average temperatures was not available, Bressler (2021) only included deaths from 2020-2100 in the MCC estimates. This study, by constrast, makes mortality projections that are a function of country-level population-weighted temperature, local long-run climate, and future income growth out to the end of the model in 2300, as discussed above and in the appendix. Finally, DICE-2016 and DICE-EMR are single region global models, so they are not able to calculate the D-MCC because all of their outputs are aggregated at the global level. Whereas in this study, the country-level spatial resolution allows me to calculate the D-MCC.

3 The Social Cost of Carbon

3.1 The Social Cost of Carbon and Valuing Excess Deaths

The SCC represents the monetized social damage from emitting one tonne of CO₂ at some point in time across all categories of damages included in the model. To calculate the SCC, I must monetize the deaths around the world caused by a pulse of emissions that were calculated

¹⁸A systematic research synthesis was undertaken to choose studies that met a set of specified criteria. Those criteria included making projections of temperature-related mortality that could be leveraged to estimate the DICE-EMR mortality damage function.

¹⁹The DICE-EMR mortality damage function was constructed by using a median weighted regression to fit a curve through mortality projections in specific warming scenarios taken from the studies chosen in the systematic research synthesis. One of the criteria for the studies that it used was that those studies should account for adaptation. However, not all of the studies used accounted for adaptation as a function of income. For instance, Hales et al. (2014) (based on Honda et al. (2014)) accounted for adaptation not as a function of income growth or other factors, but by simply reducing excess mortality in the temperature-mortality exposure response function by 50%. Thus, given the heterogeneity in the underlying assumptions that went into projections of mortality impacts net of adaptation in the underlying projections, the DICE-EMR damage function specified mortality damages only as a function of global average temperatures

in the previous section, and combine that with the broader set of non-mortality damages in other damage sectors/categories. Specifically, I use the other three damage categories that were included in the 2022 version of the GIVE model (Rennert et al., 2022): sea level rise, energy expenditures, and agricultural damages.²⁰

The D-MCC findings in the previous section have a critical implication for the SCC: the vast majority of deaths occur in lower-income countries, while comparatively few deaths occur in higher-income countries. Thus, the SCC is extremely sensitive to how the modeler chooses to value lives around the world in countries with very different income levels.

The underlying concept that informs how premature deaths are monetized in BCA is the value of statistical life (VSL). VSL is an evidence-driven estimate of how much an average individual would pay, in monetary terms, to avoid a specified mortality risk. Methodologically, it is often estimated in labor markets where there are tradeoffs between small amounts of additional safety and wage compensation. Thus, VSL is not intended to represent the government's own assessment of "the value of life," but rather, it is intended to capture the tradeoffs individuals make.

A ubiquitous finding in the VSL literature is that reducing mortality risk is a normal good: i.e., as individuals become richer, they tend to be willing to pay more to avoid mortality risk. That finding is uncontroversial. The more controversial yet necessary public policy question—that all decision-makers who assess policies that impact mortality risk must grapple with—is how to leverage this information to value deaths caused or lives saved in their analysis. Different approaches to BCA answer this question in different ways.

First, the foundational Kaldor-Hicks (Kaldor, 1939; Hicks, 1939) approach to benefit-cost analysis values all benefits and costs, including the willingness to pay to avoid mortality risk, at the best possible estimate of each individual's willingness to pay. Because willingness to pay to avoid mortality risk scales with income²¹, the Kaldor-Hicks approach values deaths among richer populations more than deaths among poorer populations.

Second, when BCA has been applied in practice, governments have generally not taken the Kaldor-Hicks approach to valuing premature deaths. Instead of valuing premature deaths among the rich more than the poor, the U.S. and the U.K. have historically monetized and

²⁰See Rennert et al. (2022) Extended Data Table 2 for further details, including a discussion of how uncertainty is represented in those damage functions. Probabilistic projections of regional changes in sea level are made using the Building Blocks for Relevant Ice and Climate Knowledge (BRICK) model (Wong et al., 2017).

²¹A variety of studies have assessed the literature to estimate the income elasticity of VSL, and a VSL income-elasticity of 1, which implies that VSL scales proportionally to income, has been presented as a standard estimate for policy analysis (Masterman and Viscusi, 2018; Robinson et al., 2019; Viscusi and Masterman, 2017). EPA (2023a) and Rennert et al. (2022) adopt a VSL income elasticity of 1 in their analysis.

continue to monetize all premature deaths at a single population average value, ²² ²³ which represents an estimate of the average VSL across the whole population. Quantitatively, this has represented a major divergence from the Kaldor-Hicks approach to BCA because the majority of benefits historically in government BCAs are directly attributable to the monetized value of reducing premature mortality.²⁴ The 2023 update to the SCC (EPA, 2023a) diverged from the U.S. status quo practice of valuing premature deaths at a single population average in favor of an approach closer to Kaldor-Hicks because it valued deaths from climate change in each country proportionally to that country's PPP-adjusted per capita income. However, that report also appeared to be the first time that the U.S. government has explicitly valued lives in other countries as part of regulatory BCA.²⁵ ²⁶

²³For the U.K., see HM Treasury (2022): "On grounds of equity . . . the valuation of a statistically prevented fatality (VPF) are based on average values from representative samples of the population (who differ in their incomes, preferences, age, states of health and other circumstances). These values are used when analysing and planning the provision of assets, goods and services at a population or sub-population level."

²⁴Colmer (2020) finds that 70% of the total benefits in BCAs of federal regulations historically were directly attributable to the monetized value of reducing early mortality. EPA (2011a) found that 85% of the benefits from the Clean Air Act Amendment are attributable to the reduction in premature mortality associated with the reduction in ambient particulate matter. See also Hemel (2022): "Lifesaving regulations are not an administrative-state sideshow—they are the main act. Really expensive regulations generally do one of three things. They (a) reduce the risk of death or serious illness from air pollution, (b) reduce the risk of death or serious injury from motor-vehicle crashes, or (c) reduce greenhouse gas emissions. Note that a primary—probably the primary—reason why we worry about greenhouse gas emissions is that global warming will lead to death and serious illness on a vast scale, so (c) is largely subsumed by (a)."

²⁵Historically in the U.S., the vast majority of regulatory impact assessments only quantify domestic benefits and costs (Gayer and Viscusi, 2016). There does not appear to be precedent for a Regulatory Impact Statement (RIA) explicitly projecting and monetizing premature deaths caused in other countries by U.S. policy decisions. A few RIAs have considered impacts in other countries but have not monetized them. For instance, the Mercury and Air Toxic Standard (MATS) RIA discussed the foreign health benefits of U.S. mercury reductions qualitatively but did not quantify them (Howard and Schwartz, 2017; EPA, 2011b). Likewise, the 1996 NASA Final tier 2 environmental impact statement for International Space Station report considered mortality impacts from falling debris in the U.S. and other countries, but did not monetize the impact (NASA, 1996).

²⁶Although two of the three underlying models that the US Government used to calculate the SCC before the 2023 update (DICE and PAGE) did not clearly specify how much (if any) of their estimated damages derived from mortality, one of the three models, FUND, did include damage from premature mortality as

²²For the U.S., see OMB (2023a): "... it is appropriate to use a value for mortality risk reductions (sometimes referred to as the value of a statistical life, or VSL) that does not depend on the income of the sub-population to which the mortality risk reduction benefits accrue..." For discussion of historical practice, see, e.g., Sunstein (2004): "For over two decades, executive orders have required regulatory agencies to engage in cost-benefit analysis of major regulations, and Congress has imposed similar requirements in several statutes. To conduct cost-benefit analysis, agencies must assign monetary values to human lives that are potentially saved by a proposed regulation. How do they come up with the numbers that they use? Do some deaths count for more than others?... No agency values the lives of poor people less than the lives of rich people. No agency distinguishes between whites and African Americans or between men and women. For statistical lives, the governing idea is that each life is worth exactly the same. With respect to cost-benefit analysis, much is disputed. But on the idea of a uniform value per life saved, there is a solid consensus, at least in terms of regulatory practice." This practice remains the same today (Sunstein, 2023).

Figure 5 shows why the choice around valuing premature deaths around the world is so consequential. The y-axis shows the country's share of deaths in the D-MCC while the x-axis shows the value assigned to a death in the country based on the EPA (2023a) methodology—i.e., proportionally to income. For instance, Niger is expected to experience nearly twice as many deaths from a pulse of emissions than all countries in Europe combined. Yet, when the modeler chooses to value deaths based on an income-elastic VSL that is proportional to PPP-adjusted income, an average death in Europe is given the same value as 29 deaths in Niger.²⁷

part of its damages. It used an income-elastic VSL to value deaths in its 16 regions (Anthoff and Tol, 2014), although premature mortality was a very small overall part of damages in that model (Cromar et al., 2021). The US Interagency Working Group did not appear to make an explicit choice around monetizing deaths, but instead adopted the model as it existed. They did not mention the choice around valuing deaths around the world in their documents (IWG, 2016, 2021). Whereas in EPA (2023a), the choice of an income-elastic VSL was an explicit modeling choice that was discussed at length.

 $^{^{27}}$ And richer countries within Europe are valued at a much higher value. E.g., each death in Ireland is given the same value as 76 deaths in Niger.

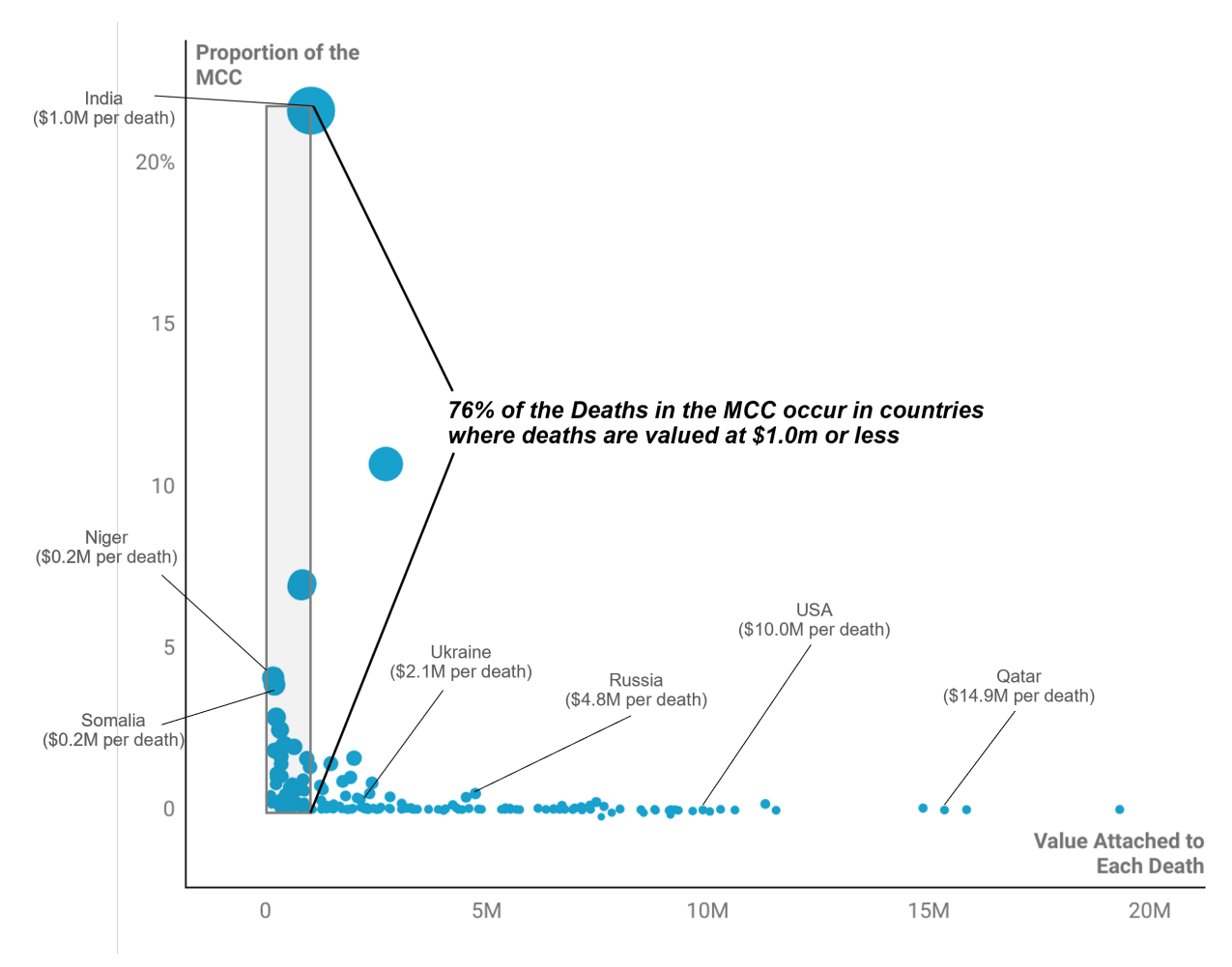


Figure 5 | Relationship between share of deaths in the distributional mortality cost of carbon and the value assigned to each death using an income-elastic VSL. The y-axis shows the share of deaths in the D-MCC by country. The x-axis shows the current period value that is attached to each death based on EPA (2023a). The size of the dots is proportional to the y-axis value.

Even when deaths are valued proportionally to income, premature deaths are still by far the largest category of damages in the SCC both in this study (see table 1 second column below) as well as in other recent studies (Rennert et al., 2022; EPA, 2023a). figure 5 provides intuition both for why the SCC is so sensitive to the choice of how to value lives around the world, and for why the SCC becomes so much larger when deaths around the world are valued more equally, as I will show below.

In the rest of the section, I will show SCC results across a range of approaches to monetization that have had significant support in the literature and/or in practice. The purpose of this study is not to argue for any particular approach, but instead to provide decision-makers with information about what the SCC is based on their preferred approach to valuing lives and livelihoods while also showing them how the SCC varies if they were to

take an alternative approach.

I will focus on four major monetization approaches, two of which I already introduced above. These are (1) Kaldor-Hicks, (2) U.S. Status Quo, (3) Income Weighting, and (4) Prioritarian Weighting. In this section, I will derive formal expression for the SCC using each of these approaches, and I will show how the SCC varies when taking these different approaches.

Throughout this section, it is critical to emphasize that the *physical* projection of damages is not changing. The only thing that is changing is how the modeler chooses to value the lives of people around the world, as well as how to value economic damages to people around the world with different incomes. Importantly, this implies that the MCC and D-MCC are the exact same across all of the different specifications that I show in this section, which lead to very different SCCs (see table 1).

3.2 Deriving the Major SCC Monetization Choices

Put simply, the SCC asks the question: how much damage is caused by emitting a marginal tonne of CO₂ at some point in time? The difference between monetization approaches is the units that those damages are represented in. The Kaldor-Hicks approach quantifies the SCC in units of money unadjusted for diminishing marginal utility across space. The incomeweighting approach quantifies the SCC in units of money that are adjusted for diminishing marginal utility across space, i.e., capturing that an additional dollar has more value to poorer individuals than richer individuals. Income weighting uses a utility function to determine the effect of damages on well-being based on an individual's income. All else equal, the more that climate damages fall on the poor relative to the rich, the higher the well-being loss. The Prioritarian approach quantifies the SCC in units of money that are both adjusted for diminishing marginal utility across space to capture the impact on wellbeing, as well as an additional adjustment that places higher weight on the wellbeing of the poor relative to the rich. Finally, the U.S. Status quo approach takes the same approach as Kaldor-Hicks to all non-mortality benefits and costs—representing damages in units of money unadjusted for diminishing marginal utility, but then it places a special carve-out for mortality damages, where all deaths are measured based on the population average willingness to pay as opposed to the individual willingness to pay. In the case of the SCC, this means that all lives are valued the same at the global average willingness to pay.

3.2.1 The Generalized Social Cost of Carbon

Abstracting from units, equation 3 represents the marginal climate damages in each time period t from a pulse of emissions in time t_0 aggregated across geographies. This is calculated as the difference in modeled damages per ton between the pulse and baseline run. This is calculated in each of the 10,000 Monte Carlo runs:

$$MD_{t_0,t} = \sum_{c=1}^{c=C} (damages with pulse_{t_0,t,c} - baseline damages_{t_0,t,c})$$
(3)

To calculate the SCC, marginal damages in each time period are multiplied by that time period's discount factor DF_t and aggregated across time:

$$SCC_{t_0} = \sum_{t=t_0}^{t=T} DF_t \times MD_{t_0,t}$$
(4)

Across monetization approaches, I calculate the SCC in each of the 10,000 Monte Carlo runs that account for uncertainty in emissions, population, economic growth, and the response of the climate system. As in EPA (2023a) and Rennert et al. (2022), I typically summarize the distribution of the 10,000 estimated SCCs by the mean, $\mathbb{E}[SCC_{t_0}]$, where the expectation operator is taken jointly over all the uncertain parameters determining DF_t and MD_{t₀,t}.

Now, we can split out the marginal damage term MD_t into a mortality and non-mortality component. As mentioned previously, the mortality cost of carbon (MCC) feeds directly into the SCC. Going back to the mortality cost of carbon (MCC) definition in equation 1, we can rewrite the mortality cost of carbon as:

$$MCC_{t_0} = \sum_{t=t_0}^{t=T} \sum_{c=1}^{c=C} MCC_{t_0,t,c}$$
 (5)

Where $MCC_{t_0,t,c}$ is the MCC broken down by both time and space: it is the number of deaths in time t in country c caused by a pulse of emissions in time t_0 :

$$MCC_{t_0,t,c} = (excess deaths with pulse_{t_0,t,c} - baseline excess deaths_{t_0,t,c})$$
 (6)

This term feeds directly into $MD_{t_0,t}$, which can be rewritten in the following way:

$$MD_{t_0,t} = \sum_{c=1}^{c=C} (MCC_{t_0,t,c} \times \text{value of life}_{t,c} + \text{non-mortality } MD_{t_0,t,c})$$
 (7)

Where value of life_{t,c} is the monetary value that the modeler places on each death in time t in country c,²⁸ and non-mortality $MD_{t_0,t,c}$ are the non-mortality damages in time t in country c caused by a pulse of emissions in time t_0 . We can use equation 7 to re-write the generalized SCC equation 4:

$$SCC_{t_0} = \sum_{t=t_0}^{t=T} DF_t \times \left[\sum_{c=1}^{c=C} (MCC_{t_0,t,c} \times \text{value of life}_{t,c} + \text{non-mortality } MD_{t_0,t,c}) \right]$$
(8)

3.2.2 The Quasi-Kaldor-Hicks SCC

I will begin to derive the Quasi-Kaldor-Hicks monetization approach. This is the monetization approach used in EPA's 2023 SCC update (EPA, 2023a) and (Rennert et al., 2022). As mentioned, this approach measures all damages in dollars unadjusted for diminishing marginal utility across space.

The Kaldor-Hicks approach to benefit-cost analysis (BCA) is based on the potential compensation criterion—which specifies that a policy is net beneficial if those who benefit from a policy could fully compensate those who are harmed and still remain gainers, regardless of if such compensation ends up occurring. This is also known as a "Potential Pareto Improvement." However, Bressler and Heal (2022) showed that there is a practical issue facing the implementation of the Kaldor-Hicks approach when estimating the SCC: the income projections most commonly used in the SCC literature—the shared socioeconomic pathways (SSPs) (Riahi et al., 2017) as well as the RFF-SPs used in this and other studies (Rennert et al., 2021)—calculate country-level income projections using purchasing power parity (PPP) instead of market exchange rates. PPP transforms current prices into adjusted prices using weights that account for the ability of money in different places to purchase fixed bundles of goods and services. The issue with PPP as it relates to the Kaldor-Hicks potential compensation criterion is that it transforms net benefits from actual units of exchange (i.e. money at current market exchange rates) to another numéraire that is hypothetical and is not an actual unit of exchange. Arguably, adjusting for PPP converts the money numéraire into

²⁸Each of the four monetization approaches use the value of statistical life (VSL) concept, which represents an estimate of willingness to pay to avoid mortality risk, to inform the value of life calculation, as I will discuss below.

units that are more relevant to what a social planner might care about: the ability of money to buy goods and services and the welfare people get from those goods and services. But this undermines the appeal to the Kaldor-Hicks potential compensation criterion. As Bressler and Heal (2022) show, a policy that yields positive net benefits measured in PPP-adjusted money will not necessarily pass the Kaldor-Hicks potential compensation test. And this is not a minor issue, as the differences between PPP-adjusted money and market-money are very large, especially in developing countries. Thus, I describe the approach in the section as Quasi-Kaldor-Hicks, since proponents of this approach have cited the Kaldor-Hicks criterion in its defense (EPA, 2023a), although it is not fully consistent with this criterion due to the PPP issue.

$$SCC_{t_0} = \sum_{t=t_0}^{t=T} SDF_t \times MD_{t_0,t}.$$
 (9)

Equation 10 yields the SCC in purchasing-power-parity dollars unadjusted for diminishing marginal utility across space so that a dollar of damages in low-income countries is counted the same as a dollar of damages in high-income countries. The marginal damages in each period, MD_t , represents the marginal damages in units of money. For the purposes of this study, I take the same approach to the discount factor as the U.S. Government's recent SCC update EPA (2023a) by using a stochastic Ramsey-like discount factor, SDF_t , which accounts for diminishing marginal utility across time when determining the rate at which damages in future time periods are converted into present value.²⁹

Plugging in equation 7 that separates out mortality and non-mortality damages:

$$SCC_{t_0} = \sum_{t=t_0}^{t=T} SDF_t \times \left[\sum_{c=1}^{c=C} (MCC_{t_0,t,c} \times \text{value of life}_{t,c} + \text{non-mortality } MD_{t_0,t,c}) \right]$$
(10)

Under this monetization approach, the value of life_{t,c} is determined based on estimating the willingness to pay to avoid mortality risk for a typical person in time t in country c, which is represented by the term $VSL_{t,c}$. Because there are no VSL estimates readily available in the literature for every country into the future, I use the same benefits transfer methodology used in EPA (2023a); Rennert et al. (2022):

 $^{^{29}}$ See section 3.2.4 for detailed comparison to other monetization approaches.

$$VSL_{t,c} = VSL_{2020,US}^{base} \times \left(\frac{y_{t,c}}{y_{2020,US}}\right)^{\epsilon}$$
(11)

This methodology uses EPA's estimate for the average U.S. VSL in 2020, VSL_{2020,US}, which is \$10.05 million, and applies this estimate to other countries based on the VSL income elasticity parameter ϵ . EPA (2023a); Rennert et al. (2022) use $\epsilon = 1$, which implies that VSL scales proportionally to income. $\epsilon = 1$ has been presented as a standard estimate for policy analysis (Masterman and Viscusi, 2018; Robinson et al., 2019; Viscusi and Masterman, 2017).

Thus, the full Quasi-Kaldor-Hicks SCC equation can be written as:

$$SCC_{t_0} = \sum_{t=t_0}^{t=T} SDF_t \times \left[\sum_{c=1}^{c=C} (MCC_{t_0,t,c} \times VSL_{t,c} + \text{non-mortality } MD_{t_0,t,c}) \right]$$
(12)

In the main body of the paper, I use $\rho = 0.2\%$, which is consistent with the main specification of EPA (2023a) and Rennert et al. (2022). In the appendix, I show a variety of alternative ρ and η values.

3.2.3 The Income Weighted SCC

Income weighting involves two main steps (Anthoff et al., 2009; Anthoff and Tol, 2010; Anthoff and Emmerling, 2019; Azar and Sterner, 1996; Broome, 2012; Errickson et al., 2021; Fankhauser et al., 1997; Hope, 2008; Kolstad et al., 2014; Mirrlees, 1978; Nordhaus, 2011; Watkiss and Hope, 2011). First, it accounts for diminishing marginal utility across space: it captures that an additional dollar has more value to someone who has a lower income than someone with a higher income. Income weighting uses a utility function to determine the effect of damages on well-being based on an individual's income. All else equal, the more that climate damages fall on low-income relative to high-income people, the higher the well-being loss. Second, income weighting converts these utility-denominated damages back into units of money, which can more easily be used in BCA. It does this by converting utility-denominated damages into units of money as valued by some person with some level of income (who is often represented as a person of average income in some "reference region", which is also sometimes referred to as a "normalization region") (Anthoff et al., 2009; Anthoff and Emmerling, 2019; Bressler and Heal, 2022; Errickson et al., 2021; Nordhaus, 2011; Scovronick et al., 2021). In this study, I often refer to this level of income as the reference point. Using a higher-income reference point increases the SCC by virtue of higher-income people valuing

an incremental dollar less, whereas using a lower-income reference point decreases the SCC by virtue of lower-income people valuing an incremental dollar more. The choice of reference point does not affect projected damages; rather, it changes the units in which these damages are represented. Different reference points do not alter the estimated damages caused by an additional tCO₂ the same way that expressing distances in miles or kilometers does not change the length of a trip (Errickson et al., 2021).

In November 2023, the U.S. Office of Management and Budget updated Circular-A-4—the U.S. government's benefit-cost analysis guidelines—for the first time in 20 years. For the first time, this new guidance explicitly allowed for the use of income weights (OMB, 2023a). Income weights adjust money-denominated benefits and costs by applying the following weight:

$$w_{t,c} = \left(\frac{y_{t,c}}{y_{ref}}\right)^{-\eta} \tag{13}$$

where $y_{t,c}$ is the average income for subgroup c in year t, y_{ref} is the reference point income level, and η is the elasticity of marginal utility.

We can derive this weight in equation 13 by considering a standard isoelastic utility function that uses the income elasticity of marginal utility parameter η (also referred to as the utility curvature parameter):

$$u(y) = \frac{y^{1-\eta}}{1-\eta} \tag{14}$$

Using the standard social welfare function (SWF) that aggregates utilities across a population of N individuals across time and discounted to present value using the pure rate of time preference parameter ρ :

$$W = \sum_{t=t_0}^{t=T} \sum_{i=1}^{N_t} u(y_{t,i}) \frac{1}{(1+\rho)^{t-t_0}}$$
(15)

The utility-denominated SCC, which we can label as SCC-u, is equivalent to the marginal damage caused by a marginal pulse of SCC emissions in time t_0 :

$$SCC-u_{t_0} = \frac{\partial W}{\partial E_0} = \frac{\partial \sum_{t=t_0}^{t=T} \sum_{i=1}^{N_t} u(y_{t,i}) \frac{1}{(1+\rho)^{t-t_0}}}{\partial E_0}$$
(16)

Which is equivalent to:

$$SCC-u_{t_0} = \sum_{t=t_0}^{t=T} \sum_{i=1}^{N_t} \frac{\partial u(y_{t,i})}{\partial E_0} \frac{1}{(1+\rho)^{t-t_0}}$$
(17)

Applying the chain rule:

$$SCC-u_{t_0} = \sum_{t=t_0}^{t=T} \sum_{i=1}^{N_t} \frac{\partial u(y_{t,i})}{\partial y_{t,i}} \frac{\partial y_{t,i}}{\partial E_0} \frac{1}{(1+\rho)^{t-t_0}}$$
(18)

The term $\frac{\partial y_{t,i}}{\partial E_0}$ represents the marginal damage to person i in time t from the emission E in time t_0 , so we can replace that term with $MD_{t_0,t,i}$:

$$SCC-u_{t_0} = \sum_{t=t_0}^{t=T} \sum_{i=1}^{N_t} \frac{\partial u(y_{t,i})}{\partial y_{t,i}} \frac{1}{(1+\rho)^{t-t_0}} MD_{t_0,t,i}$$
(19)

No integrated assessment models used to calculate the SCC are able to project damages at the level of individuals, so we can instead represent damages at the aggregated country level c:

$$SCC-u_{t_0} = \sum_{t=t_0}^{t=T} \sum_{c=1}^{c=C} \frac{\partial u(y_{t,c})}{\partial y_{t,c}} \frac{1}{(1+\rho)^{t-t_0}} MD_{t_0,t,c}$$
(20)

where $y_{t,c}$ represents the average income of region c at time t. This SCC in equation 20 is in units of utility. Indeed, this can be used directly in BCA, but this tends to be inconvenient because other benefits and costs are usually measured in dollars (Anthoff et al., 2009). For practical application in BCA, this utility-denominated SCC must be converted into dollars. When income weighting, this is done with the following inverse marginal utility weight:

$$\mu_{ref} = \frac{1}{\frac{\partial u(y_{ref})}{\partial y_{ref}}}.$$
(21)

 μ_{ref} represents the inverse marginal utility of some person with the reference point income level y_{ref} . Thus, this factor converts the SCC from units of utility into units of money as it is valued by someone with the reference point level of income:

$$SCC_{t_0} = \sum_{t=t_0}^{t=T} \sum_{c=1}^{c=C} \mu_{ref} \frac{\partial u(y_{t,c})}{\partial y_{t,c}} \frac{1}{(1+\rho)^{t-t_0}} MD_{t_0,t,c} = \sum_{t=t_0}^{t=T} \sum_{c=1}^{c=C} \frac{\frac{\partial u(y_{t,c})}{\partial y_{t,c}}}{\frac{\partial u(y_{ref})}{\partial y_{ref}}} \frac{1}{(1+\rho)^{t-t_0}} MD_{t_0,t,c}$$
(22)

Now, the marginal damage in time t in region c $(MD_{t_0,t,c})$ is multiplied by the ratio of the marginal utility for an average person in that region at that time $(\frac{\partial u(y_{t,c})}{\partial y_{t,c}})$ and the marginal utility at the reference point income level $(\frac{\partial u(y_{ref})}{\partial y_{ref}})$. Because of diminishing marginal utility, marginal utility for people at lower income levels is higher (i.e., a dollar is more valuable to someone with lower income), whereas the marginal utility for those at higher income levels is lower (i.e., a dollar is less valuable to someone with higher income). Thus, equation 22 shows mathematically how income weighting upweights marginal damages in lower-income regions (because $\frac{\partial u(y_{t,c})}{\partial y_{t,c}}$ in the numerator is larger) and downweights marginal damages in higher-income regions (because $\frac{\partial u(y_{t,c})}{\partial y_{t,c}}$ is smaller).

Furthermore, equation 22 illustrates the importance of the reference point income level. When one chooses a higher reference point income level (e.g., average income in the U.S.), this increases the SCC because $\frac{\partial u(y_{ref})}{\partial y_{ref}}$ (in the denominator) is lower. Whereas if one chooses a lower reference point income level (e.g., average income in India), this decreases the SCC because $\frac{\partial u(y_{ref})}{\partial y_{ref}}$ is higher. This mathematically illustrates the intuition that using a higher-income reference region increases the SCC just by virtue of people in that region valuing money less. Whereas using a lower-income reference region decreases the SCC just by virtue of people in that region valuing money more.

One reason for choosing a particular reference point is based on which region will bear the cost of emissions reductions (Anthoff et al., 2009). For instance, if emissions reductions are taking place in the U.S., using U.S. average income as the reference point converts this value into units of money as it is valued by a typical individual in the U.S. For a given income-weighted benefit-cost analysis, using the same reference point for all benefits and costs—both climate and non-climate—ensures that all these benefits and costs are represented in the same units. Thus, conclusions based on net benefits in an income-weighted BCA will be the same, regardless of reference point (Anthoff et al., 2009).

We can simplify equation 22 further by assuming isoelastic utility (plugging in equation 14):

$$SCC_{t_0} = \sum_{t=t_0}^{t=T} \sum_{c=1}^{c=C} \frac{y_{t,c}^{-\eta}}{y_{ref}^{-\eta}} \frac{1}{(1+\rho)^{t-t_0}} MD_{t_0,t,c} = \sum_{t=t_0}^{t=T} \sum_{c=1}^{c=C} \left(\frac{y_{t,c}}{y_{ref}}\right)^{-\eta} \frac{1}{(1+\rho)^{t-t_0}} MD_{t_0,t,c}$$
(23)

We can see that the term is $\left(\frac{y_{t,c}}{y_{ref}}\right)^{-\eta}$ is exactly equal to the weight given in equation 13.

Now, we can split the marginal damage term from equation 23 into mortality and non-mortality components as we did for Quasi-Kaldor-Hicks in equation 12:

$$SCC_{t_0} = \sum_{t=t_0}^{t=T} \sum_{c=1}^{c=C} \left(\frac{y_{t,c}}{y_{ref}}\right)^{-\eta} \frac{1}{(1+\rho)^{t-t_0}} \left[MCC_{t_0,t,c} \times VSL_{t,c} + \text{non-mortality } MD_{t_0,t,c}\right]$$
(24)

And we can plug in equation 11 for $VSL_{t,c}$:

$$SCC_{t_0} = \sum_{t=t_0}^{t=T} \sum_{c=1}^{c=C} \left(\frac{y_{t,c}}{y_{ref}}\right)^{-\eta} \frac{1}{(1+\rho)^{t-t_0}} \left[MCC_{t_0,t,c} \times VSL_{2020,US}^{\text{base}} \left(\frac{y_{t,c}}{y_{2020,US}}\right)^{\epsilon} + \text{non-mortality } MD_{t_0,t,c}\right]$$
(25)

This allows us to split out the income-weighted SCC into two separate mortality and non-mortality components:

Mortality Partial
$$SCC_{t_0} = \sum_{t=t_0}^{t=T} \sum_{c=1}^{c=C} \frac{1}{(1+\rho)^{t-t_0}} \left(\frac{y_{t,c}}{y_{ref}}\right)^{-\eta} \left(\frac{y_{t,c}}{y_{2020,US}}\right)^{\epsilon} VSL_{2020,US}^{\text{base}} \times MCC_{t_0,t,c}$$
(26)

Non-Mortality Partial
$$SCC_{t_0} = \sum_{t=t_0}^{t=T} \sum_{c=1}^{c=C} \frac{1}{(1+\rho)^{t-t_0}} \left(\frac{y_{t,c}}{y_{ref}}\right)^{-\eta} \times \text{non-mortality } MD_{t_0,t,c}$$
 (27)

Equation 26 provides some intuition for how income-weighting treats mortality impacts. The VSL term $\left(\frac{y_{t,c}}{y_{2020,US}}\right)^{\epsilon} \times \text{VSL}_{2020,US}^{\text{base}}$ uses benefits transfer to scale the baseline 2020 U.S. VSL (recall from above was \$10.05 million) based on the VSL income elasticity ϵ . This captures that as people become richer, they are willing to pay more to avoid mortality risk. However, the income weighting term $\left(\frac{y_{t,c}}{y_{ref}}\right)^{-\eta}$ adjusts this willingness-to-pay-based VSL term into dollars that are adjusted for diminishing marginal utility. The interpretation of this is that poorer people are willing to pay less to avoid mortality risk not necessarily because they value their lives less, but because they value marginal dollars more (Bressler and Heal, 2022; Broome, 2012; Kolstad et al., 2014).

What does this imply in terms of the value that is placed on lives under income weighting? It depends on the relative values of the VSL income elasticity ϵ and the utility curvature η . In the case when $\epsilon = \eta$, this implies that the VSL-income scaling and utility-income scaling exactly offset each other. In this case, all lives across space are valued equally at the 2020 U.S. VSL VSL $_{2020,US}^{\text{base}}$ scaled by the constant $\left(\frac{y_{ref}}{y_{2020,US}}\right)^{\eta}$, and are only discounted in the future by the pure rate of time preference ρ :

Mortality Partial
$$SCC_{t_0} = \sum_{t=t_0}^{t=T} \sum_{c=1}^{c=C} \frac{1}{(1+\rho)^{t-t_0}} \left(\frac{y_{ref}}{y_{2020,US}}\right)^{\eta} VSL_{2020,US}^{\text{base}} \times MCC_{t_0,t,c}$$
 (28)

In fact, because $\epsilon = \eta$ in this case, the term $\left(\frac{y_{ref}}{y_{2020,US}}\right)^{\eta} \times \text{VSL}_{2020,US}^{\text{base}}$ is just rewriting the VSL benefits transfer equation 11 for calculating the VSL at the reference income level: VSL_{ref}. So we can rewrite equation 28 as:

Mortality Partial
$$SCC_{t_0} = \sum_{t=t_0}^{t=T} \sum_{c=1}^{c=C} \frac{1}{(1+\rho)^{t-t_0}} VSL_{ref} \times MCC_{t_0,t,c}$$
 (29)

3.2.4 Comparing the Quasi-Kaldor-Hicks and the Income-Weighted SCC

We can compare the expression for the income-weighted SCC in equation 4. We can write out the full expression for the Quasi-Kaldor-Hicks SCC from equation 4, including the Ramsey-like SDF, which is defined as (Bressler et al., nd; EPA, 2023a; Rennert et al., 2022):

$$SDF_{t} = \frac{1}{(1+\rho)^{t-t_{0}}} \left(\frac{y_{t,avg}}{y_{t_{0},avg}} \right)^{-\eta}$$
(30)

where $y_{t,avg}$ is world average per capita income in year t and ρ is the pure rate of time preference. Plugging this into equation 4:

$$SCC_{t_0} = \sum_{t=t_0}^{t=T} \frac{1}{(1+\rho)^{t-t_0}} \left(\frac{y_{t,avg}}{y_{t_0,avg}}\right)^{-\eta} \sum_{c=1}^{c=C} MD_{t_0,t,c}$$
(31)

Since the term $\left(\frac{1}{y_{t_0,avg}}\right)^{-\eta}$ is a constant—it is simply world average per capita income in the year of the pulse—we can move it to the front of the expression. Since $\mathrm{MD}_{t_0,t,c}$ is just the sum of marginal damage across all regions in time t, we can rewrite this expression as:

$$SCC_{t_0} = (y_{t_0,avg})^{\eta} \sum_{t=t_0}^{t=T} \frac{1}{(1+\rho)^{t-t_0}} (y_{t,avg})^{-\eta} \sum_{c=1}^{c=C} MD_{t_0,t,c}$$
(32)

Now consider a special case of the income-weighted SCC (equation 23) where global average income in 2020 is the reference point income level (the reference point income level that we used in multiple results in the main text):

$$SCC_{t_0} = (y_{t_0,avg})^{\eta} \sum_{t=t_0}^{t=T} \frac{1}{(1+\rho)^{t-t_0}} \sum_{c=1}^{c=C} (y_{t,c})^{-\eta} M D_{t_0,t,c}$$
(33)

To summarize, equation 32 is the Quasi-Kaldor-Hicks SCC, and equation 33 is the incomeweighted SCC (using global average income as the reference point, which is the most directly comparable to the SCC before income weighting). The only difference between these two equations is that, after income weighting (equation 33), the marginal damage in each region in each time period is multiplied by the marginal utility in that region at that time, $(y_{t,c})^{-\eta}$. Whereas before income weighting (equation 32), marginal damages are first aggregated across all regions in each time period and then multiplied by the global average marginal utility $(y_{t,avg})^{-\eta}$. Thus, the income-weighted SCC (equation 33) accounts for differences in marginal utility across both time and across regions. Whereas the SCC before income weighting (equation 32) does not account for differences in marginal utility across regions, it does account for global average differences in marginal utility across time.

We can see quantitatively the differential impact of the utility curvature parameter, η , in the Quasi-Kaldor-Hicks approach to the SCC versus the income-weighted approach in Fig. ??, which holds all parts of the model fixed except η . A higher η indicates a more curved utility function. This implies that the marginal utility gained from a marginal dollar declines more rapidly compared to a lower η value. Before income weighting, η affects the SCC in two ways (EPA, 2023a; Rennert et al., 2022). First, it accounts for diminishing marginal utility across time (see Methods section for details). A higher η tends to place less weight on future damages because a marginal dollar of damages to comparatively higher-income people in the future will be considered less harmful than a marginal dollar of damages to comparatively lower-income people today. Second, it accounts for risk aversion across uncertain potential future states of the world. A higher η implies higher risk aversion. Income weighting adds a third role for η : it accounts for diminishing marginal utility across space. That is, a higher η places more weight on damages in low-income locations (Broome, 2012; Kolstad et al., 2014).

3.2.5 U.S. Status Quo SCC

The U.S. Status quo approach takes the same approach as Quasi-Kaldor-Hicks to all non-mortality benefits and costs— representing damages in units of money unadjusted for diminishing marginal utility, but then it places a special carve-out for mortality damages, where all deaths are measured based on the population average willingness to pay as opposed to the individual willingness to pay. In the case of the SCC, this means that all lives are valued the same at the global average willingness to pay.

Mathematically, we can take the Kaldor-Hicks SCC (equation 12), but then monetize each death around the world at the same uniform VSL based on the global population average willingness to pay in each time period t, which I label as $VSL_{t,avq}$:

$$SCC_{t_0} = \sum_{t=t_0}^{t=T} SDF_t \left[\sum_{c=1}^{c=C} (MCC_{t_0,t,c} \times VSL_{t,avg} + \text{non-mortality } MD_{t_0,t,c}) \right]$$
(34)

This represents the general equation for the U.S. Status quo SCC. At every point in time, every life around the world is valued at the same $VSL_{t,avg}$. If global average income increases in the future, then $VSL_{t,avg}$ also increases in the future because VSL has a positive income elasticity. But this is counteracted by the stochastic Ramsey-like discount factor SDF_t , which accounts for diminishing marginal utility across time by discounting richer periods at a higher

rate, and which also discounts all future periods at the pure rate of time preference, ρ , as shown in equation 35 below. The exact present value of future lives depends on the relative values of the VSL income elasticity ϵ , the utility curvature η , and the pure rate of time preference ρ , as shown in equation 35.

Plugging in equation 30 for SDF_t and equation 11 for VSL_{t,avg}:

$$SCC_{t_0} = \sum_{t=t_0}^{t=T} \sum_{c=1}^{c=C} \frac{1}{(1+\rho)^{t-t_0}} \left(\frac{y_{t,avg}}{y_{t_0,avg}} \right)^{-\eta} \left[MCC_{t_0,t,c} \times VSL_{2020,US}^{\text{base}} \left(\frac{y_{t,avg}}{y_{2020,US}} \right)^{\epsilon} + \text{non-mortality } MD_{t_0,t,c} \right]$$
(35)

$$SCC_{t_0} = \sum_{t=t_0}^{t=T} \sum_{c=1}^{c=C} \frac{1}{(1+\rho)^{t-t_0}} \left(\frac{y_{t,avg}}{y_{t_0,c}} \right)^{-\eta} \left[MCC_{t_0,t,c} \times VSL_{2020,US}^{\text{base}} \left(\frac{y_{t,avg}}{y_{2020,US}} \right)^{\epsilon} + \text{non-mortality } MD_{t_0,t,c} \right]$$
(36)

This allows us to split out the U.S. status quo SCC into two separate mortality and non-mortality components:

Mortality Partial
$$SCC_{t_0} = \sum_{t=t_0}^{t=T} \sum_{c=1}^{c=C} \frac{1}{(1+\rho)^{t-t_0}} \left(\frac{y_{t,avg}}{y_{t_0,avg}}\right)^{-\eta} \left(\frac{y_{t,avg}}{y_{2020,US}}\right)^{\epsilon} VSL_{2020,US}^{\text{base}} \times MCC_{t_0,t,c}$$
(37)

Non-Mortality Partial
$$SCC_{t_0} = \sum_{t=t_0}^{t=T} \sum_{c=1}^{c=C} \frac{1}{(1+\rho)^{t-t_0}} \left(\frac{y_{t,avg}}{y_{t_0,avg}}\right)^{-\eta} \times \text{non-mortality } MD_{t_0,t,c}$$
(38)

In fact, the U.S. status quo mortality partial SCC is equivalent to the income-weighted mortality partial SCC that uses global average income as the reference point when the utility curvature, η , is equivalent to the income elasticity of the VSL, ϵ . We can see this by taking equation 37 and assuming that $\eta = \epsilon$. This allows us to simplify equation 37 to:

Mortality Partial
$$SCC_{t_0} = \sum_{t=t_0}^{t=T} \sum_{c=1}^{c=C} \frac{1}{(1+\rho)^{t-t_0}} \left(\frac{y_{t_0,avg}}{y_{2020,US}}\right)^{\eta} VSL_{2020,US}^{\text{base}} \times MCC_{t_0,t,c}$$
 (39)

In fact, because $\epsilon = \eta$ in this case, the term $\left(\frac{y_{t_0,avg}}{y_{2020,US}}\right)^{\epsilon} \times \text{VSL}_{2020,US}^{\text{base}}$ is just rewriting the VSL benefits transfer equation 11 for calculating the global average VSL at time of the pulse t_0 : VSL_{t_0,avg}. So we can rewrite equation 28 as:

Mortality Partial
$$SCC_{t_0} = \sum_{t=t_0}^{t=T} \sum_{c=1}^{c=C} \frac{1}{(1+\rho)^{t-t_0}} VSL_{t_0,avg} \times MCC_{t_0,t,c}$$
 (40)

This is identical to the income-weighted partial SCC when current global average income is used as the reference income level and $\epsilon = \eta$ shown in equation 29. QED.

Furthermore, I prove this numerically, as shown in table 4. For the rows where $\eta = 1$, which is the same value as the income elasticity of VSL ($\epsilon = 1$), we can see that the mortality partial SCC yields the exact same value for the U.S. Status Quo approach and Income Weighting approach using global average income as the reference region.

3.2.6 The Prioritarian SCC

Like income-weighting, prioritarian-weighting uses a utility function to estimate the effect of damages on wellbeing. But while income-weighting values everyone's wellbeing the same, prioritarian-weighting places extra weight on the wellbeing of the worse off (i.e., those with lower incomes). Prioritarian-weighting has support in the academic literature (Adler et al., 2017; Adler and Treich, 2015; Ferranna and Fleurbaey, 2020), but it is not yet used as far as I am aware in benefit-cost analysis for government policymaking in the U.S. or other countries.

To calculate the prioritarian SCC, I follow the approach used in Adler et al. (2017). Like the income-weighted social welfare function (SWF) defined in equation 15, the Prioritarian SWF aggregates utilities across a population of N individuals, but it applies an additional concave function g(u()) that transforms the wellbeing value determined by the utility function u() into Prioritarian-transformed wellbeing that places extra weight on those with lower wellbeing levels. This g(u()) function could, in principle, take a number of forms, so I focus here on the central parameter values given in Adler et al. (2017), which uses a log function for g(u()). The Prioritarian SWF is defined as:

$$W = \sum_{t=t_0}^{t=T} \sum_{i=1}^{N_t} \log\left[u^*(y_{t,i})\right] \frac{1}{(1+\rho)^{t-t_0}}$$
(41)

Where $u^*(y_{t,i}) = u(y_{t,i}) - u(y^{zero})$ is the wellbeing of individual i in time t rescaled by the utility at subsistence level, which is determined by the World Bank's extreme poverty level

(Bank, 2024).

The prioritarian welfare-denominated SCC, which we can label as SCC-w, is equivalent to the marginal damage caused by a marginal pulse of SCC emissions in time t_0 :

$$SCC-w_{t_0} = \sum_{t=t_0}^{t=T} \sum_{i=1}^{N_t} \frac{\partial log \left[u^*(y_{t,i}) \right]}{\partial E_0} \frac{1}{(1+\rho)^{t-t_0}}$$
(42)

Applying the chain rule:

$$SCC-w_{t_0} = \sum_{t=t_0}^{t=T} \sum_{i=1}^{N_t} \left(\frac{1}{u^*(y_{t,i})} \frac{\partial u^*(y_{t,i})}{\partial y_{t,i}} \frac{\partial y_{t,i}}{\partial E_0} \right) \frac{1}{(1+\rho)^{t-t_0}}$$
(43)

As in the income-weighting derivation, we can notice that $\frac{\partial y_{t,i}}{\partial E_0}$ represents the marginal damage to person i in time t from the emission E in time t_0 , so we can replace that term with $MD_{t_0,t,i}$. And, since no integrated assessment models used to calculate the SCC are able to project damages at the level of individuals, we can instead represent damages at the aggregated country level c:

$$SCC-w_{t_0} = \sum_{t=t_0}^{t=T} \sum_{c=1}^{c=C} \left(\frac{1}{u^*(y_{t,c})} \frac{\partial u^*(y_{t,c})}{\partial y_{t,c}} MD_{t_0,t,c} \right) \frac{1}{(1+\rho)^{t-t_0}}$$
(44)

Equation 44 is in units of prioritarian social welfare, which can be used directly in BCA, although this tends to be inconvenient because other benefits and costs are usually measured in dollars. To convert this into dollars, we apply the following inverse social welfare function weight:

$$\frac{1}{\frac{\partial W}{\partial y_{ref}}}$$

Where $\frac{\partial W}{\partial y_{ref}}$ represents the increase in social welfare per dollar added to the consumption of some person with the reference point income level y_{ref} .

We can then plug this into equation 44 to yield the prioritarian-weighted SCC in units of money:

$$SCC-w_{t_0} = \frac{\sum_{t=t_0}^{t=T} \sum_{c=1}^{c=C} \left(\frac{1}{u^*(y_{t,c})} \frac{\partial u^*(y_{t,c})}{\partial y_{t,c}} M D_{t_0,t,c} \right) \frac{1}{(1+\rho)^{t-t_0}}}{\frac{\partial W}{\partial y_{ref}}}$$
(45)

This equation is the analog of equation 3 in Adler et al. (2017) in this setting.

3.3 Results

Table 1 shows the SCC across the four monetization approaches. As these results show, the value of the SCC varies by a factor of 50 simply by making different choices around valuing lives and livelihoods. Importantly, the physical climate damages are the exact same across each of these four approaches: the underlying mortality cost of carbon and the physical damages in the other sectors are the exact same. The only difference is how these approaches value the lives of people in poorer versus richer countries and how they value a dollar of market damages to people in poorer versus richer countries. Model parameters, including the pure rate of time preference (ρ) and utility curvature (η), are held constant across all of these calculations to ensure maximum comparability. I use $\eta = 1.4$, which follows OMB (2023a)'s recent guidance³⁰, and I use $\rho = 0.2\%$, which follows the central specification in (EPA, 2023a). SCCs across a range of η and ρ values and across the four monetization approaches are shown below in table 3.

 $^{^{30}}$ OMB conducted an in-depth review of the literature on η as part of its update to Circular A-4 (see section 9.d of OMB (2023b) for details). This review extended Acland and Greenberg's 2023 review Acland and Greenberg (2023). Acland and Greenberg tentatively concluded using $\eta=1.6$ with lower and upper bound sensitivity testing at 1.2 and 1.6. OMB determined that $\eta=1.4$ is a reasonable estimate for income weighting in regulatory analysis. I thus use income weighting with $\eta=1.4$ in the main specifications in the main text. Likewise, the U.K. Green Book also suggests constructing weights based on income (what it calls "distributional weights") using an income elasticity of marginal utility of $\eta=1.3$ (HM Treasury, 2022). The German government uses $\eta=1$ to calculate the SCC.

Table 1

	Quasi-Kaldor Hicks	U.S. Status Quo	Income Weighting (U.S.)	Prioritarian Weighting (U.S.)	
2025 SCC [2.5th-97.5th Percentile]	\$237 [-\$93, \$861]	\$380 [-\$8, \$1,302]	\$3,567 [\$172, \$11,640]	\$11,839 [-\$1,220, \$16,870]	
SCC Breakdown by Impact Category					
Mortality	\$145	\$287	\$2,723	\$10,880	
Agriculture	\$81	\$81	\$736	\$754	
Energy	\$8	\$8	\$85	\$181	
Sea Level Rise	\$4	\$4	\$23	\$25	

Table 1 | Social Cost of Carbon Sensitivity to Choices Around Valuing Lives and Livelihoods. The table shows the Social Cost of Carbon (SCC) across the four major monetization approaches. The central SCCs are the mean SCC value across 10,000 draws in a Monte Carlo simulation, which captures uncertainty in socioeconomic and emissions scenarios (RFF-SPs), uncertainty in climate (FaIR v1.6.2), and mortality damage function uncertainty.

Table 2: Social Cost of Carbon Sensitivity to Discounting

			Social Cost o	f Carbon
Specification	Pure Rate of Time Preference (ρ)	Utility Curvature (η)	Quasi-Kaldor Hicks	U.S. Status Quo
${\text{High } \rho \text{ High } \eta}$	2.00%	2.00	\$55	\$88
DICE-2007	1.50%	2.00	\$72	\$114
DICE-2016	1.50%	1.45	\$81	\$134
DICE-2023	1.00%	1.50	\$111	\$180
EPA 2023 2.5%	0.46%	1.42	\$179	\$288
Main Specification	0.20%	1.40	\$237	\$380
EPA 2023 2%	0.20%	1.24	\$252	\$411
Stern Discounting	0.10%	1.00	\$317	\$536
EPA 2023 1.5%	0.01%	1.02	\$350	\$590
Low ρ Low η	0.00%	1.00	\$357	\$603

Table 2 shows the SCCs sensitivity to discounting. Each row varies the ρ and η parameters, which, together with the growth rate, determine the Ramsey-like stochastic discount factor as discussed above in equations 30 and 35. This table focuses just on the two monetization approaches—Quasi-Kaldor-Hicks and U.S. Status Quo—that account for diminishing marginal across time, but not across space. In these approaches, η affects the SCC in two ways. First, a higher η tends to place less weight on future damages because a marginal dollar of damages to comparatively higher-income people in the future will be considered less harmful than a marginal dollar of damages to comparatively lower-income people today. Second, it accounts for risk aversion across uncertain potential future states of the world. A higher η implies higher risk aversion. Thus, as table 2 shows, lower η values and lower ρ values tend to lead

to a lower SCC.

As past literature has pointed out and as table 2 shows, the SCC is indeed quite sensitive to these discount rate parameters. In 2007, Nicholas Stern and William Nordhaus had a spirited and notable debate about what the correct SCC should be, which focused on the values that should be chosen for these discounting parameters. Nicholas Stern argued for a lower discount rate, which included a pure rate of time preference of 0.1% and utility curvature of 1. Whereas William Nordhaus argued for a higher discount rate, which included a pure rate of time preference of 1.5% and utility curvature of 2. As table 2 shows, this leads to a 4.4x difference in the SCC in my model when taking the Quasi-Kaldor-Hicks approach to monetization (\$72 for Nordhaus's preferred discounting approach in 2007 vs. \$317 for Stern's preferred approach to discounting) and a 4.7x difference when taking the U.S. Status Quo approach to monetization (\$114 for Nordhaus's preferred discounting approach in 2007 vs. \$536 for Stern's preferred approach to discounting). Importantly, this debate took place in 2007 in a higher interest rate environment. Nordhaus, who prefers to take a descriptive approach to discounting that aligns the money discount rate with market interest rates, has since lowered his discount rate parameters in his DICE model to $\eta = 1.5$ and $\rho = 1\%$. This now leads to less disagreement with Stern: DICE-2023 discounting leads to a 2.9x higher SCC than Stern discounting under Quasi-Kaldor-Hicks (\$111 vs. \$317) and to a 3.0x higher SCC under U.S. Status Quo (\$180 vs. \$536). The crucial point is that these 3-5x differences in the SCC across discounting parameters are quite small compared to the 50x difference due to different approaches to valuing lives and livelihoods shown in table 1. This underscores the importance of choices around valuing lives and livelihoods.

Table 3: Social Cost of Carbon Sensitivity Across Monetization Approaches and η and ρ Specification

					Social C	ost of Carbon		
Specification	Pure Rate of Time Preference (ρ)	Utility Curvature (η)	Quasi- Kaldor Hicks	U.S. Status Quo	Income Weighting (Global)	Prioritarian Weighting (Global)	Income Weighting (US)	Prioritarian Weighting (US)
High ρ High η	2.00%	2.00	\$55	\$88	\$279	\$621	\$3,852	\$7,793
DICE-2007	1.50%	2.00	\$72	\$114	\$358	\$1,034	\$4,934	\$12,638
DICE-2016	1.50%	1.45	\$81	\$134	\$215	\$514	\$1,427	\$3,202
DICE-2023	1.00%	1.50	\$111	\$180	\$303	\$913	\$2,154	\$5,945
EPA 2023 2.5%	0.46%	1.42	\$179	\$288	\$446	\$1,548	\$2,852	\$9,029
Main Specification	0.20%	1.40	\$237	\$380	\$574	\$2,095	\$3,567	\$11,839
EPA 2023 2%	0.20%	1.24	\$252	\$411	\$536	\$1,759	\$2,712	\$8,232
Stern Discounting	0.10%	1.00	\$317	\$536	\$565	\$1,573	\$2,074	\$5,464
EPA 2023 1.5%	0.01%	1.02	\$350	\$590	\$630	\$1,788	\$2,360	\$6,319
Low ρ Low η	0.00%	1.00	\$357	\$603	\$635	\$1,786	\$2,332	\$6,195

Table 3 further emphasizes this point. Compared to Quasi-Kaldor-Hicks and U.S. Status Quo, Income weighting and Prioritarian weighting add a third role for η : it accounts for

diminishing marginal utility across space. That is, a higher η places more weight on damages in low-income locations. The difference in the SCC across columns shows how sensitive the SCC is to valuing lives and livelihoods for a given η and ρ combination. Ironically, the η and ρ combination that leads to the highest income-weighted and highest prioritarian-weighted SCC when the U.S. is used as the reference region is Nordhaus's DICE-2007 preferred approach ($\eta = 2$ and $\rho = 1.5\%$) because it has a comparatively high utility curvature (η). Higher η values in income weighting and prioritarian weighting place more weight on damages in poorer locations. This is counteracted to some extent by η 's role in placing less weight on comparatively better-off future generations, but as we can see, the role of intragenerational diminishing marginal utility dominates the role of intergenerational diminishing marginal utility in this setting.

As discussed above, the choice of valuing lives and livelihoods leads to a 50x difference in the SCC in this study's main η and ρ specification ($\eta = 1.4$ and $\rho = 0.2\%$). But under higher η values, this difference is even wider. For instance, under the DICE-2007 parameter values, the SCC varies by a factor of 175 (\$72 under Quasi-Kaldor-Hicks to \$12,698 under Prioritarian Weighting with the U.S. reference region). Indeed, as table 3 shows, the choice of reference region in income and prioritarian weighting is itself also an important choice that the modeler must make around valuing lives and livelihoods. There are reasonable arguments for multiple potential choices of reference region, over which reasonable experts may disagree. E.g., an analyst conducting benefit cost analysis (BCA) in the U.S. may use U.S. average income as the reference point because they want their climate benefits and costs to be in units of money as valued by a typical individual in the U.S. This ensures that these climate benefits and costs are in the same units as the rest of the non-climate domestic benefits and costs in their analysis. On the other hand, the analyst may consider that climate change is a global collective action problem. From this perspective, the analyst may want to measure the SCC in units of money as valued by someone with global average income. Furthermore, they may want to align the SCC value used in U.S. BCA with SCC values that are used in BCA in other countries with different income levels. And, as discussed in section 3.2, using global average income as the reference point is more directly comparable mathematically to the Quasi-Kaldor-Hicks and U.S. Status Quo approaches. In any case, it is useful to know what the SCC is under multiple reference regions, and how sensitive the SCC is to the choice of reference region.

Table 4: The Partial Mortality Social Cost of Carbon Sensitivity Across Monetization Approaches and η and ρ Specification

					Social C	ost of Carbon		
Specification	Pure Rate of Time Preference (ρ)	Utility Curvature (η)	Quasi- Kaldor Hicks	U.S. Status Quo	Income Weighting (Global)	Prioritarian Weighting (Global)	Income Weighting (US)	Prioritarian Weighting (US)
High ρ High η	2.00%	2.00	\$38	\$72	\$237	\$571	\$3,269	\$7,109
DICE-2007	1.50%	2.00	\$49	\$92	\$303	\$965	\$4,170	\$11,709
DICE-2016	1.50%	1.45	\$53	\$106	\$168	\$460	\$1,120	\$2,846
DICE-2023	1.00%	1.50	\$71	\$140	\$238	\$835	\$1,691	\$5,398
EPA 2023 2.5%	0.46%	1.42	\$111	\$220	\$343	\$1,426	\$2,193	\$8,265
Main Specification	0.20%	1.40	\$145	\$287	\$438	\$1,936	\$2,724	\$10,880
EPA 2023 2%	0.20%	1.24	\$147	\$306	\$394	\$1,602	\$1,998	\$7,455
Stern Discounting	0.10%	1.00	\$162	\$381	\$381	\$1,398	\$1,399	\$4,827
EPA 2023 1.5%	0.01%	1.02	\$179	\$419	\$426	\$1,593	\$1,597	\$5,598
Low ρ Low η	0.00%	1.00	\$180	\$427	\$427	\$1,588	\$1,565	\$5,479

Table 4 is similar to table 3 except that it only shows the partial mortality social cost of carbon. I.e., it shows only the portion of the SCC that comes from mortality. It leaves out climate damages in other sectors in the model (agriculture, energy, and sea level rise). Table 5 shows the percentage of the SCC that comes from mortality across η and ρ combinations and across approaches to valuing lives and livelihoods. Indeed, as these tables show, mortality damages are the majority of damages in the SCC across all η and ρ combinations and across all approaches to valuing lives and livelihoods. Even when lives are valued proportionally to income without any other adjustments under the Quasi-Kaldor-Hicks approach that was favored by EPA (2023a), the majority of climate damages still comes from premature mortality across all η and ρ combinations. In addition, the percentage of the SCC that comes from premature mortality tends to be higher under higher ρ and higher η values. This is because mortality damages tend to be more disproportionally concentrated in poorer populations in the near term compared to other climate damages.

Table 5: The Percentage of the SCC that Comes from Mortality

					Social C	ost of Carbon		
Specification	Pure Rate of Time Preference (ρ)	Utility Curvature (η)	Quasi- Kaldor Hicks	U.S. Status Quo	Income Weighting (Global)	Prioritarian Weighting (Global)	Income Weighting (US)	Prioritarian Weighting (US)
High ρ High η	2.00%	2.00	69%	82%	85%	92%	85%	91%
DICE-2007	1.50%	2.00	69%	80%	85%	93%	85%	93%
DICE-2016	1.50%	1.45	65%	79%	78%	90%	78%	89%
DICE-2023	1.00%	1.50	64%	78%	78%	91%	78%	91%
EPA 2023 2.5%	0.46%	1.42	62%	76%	77%	92%	77%	92%
Main Specification	0.20%	1.40	61%	76%	76%	92%	76%	92%
EPA 2023 2%	0.20%	1.24	58%	74%	74%	91%	74%	91%
Stern Discounting	0.10%	1.00	51%	71%	68%	89%	67%	88%
EPA 2023 1.5%	0.01%	1.02	51%	71%	68%	89%	68%	89%
Low ρ Low η	0.00%	1.00	50%	71%	67%	89%	67%	88%

4 The Benefits of the Inflation Reduction Act

Table 6 uses the MCC estimates from section 2 to estimate how many lives the 2022 Inflation Reduction Act (IRA) is projected to save just from reducing greenhouse gas emissions.³¹ The table shows the projected reduction in emissions every year from 2025-2050 versus a counterfactual without the IRA using estimates from Bistline et al. (2023).³² For instance, the IRA is projected to save 188 megatons of CO₂-equivalent emissions in 2025. The MCC estimate that accounts for additional heat-vulnerability reduction from rising incomes (shown in the third column) estimates that this will save 25,691 lives in expectation from 2025-2300. The MCC estimate that assumes that future populations will be as vulnerable to heat as populations today (fifth column) estimates that this will save 73,878 lives from 2025-2300.³³ When aggregating across all of the IRA's expected emissions reductions from 2025-2050, I find that the IRA is expected to save 2.8 million lives when accounting for additional heat-vulnerability reduction from rising incomes, and 8.6 million lives when we assume that future populations will be as vulnerable to heat as current populations.

If one prefers to aggregate deaths over a shorter period than to 2300, the underlying data from figure 3 can be used. E.g., as discussed above and as shown in that figure, half of the lives saved in the MCC that assumes future heat-vulnerability reduction will be saved within 100 years of the pulse of the emissions. I.e., if we only were to include the estimate lives that were saved within 100 years of the reduction in emissions, the IRA saves approximately 1.4 million lives.³⁴ If one wishes to understand how those saved lives are broken down spatially, the D-MCC estimates shown in table A.1 can be leveraged.³⁵

³¹Note that these calculations exclude other potential lifesaving benefits of the IRA, such as reductions in local air pollution. These calculations simply apply the MCC estimates from this paper, which, as discussed above, only capture the direct impact of climate change on temperature-related mortality.

³²Bistline et al. (2023) gives data in 5-year time-steps; years between the data given in the 5-year time-steps are linearly interpolated.

³³Note that for this study, I've calculated the MCC in 5-year increments (2025, 2030, 2035, 2040, 2045, and 2050), and in the chart I've assigned the MCC value for each year based on the closest year. This is because it takes significant time and computing power to generate each MCC estimate given that I need to run 10,000 monte carlo simulations that sample across all of the uncertainties in the model discussed above to estimate the expected MCC in each year. In future iterations of the study, I may provide exact-year values for the MCC, but my results suggest that using the 5-year estimates are a fairly close approximation, especially because there is not a large change in the MCC for pulses in different years as shown in table 6

³⁴This estimate assumes that the underlying dynamics MCC dynamics observed for a 2025 as shown in figure 3 stay fairly constant for future emissions pulses. I have run the model with yearly breakdowns for a 2030, 2040, and 2050 pulse, and I have found this to be true in those future years. Due to space limitations, I am not providing the full tables for those 2030, 2040, and 2050 pulse results as I do for a pulse of 2025 emissions.

³⁵I have run D-MCC estimated for emissions pulses in some future years, but due to space limitations, I am not providing the full tables for those results as I do for a 2025 pulse in table A.1. However, the D-MCC

Table 6

		Vulneral	g for Additional Heat- bility Reduction from Rising Incomes	Heat-Vu	ounting for Additional Inerability Reduction n Rising Incomes
Year	Emissions Reduction from IRA (MT CO2-eq)	MCC	Expected Lives Saved from Emissions Reduction	MCC	Expected Lives Saved from Emissions Reduction
2025	188	1.37E-04	25,691	3.93E-04	73,878
2026	285	1.37E-04	39,014	3.93E-04	112,189
2027	383	1.37E-04	52,337	3.93E-04	150,500
2028	480	1.34E-04	64,188	3.90E-04	187,079
2029	577	1.34E-04	77,212	3.90E-04	225,038
2030	675	1.34E-04	90,236	3.90E-04	262,998
2031	727	1.34E-04	97,241	3.90E-04	283,414
2032	779	1.34E-04	104,246	3.90E-04	303,830
2033	832	1.34E-04	111,251	3.86E-04	324,246
2034	884	1.34E-04	118,256	3.86E-04	344,663
2035	937	1.34E-04	125,261	3.86E-04	365,079
2036	957	1.27E-04	121,793	3.86E-04	373,217
2037	978	1.27E-04	124,449	3.86E-04	381,356
2038	999	1.27E-04	127,105	3.83E-04	389,494
2039	1,020	1.27E-04	129,761	3.83E-04	397,633
2040	1,041	1.27E-04	132,417	3.83E-04	405,772
2041	1,037	1.27E-04	131,960	3.83E-04	404,370
2042	1,034	1.27E-04	131,502	3.83E-04	402,969
2043	1,030	1.27E-04	131,045	3.79E-04	$401,\!567$
2044	1,027	1.27E-04	130,588	3.79E-04	400,166
2045	1,023	1.27E-04	130,130	3.79E-04	398,764
2046	1,021	1.20E-04	122,695	3.79E-04	397,815
2047	1,018	1.20E-04	122,402	3.79E-04	396,866
2048	1,016	1.20E-04	122,109	3.75E-04	395,917
2049	1,013	1.20E-04	121,817	3.75E-04	394,968
2050	1,011	1.20E-04	121,524	3.75E-04	394,019
Total	21,972		2,806,234		8,567,807

Table 6 | Using the Mortality Cost of Carbon to Estimate the Lives Saved from the Inflation Reduction Act. The table shows the number of expected lives saved by the 2022 Inflation Reduction Act (IRA). The emissions reductions estimates come from Bistline et al. (2023) and are represented in megatons of carbon dioxide equivalents (MT CO2-eq). The MCC estimates for each year represent the number of expected lives saved by reducing one metric tonne of CO_2 emissions in that year out to the end of the model period in 2300. E.g., the 2025 MCC values here correspond to the 2025 MCC values shown in figures 2 and 3.

spatial distribution does stay fairly constant over time, so I have found that the percentage breakdowns provided in table A.1 do remain fairly stable for emissions pulses in future years. Thus, if one were to apply the D-MCC spatial breakdown of a 2025 pulse to, e.g., a 2040 pulse, this would be a reasonable approximation.

Table 7

		Relevant	SCC (acc	counting for l	Relevant SCC (accounting for heat-vulnerability	Tot	al Benefit from that	Total Benefit from that Year's Emissions Reductions	ctions
			reduction from	from rising i	rising incomes)		(converted to 205	(converted to 2025 net present value)	
	Emissions	Quasi-	U.S.	Income	Prioritarian	Quasi-	U.S.	Income	Prioritarian
Year	Reduction with	Kaldor-	Status	Weighted	Weighted	Kaldor-	$\operatorname*{Status}_{\widehat{}}$	Weighted	Weighted
	IRA (MT CO2-eq)	Hicks	Ono	(U.S.)	(U.S.)	Hicks	Quo	(U.S.)	(U.S.)
2025	188	\$237	\$380	\$3,567	\$11,839	\$44,567,197,556	\$71,324,847,383	\$669,785,764,681	\$8,037,429,176,176
2026	285	\$237	\$380	\$3,567	\$11,839	\$66,351,748,451	\$106,188,600,391	\$997,178,620,399	\$11,966,143,444,785
2027	383	\$237	\$380	\$3,567	\$11,839	\$87,264,868,593	\$139,657,725,312	\$1,311,475,029,731	\$15,737,700,356,771
2028	480	\$255	\$409	\$3,921	\$18,770	\$115,356,493,465	\$185,038,209,214	\$1,773,478,750,481	\$21,281,745,005,775
2029	577	\$255	\$409	\$3,921	\$18,770	\$136,042,369,001	\$218,219,500,099	\$2,091,501,252,684	\$25,098,015,032,209
2030	675	\$255	\$409	\$3,921	\$18,770	\$155,872,682,907	\$250,028,422,710	\$2,396,370,439,249	\$28,756,445,270,983
2031	727	\$255	\$409	\$3,921	\$18,770	\$164,679,236,664	\$264,154,623,044	\$2,531,761,482,132	\$30,381,137,785,587
2032	779	\$255	\$409	\$3,921	\$18,770	\$173,080,507,390	\$277,630,726,933	\$2,660,921,745,772	\$31,931,060,949,265
2033	832	\$267	\$430	\$4,173	\$21,133	\$189,769,730,912	\$305,347,561,891	\$2,962,592,361,713	\$35,551,108,340,551
2034	884	\$267	\$430	\$4,173	\$21,133	\$197,763,276,351	\$318,209,516,213	\$3,087,383,689,329	\$37,048,604,271,948
2035	937	\$267	\$430	\$4,173	\$21,133	\$205,370,389,124	\$330,449,683,953	\$3,206,142,218,876	\$38,473,706,626,512
2036	957	\$267	\$430	\$4,173	\$21,133	\$205,832,007,485	\$331,192,447,514	\$3,213,348,779,290	\$38,560,185,351,482
2037	826	\$267	\$430	\$4,173	\$21,133	\$206,196,564,923	\$331,779,035,924	\$3,219,040,071,968	\$38,628,480,863,621
2038	666	\$284	\$461	\$4,592	\$27,670	\$219,547,106,083	\$332,215,288,130	\$3,223,272,748,487	\$38,679,272,981,839
2039	1,020	\$284	\$461	\$4,592	\$27,670	\$219,739,803,012	\$332,506,874,147	\$3,226,101,821,361	\$38,713,221,856,334
2040	1,041	\$284	\$461	\$4,592	\$27,670	\$219,840,534,470	\$332,659,299,432	\$3,227,580,706,546	\$38,730,968,478,549
2041	1,037	\$284	\$461	\$4,592	\$27,670	\$214,785,536,931	\$325,010,155,273	\$3,153,365,946,425	\$37,840,391,357,100
2042	1,034	\$284	\$461	\$4,592	\$27,670	\$209,844,253,045	\$317,533,080,858	\$3,080,820,669,128	\$36,969,848,029,540
2043	1,030	\$299	\$489	\$4,828	\$28,437	\$215,719,216,862	\$310,224,269,202	\$3,009,907,937,905	\$36,118,895,254,866
2044	1,027	\$599	\$489	\$4,828	\$28,437	\$210,751,336,929	\$303,079,996,457	\$2,940,591,622,644	\$35,287,099,471,728
2045	1,023	\$299	\$489	\$4,828	\$28,437	\$205,895,338,787	\$296,096,620,117	\$2,872,836,382,438	\$34,474,036,589,254
2046	1,021	\$299	\$489	\$4,828	\$28,437	\$201,377,767,307	\$289,599,932,751	\$2,809,803,174,483	\$33,717,638,093,799
2047	1,018	\$299	\$489	\$4,828	\$28,437	\$196,958,195,425	\$283,244,177,908	\$2,748,137,344,779	\$32,977,648,137,348
2048	1,016	\$315	\$521	\$5,239	\$23,531	\$203,129,573,917	\$277,026,326,587	\$2,687,809,504,869	\$32,253,714,058,430
2049	1,013	\$315	\$521	\$5,239	\$23,531	\$198,669,278,109	\$270,943,414,388	\$2,628,790,893,074	\$31,545,490,716,886
2050	1,011	\$315	\$521	\$5,239	\$23,531	\$194,305,799,140	\$264,992,540,142	\$2,571,053,361,209	\$30,852,640,334,505
Total	21,972					\$4,658,710,812,838	\$7,064,352,875,971	\$74,175,077,627,356	\$392,150,216,924,616

reductions to estimate the IRA's in-year period climate benefit (not shown in the table here due to space constraints). In the last four columns, those reductions are the exact same as in table 6. The SCC estimates in each year represent the monetized benefit of removing one metric tonne of CO₂ period benefits are then converted into 2025 present value using a 2% discount rate, following the recent U.S. government guidance (OMB, 2023a). Table 7 | Using the Social Cost of Carbon to Estimate the Monetized Climate Benefits from the Inflation Reduction Act. This table shows the emissions in that year. E.g., the 2025 SCC values here correspond to the SCC values in table 1. Those values are multiplied by the emissions monetized climate benefits from the Inflation Reduction Act across the four monetization approaches considered in this study. The emissions

Table 7 uses the SCC estimates from section 3 to estimate monetized climate benefits from the Inflation Reduction Act (IRA). The IRA's yearly emissions reduction estimates are the exact same as in table 6 discussed above. As in section 3, all of these SCC estimates account for additional heat-vulnerability reduction from rising incomes. When taking the Quasi-Kaldor-Hicks approach that EPA (2023a) took, I find that the total monetized climate benefits from the IRA are \$4.7 trillion. This is similar to Levinson et al. (2024), which also used the Bistline et al. (2023) estimates of the IRA's emissions reductions and used the SCC estimates directly from EPA (2023a). They find a similar result: that the IRA led to \$5.6 trillion in climate benefits.

Importantly, as discussed at length in section 3, these estimates that use the Quasi-Kaldor-Hicks approach value the lives of people in richer countries more than the lives of people in poorer countries, and also count a dollar of damages to the rich the same as to the poor. If, instead, we took the U.S. status quo approach and valued all lives at the population average value, the monetized benefits of the IRA would be \$7.1 trillion as shown in table 7. If, instead, we were to use income-weighting and used U.S. average income as the reference region, the monetized benefits of the IRA are \$74 trillion. As mentioned above, income weighting is now sanctioned in U.S. benefit cost analysis as of the 2023 comprehensive update OMB (2023a). Finally, prioritarian weighting—which has some support in the academic literature, but which is not yet used as far as I am aware in regulatory benefit-cost analysis—yields a much higher number, since the wellbeing of the worst off, who are most impacted by climate damages, are given extra value. Under prioritarian weighting, the IRA is estimated to yield \$392 trillion in benefits. As these results show, of the approaches that EPA (2023a) might have taken toward valuing lives and livelihoods that have significant support in the literature and practice, they ended up taking the approach that assigns the lowest value to climate benefits.

References

- Acland, D. and D. H. Greenberg (2023). The Elasticity of Marginal Utility of Income for Distributional Weighting and Social Discounting: A Meta-Analysis. *Journal of Benefit-Cost Analysis* 14(2), 386–405.
- Adler, M., D. Anthoff, V. Bosetti, G. Garner, K. Keller, and N. Treich (2017, June). Priority for the worse-off and the social cost of carbon. *Nature Climate Change* 7(6), 443–449.
- Adler, M. D. and N. Treich (2015, October). Prioritarianism and Climate Change. *Environmental and Resource Economics* 62(2), 279–308.
- Anthoff, D. and J. Emmerling (2019, March). Inequality and the Social Cost of Carbon. Journal of the Association of Environmental and Resource Economists 6(2), 243–273. Publisher: The University of Chicago Press.
- Anthoff, D., C. Hepburn, and R. S. J. Tol (2009, January). Equity weighting and the marginal damage costs of climate change. *Ecological Economics* 68(3), 836–849.
- Anthoff, D. and R. Tol (2014). FUND Technical Description, Version 3.8. www.fund-model.org, 26.
- Anthoff, D. and R. S. J. Tol (2010, July). On international equity weights and national decision making on climate change. *Journal of Environmental Economics and Management* 60(1), 14–20.
- Armstrong, B., F. Sera, A. M. Vicedo-Cabrera, R. Abrutzky, D. O. Åström, M. L. Bell, B.-Y. Chen, M. de Sousa Zanotti Stagliorio Coelho, P. M. Correa, T. N. Dang, et al. (2019). The role of humidity in associations of high temperature with mortality: a multicountry, multicity study. *Environmental health perspectives* 127(9), 097007.
- Azar, C. and T. Sterner (1996, November). Discounting and distributional considerations in the context of global warming. *Ecological Economics* 19(2), 169–184.
- Baldwin, J. W., T. Benmarhnia, K. L. Ebi, O. Jay, N. J. Lutsko, and J. K. Vanos (2023, May). Humidity's role in heat-related health outcomes: A heated debate. *Environmental Health Perspectives* 131(5), 055001.
- Bank, W. (2024). Pathways Out of the Polycrisis. Technical report, World Bank Group.
- Barrage, L. and W. Nordhaus (2024, March). Policies, projections, and the social cost of carbon: Results from the DICE-2023 model. *Proceedings of the National Academy of Sciences* 121(13), e2312030121.
- Barreca, A., K. Clay, O. Deschenes, M. Greenstone, and J. S. Shapiro (2016). Adapting to climate change: The remarkable decline in the us temperature-mortality relationship over the twentieth century. *Journal of Political Economy* 124(1), 105–159.

- Bistline, J., G. Blanford, M. Brown, D. Burtraw, M. Domeshek, J. Farbes, A. Fawcett, A. Hamilton, J. Jenkins, R. Jones, B. King, H. Kolus, J. Larsen, A. Levin, M. Mahajan, C. Marcy, E. Mayfield, J. McFarland, H. McJeon, R. Orvis, N. Patankar, K. Rennert, C. Roney, N. Roy, G. Schivley, D. Steinberg, N. Victor, S. Wenzel, J. Weyant, R. Wiser, M. Yuan, and A. Zhao (2023, June). Emissions and energy impacts of the Inflation Reduction Act. *Science* 380 (6652), 1324–1327. Publisher: American Association for the Advancement of Science.
- Bressler, R. D. (2021, July). The mortality cost of carbon. *Nature Communications* 12(1), 4467. Number: 1 Publisher: Nature Publishing Group.
- Bressler, R. D. and G. Heal (2022, November). Valuing Excess Deaths Caused by Climate Change. *NBER Working Paper No. 30648*.
- Bressler, R. D., F. C. Moore, K. Rennert, and D. Anthoff (2021, October). Estimates of country level temperature-related mortality damage functions. *Scientific Reports* 11(1), 20282. Number: 1 Publisher: Nature Publishing Group.
- Bressler, R. D., N. Shimberg, L. Rennels, B. Parthum, D. Smith, F. Errickson, and D. Anthoff (n.d.). Large Disproportionate Mortality Effects on the Global Poor Drive a Higher Income-Weighted Social Cost of CO2. *Revision Invited at Nature*.
- Broome, J. (2012, July). Climate Matters: Ethics in a Warming World (Norton Global Ethics Series). W. W. Norton & Company. Google-Books-ID: RjrYYEk8GYQC.
- Broome, J. (2024, September). The Value of Life in the Social Cost of Carbon: A Critique and a Proposal. *Journal of Benefit-Cost Analysis*, 1–17.
- Buzan, J. R. and M. Huber (2020). Moist heat stress on a hotter earth. pp. 35.
- Carleton, T., M. Delgado, M. Greenstone, T. Houser, S. Hsiang, A. Hultgren, A. Jina, R. E. Kopp, K. McCusker, I. Nath, J. Rising, A. Rode, H. K. Seo, J. Simcock, A. Viaene, J. Yuan, and A. T. Zhang (2020). Valuing the Global Mortality Consequences of Climate Change Accounting for Adaptation Costs and Benefits. NBER Working Paper.
- Carleton, T., A. Jina, M. Delgado, M. Greenstone, T. Houser, S. Hsiang, A. Hultgren, R. E. Kopp, K. E. McCusker, I. Nath, J. Rising, A. Rode, H. K. Seo, A. Viaene, J. Yuan, and A. T. Zhang (2022, November). Valuing the Global Mortality Consequences of Climate Change Accounting for Adaptation Costs and Benefits*. The Quarterly Journal of Economics 137(4), 2037–2105.
- Clarke, L., J. Eom, E. H. Marten, R. Horowitz, P. Kyle, R. Link, B. K. Mignone, A. Mundra, and Y. Zhou (2018, May). Effects of long-term climate change on global building energy expenditures. *Energy Economics* 72, 667–677.
- Cohen, F. and A. Dechezleprêtre (2022). Mortality, temperature, and public health provision: evidence from mexico. *American Economic Journal: Economic Policy* 14(2), 161–192.

- Colmer, J. (2020, September). What is the meaning of (statistical) life? Benefit—cost analysis in the time of COVID-19. Oxford Review of Economic Policy 36 (Supplement_1), S56–S63.
- Cromar, K., P. Howard, V. N. Vásquez, and D. Anthoff (2021, August). Health Impacts of Climate Change as Contained in Economic Models Estimating the Social Cost of Carbon Dioxide. *GeoHealth* 5(8).
- Cromar, K. R., S. C. Anenberg, J. R. Balmes, A. A. Fawcett, M. Ghazipura, J. M. Gohlke, M. Hashizume, P. Howard, E. Lavigne, K. Levy, J. Madrigano, J. A. Martinich, E. A. Mordecai, M. B. Rice, S. Saha, N. C. Scovronick, F. Sekercioglu, E. R. Svendsen, B. F. Zaitchik, and G. Ewart (2022, July). Global Health Impacts for Economic Models of Climate Change: A Systematic Review and Meta-Analysis. Annals of the American Thoracic Society 19(7), 1203–1212.
- Davies-Jones, R. (2008, July). An Efficient and Accurate Method for Computing the Wet-Bulb Temperature along Pseudoadiabats. *Monthly Weather Review* 136(7), 2764–2785.
- Deschênes, O. and M. Greenstone (2011). Climate Change, Mortality, and Adaptation: Evidence from Annual Fluctuations in Weather in the US. American Economic Journal: Applied Economics 3(4), 152–185.
- Diaz, D. B. (2016, July). Estimating global damages from sea level rise with the Coastal Impact and Adaptation Model (CIAM). *Climatic Change* 137(1), 143–156.
- Dietz, S., F. van der Ploeg, A. Rezai, and F. Venmans (2021, September). Are Economists Getting Climate Dynamics Right and Does It Matter? *Journal of the Association of Environmental and Resource Economists* 8(5), 895–921.
- Dougenik, J. A., N. R. Chrisman, and D. R. Niemeyer (1985, February). AN ALGORITHM TO CONSTRUCT CONTINUOUS AREA CARTOGRAMS. *The Professional Geographer* 37(1), 75–81.
- Ebi, K. L., A. Capon, P. Berry, C. Broderick, R. de Dear, G. Havenith, Y. Honda, R. S. Kovats, W. Ma, A. Malik, N. B. Morris, L. Nybo, S. I. Seneviratne, J. Vanos, and O. Jay (2021, August). Hot weather and heat extremes: health risks. *The Lancet 398* (10301), 698–708.
- EPA (2011a). The benefits and costs of the Clean Air Act from 1990 to 2020.
- EPA (2011b). Regulatory impact analysis for the final mercury and air toxics standards. Technical report, United States Government.
- EPA (2023a, November). EPA Report on the Social Cost of Greenhouse Gases: Estimates Incorporating Recent Scientific Advances. Supplementary Material for the Regulatory Impact Analysis for the Final Rulemaking, "Standards of Performance for New, Reconstructed, and Modified Sources and Emissions Guidelines for Existing Sources: Oil and Natural Gas Sector Climate Review".

- EPA (2023b). Pattern scaling of global climate variables to local climate variables for use in probabilistic integrated assessment models. https://github.com/usepa/pattern-scaled-climate-variables.
- EPA, U. (2019). Greenhouse gas equivalencies calculator.
- Errickson, F. C., K. Keller, W. D. Collins, V. Srikrishnan, and D. Anthoff (2021, April). Equity is more important for the social cost of methane than climate uncertainty. *Nature* 592 (7855), 564–570.
- Eyring, V., S. Bony, G. A. Meehl, C. A. Senior, B. Stevens, R. J. Stouffer, and K. E. Taylor (2016). Overview of the coupled model intercomparison project phase 6 (cmip6) experimental design and organization. *Geoscientific Model Development* 9(5), 1937–1958.
- Fankhauser, S., R. S. Tol, and D. W. Pearce (1997, October). The Aggregation of Climate Change Damages: a Welfare Theoretic Approach. *Environmental and Resource Economics* 10(3), 249–266.
- Ferranna, M. and M. Fleurbaey (2020). Prioritarianism and Climate Change. SSRN.
- Folini, D., A. Friedl, F. Kübler, and S. Scheidegger (2024, January). The Climate in Climate Economics*. *The Review of Economic Studies*, rdae011.
- Gallo, E., M. Quijal-Zamorano, R. Fernando Mendez Turrubiates, C. Tonne, X. Basagana, H. Achebak, and J. Ballester (2024). Heat-related mortality in Europe during 2023 and the role of adaptation in protecting health. *Nature Medicine*.
- Gasparrini, A. (2011). Distributed lag linear and non-linear models in r: the package dlnm. Journal of statistical software 43(8), 1.
- Gasparrini, A., Y. Guo, M. Hashizume, E. Lavigne, A. Zanobetti, J. Schwartz, A. Tobias, S. Tong, J. Rocklöv, B. Forsberg, M. Leone, M. De Sario, M. L. Bell, Y.-L. L. Guo, C.-f. Wu, H. Kan, S.-M. Yi, M. de Sousa Zanotti Stagliorio Coelho, P. H. N. Saldiva, Y. Honda, H. Kim, and B. Armstrong (2015, July). Mortality risk attributable to high and low ambient temperature: a multicountry observational study. *The Lancet* 386 (9991), 369–375.
- Gasparrini, A., Y. Guo, F. Sera, A. M. Vicedo-Cabrera, V. Huber, S. Tong, M. d. S. Z. S. Coelho, P. H. N. Saldiva, E. Lavigne, P. M. Correa, N. V. Ortega, H. Kan, S. Osorio, J. Kyselý, A. Urban, J. J. K. Jaakkola, N. R. I. Ryti, M. Pascal, P. G. Goodman, A. Zeka, P. Michelozzi, M. Scortichini, M. Hashizume, Y. Honda, M. Hurtado-Diaz, J. C. Cruz, X. Seposo, H. Kim, A. Tobias, C. Iñiguez, B. Forsberg, D. O. Åström, M. S. Ragettli, Y. L. Guo, C.-f. Wu, A. Zanobetti, J. Schwartz, M. L. Bell, T. N. Dang, D. D. Van, C. Heaviside, S. Vardoulakis, S. Hajat, A. Haines, and B. Armstrong (2017, December). Projections of temperature-related excess mortality under climate change scenarios. *The Lancet Planetary Health* 1(9), e360–e367. Publisher: Elsevier.
- Gayer, T. and W. K. Viscusi (2016, July). Determining the Proper Scope of Climate Change Policy Benefits in U.S. Regulatory Analyses: Domestic versus Global Approaches. *Review*

- of Environmental Economics and Policy 10(2), 245-263. Publisher: The University of Chicago Press.
- Geruso, M. and D. Spears (2018). Heat, Humidity, and Infant Mortality in the Developing World. NBER Working Paper No. 24870, 31.
- Hajat, S., S. Vardoulakis, C. Heaviside, and B. Eggen (2014, July). Climate change effects on human health: projections of temperature-related mortality for the UK during the 2020s, 2050s and 2080s. *J Epidemiol Community Health* 68(7), 641–648.
- Hales, S., S. Kovats, S. Lloyd, D. Campbell-Lendrum, World Health Organization, World Health Organization, and Health Security and Environment Cluster (2014). Quantitative risk assessment of the effects of climate change on selected causes of death, 2030s and 2050s. OCLC: 897764432.
- Harrell, F. E. (2015). Regression Modeling Strategies: With Applications to Linear Models, Logistic and Ordinal Regression, and Survival Analysis. Springer International Publishing.
- Havenith, G. and D. Fiala (2011). Thermal indices and thermophysiological modeling for heat stress. Comprehensive Physiology 6(1), 255–302. Publisher: Wiley Online Library.
- Heal, G. (2017, September). The Economics of the Climate. *Journal of Economic Literature* 55(3), 1046–1063.
- Hemel, D. (2022, May). Regulation and Redistribution with Lives in the Balance. *The University of Chicago Law Review 89*(3), 649–734. Num Pages: 649-734 Place: Chicago, United States Publisher: University of Chicago, acting on behalf of the University of Chicago Law Review.
- Hersher, R., R. Ramirez, A. Scott, and M. Cirino (2023, February). EPA's proposal to raise the cost of carbon is a powerful tool and ethics nightmare. *NPR*.
- Hicks, J. R. (1939). The Foundations of Welfare Economics. *The Economic Journal* 49(196), 696–712. Publisher: [Royal Economic Society, Wiley].
- HM Treasury (2022). The Green Book: appraisal and evaluation in central government.
- Honda, Y., M. Kondo, G. McGregor, H. Kim, Y.-L. Guo, Y. Hijioka, M. Yoshikawa, K. Oka, S. Takano, S. Hales, and R. S. Kovats (2014, January). Heat-related mortality risk model for climate change impact projection. *Environmental Health and Preventive Medicine* 19(1), 56–63.
- Hope, C. (2008, May). Discount rates, equity weights and the social cost of carbon. *Energy Economics* 30(3), 1011-1019.
- Houser, T., S. Hsiang, R. Kopp, K. Larsen, M. Delgado, A. Jina, M. Mastrandrea, S. Mohan, R. Muir-Wood, D. J. Rasmussen, J. Rising, and P. Wilson (2015, August). *Economic Risks of Climate Change: An American Prospectus*. Columbia University Press. Google-Books-ID: 0QTSBgAAQBAJ.

- Howard, P. and J. Schwartz (2017). Think Global: International Reciprocity as Justification for a Global Social Cost of Carbon. *Columbia Journal of Environmental Law* 42(S). Number: S.
- Hsu, A., G. Sheriff, T. Chakraborty, and D. Manya (2021, May). Disproportionate exposure to urban heat island intensity across major US cities. *Nature Communications* 12(1), 2721. Number: 1 Publisher: Nature Publishing Group.
- IWG (2016, August). Technical update of the social cost of carbon for regulatory impact analysis. Technical report, United States Government.
- IWG (2021, November). Technical update of the social cost of carbon for regulatory impact analysis. Technical report, United States Government.
- Jáuregui-Díaz, J. A., M. d. J. Á. Sánchez, and R. T. Cabañas (2020). Cambios en la mortalidad por eventos climáticos extremos en méxico entre el 2000 y 2015. Revista de Estudios Latinoamericanos sobre Reducción del Riesgo de Desastres REDER 4(1), 80–94.
- Jeworutzki, S. (2016). cartogram: Create Cartograms with R.
- Kaldor, N. (1939). Welfare propositions of economics and interpersonal comparisons of utility. The economic journal 49(195), 549–552. Publisher: Oxford University Press Oxford, UK.
- Kelleher, J. P. (2024). The Social Cost of Carbon. Oxford University Press.
- Kim, D.-W., R. C. Deo, J.-H. Chung, and J.-S. Lee (2016, January). Projection of heat wave mortality related to climate change in Korea. *Natural Hazards* 80(1), 623–637.
- Kjellström, T., N. Maître, C. Saget, M. Otto, and T. Karimova (2019). Working on a warmer planet: The impact of heat stress on labour productivity and decent work. ILO.
- Kolstad, C., K. Urama, J. Broome, A. Bruvoll, M. Cariño-Olvera, D. Fullerton, C. Gollier, W. M. Hanemann, R. Hassan, and F. Jotzo (2014). Social, economic and ethical concepts and methods. Climate Change 2014: Mitigation of Climate Change. Contribution of Working Group III to the Fifth Assessment Report of the Intergovern- mental Panel on Climate Change. Publisher: Cambridge University Press.
- Lab, F. C. and C. for International Earth Science Information Network CIESIN Columbia University (2016). High Resolution Settlement Layer (HRSL). Source imagery for HRSL © 2016 DigitalGlobe.
- Lee, J. Y. and H. Kim (2016, September). Projection of future temperature-related mortality due to climate and demographic changes. *Environment International 94*, 489–494.
- Levinson, A., K. D. Werner, M. Ashenfarb, and A. Britten (2024). The Inflation Reduction Act's Benefits and Costs. *US Department of the Treasury, March 1*.
- Li, T., R. M. Horton, D. A. Bader, M. Zhou, X. Liang, J. Ban, Q. Sun, and P. L. Kinney (2016, June). Aging Will Amplify the Heat-related Mortality Risk under a Changing Climate: Projection for the Elderly in Beijing, China. *Scientific Reports* 6(1), 28161.

- Lynch, C., C. Hartin, B. Bond-Lamberty, and B. Kravitz (2017). An open-access cmip5 pattern library for temperature and precipitation: description and methodology. *Earth System Science Data* 9(1), 281–292.
- Masterman, C. J. and W. K. Viscusi (2018). The income elasticity of global values of a statistical life: stated preference evidence. *Journal of Benefit-Cost Analysis* 9(3), 407–434. Publisher: Cambridge University Press.
- Meyer, A. and T. Cooper (1995). A recalculation of the social costs of climate change. *The Ecologist*.
- Millar, R. J., Z. R. Nicholls, P. Friedlingstein, and M. R. Allen (2017, June). A modified impulse-response representation of the global near-surface air temperature and atmospheric concentration response to carbon dioxide emissions. *Atmospheric Chemistry and Physics* 17(11), 7213–7228.
- Mirrlees, J. A. (1978, February). Social benefit-cost analysis and the distribution of income. World Development 6(2), 131–138.
- Moore, F. C., U. Baldos, T. Hertel, and D. Diaz (2017, November). New science of climate change impacts on agriculture implies higher social cost of carbon. *Nature Communications* 8(1), 1607. Number: 1 Publisher: Nature Publishing Group.
- Mora, C., B. Dousset, I. R. Caldwell, F. E. Powell, R. C. Geronimo, C. R. Bielecki, C. W. W. Counsell, B. S. Dietrich, E. T. Johnston, L. V. Louis, M. P. Lucas, M. M. McKenzie, A. G. Shea, H. Tseng, T. W. Giambelluca, L. R. Leon, E. Hawkins, and C. Trauernicht (2017, July). Global risk of deadly heat. *Nature Climate Change* 7(7), 501–506.
- Murakami, D. and Y. Yamagata (2019). Estimation of gridded population and gdp scenarios with spatially explicit statistical downscaling. *Sustainability* 11(7), 2106.
- NASA (1996). Final tier 2 environmental impact statement for international space station. Technical report, United States Government.
- NASEM (2017). Valuing Climate Changes: Updating Estimation of the Social Cost of Carbon Dioxide. Washington, D.C.: National Academies Press.
- Nordhaus, W. D. (2007, September). A Review of the Stern Review on the Economics of Climate Change. Journal of Economic Literature 45(3), 686–702.
- Nordhaus, W. D. (2011, October). Estimates of the Social Cost of Carbon: Background and Results from the RICE-2011 Model.
- Nordhaus, W. D. (2017, February). Revisiting the social cost of carbon. *Proceedings of the National Academy of Sciences* 114(7), 1518–1523. Publisher: Proceedings of the National Academy of Sciences.
- Nordhaus, W. D. and A. Moffat (2017). A survey of global impacts of climate change: Replication, survey methods, and a statistical analysis. Technical report, National Bureau of Economic Research.

- Oehlsen, E. (2024, May). Philanthropic Cause Prioritization. *Journal of Economic Perspectives* 38(2), 63–82.
- OMB (2023a). Circular A-4. Technical report, United States Government.
- OMB (2023b). Circular A-4 Explanation and Response to Public Input. Technical report, United States Government.
- Parsons, K. (2014). Human thermal environments: the effects of hot, moderate, and cold environments on human health, comfort, and performance. CRC press.
- Pindyck, R. S. (2013). Climate change policy: what do the models tell us? *Journal of Economic Literature* 51(3), 860–72.
- Powis, C. M., D. Byrne, Z. Zobel, K. N. Gassert, A. C. Lute, and C. R. Schwalm (2023, September). Observational and model evidence together support wide-spread exposure to noncompensable heat under continued global warming. *Science Advances* 9(36), eadg9297. Publisher: American Association for the Advancement of Science.
- Prest, B. C., L. Rennels, F. Errickson, and D. Anthoff (2024, August). Equity weighting increases the social cost of carbon. *Science* 385(6710), 715–717. Publisher: American Association for the Advancement of Science.
- Raymond, C., T. Matthews, and R. M. Horton (2020). The emergence of heat and humidity too severe for human tolerance. *Science Advances* 6(19), eaaw1838.
- Rennert, K., F. Errickson, B. C. Prest, L. Rennels, R. G. Newell, W. Pizer, C. Kingdon, J. Wingenroth, R. Cooke, B. Parthum, D. Smith, K. Cromar, D. Diaz, F. C. Moore, U. K. Müller, R. J. Plevin, A. E. Raftery, H. Ševčíková, H. Sheets, J. H. Stock, T. Tan, M. Watson, T. E. Wong, and D. Anthoff (2022, October). Comprehensive evidence implies a higher social cost of CO2. *Nature* 610 (7933), 687–692. Number: 7933 Publisher: Nature Publishing Group.
- Rennert, K., B. C. Prest, W. A. Pizer, R. G. Newell, D. Anthoff, C. Kingdon, L. Rennels, R. Cooke, A. E. Raftery, and H. Ševčíková (2021). The Social Cost of Carbon: Advances in Long-Term Probabilistic Projections of Population, GDP, Emissions, and Discount Rates. *Brookings Papers on Economic Activity*.
- Riahi, K., D. P. van Vuuren, E. Kriegler, J. Edmonds, B. C. O'Neill, S. Fujimori, N. Bauer, K. Calvin, R. Dellink, O. Fricko, W. Lutz, A. Popp, J. C. Cuaresma, S. Kc, M. Leimbach, L. Jiang, T. Kram, S. Rao, J. Emmerling, K. Ebi, T. Hasegawa, P. Havlik, F. Humpenöder, L. A. Da Silva, S. Smith, E. Stehfest, V. Bosetti, J. Eom, D. Gernaat, T. Masui, J. Rogelj, J. Strefler, L. Drouet, V. Krey, G. Luderer, M. Harmsen, K. Takahashi, L. Baumstark, J. C. Doelman, M. Kainuma, Z. Klimont, G. Marangoni, H. Lotze-Campen, M. Obersteiner, A. Tabeau, and M. Tavoni (2017, January). The Shared Socioeconomic Pathways and their energy, land use, and greenhouse gas emissions implications: An overview. *Global Environmental Change* 42, 153–168.

- Robinson, L. A., J. K. Hammitt, and L. O'Keeffe (2019). Valuing Mortality Risk Reductions in Global Benefit-Cost Analysis. *Journal of Benefit-Cost Analysis* 10(S1), 15–50.
- Schwartz, J. (2000). Harvesting and long term exposure effects in the relation between air pollution and mortality. *American Journal of Epidemiology* 151(5), 440–448.
- Scovronick, N., D. Anthoff, F. Dennig, F. Errickson, M. Ferranna, W. Peng, D. Spears, F. Wagner, and M. Budolfson (2021, May). The importance of health co-benefits under different climate policy cooperation frameworks. *Environmental Research Letters* 16(5), 055027.
- Sherwood, S. C. and M. Huber (2010). An adaptability limit to climate change due to heat stress. *Proceedings of the National Academy of Sciences* 107(21), 9552–9555.
- Smith, C. J., P. M. Forster, M. Allen, N. Leach, R. J. Millar, G. A. Passerello, and L. A. Regayre (2018, June). FAIR v1.3: a simple emissions-based impulse response and carbon cycle model. *Geoscientific Model Development* 11(6), 2273–2297. Publisher: Copernicus GmbH.
- Steadman, R. G. (1979). The assessment of sultriness. Part I: A temperature-humidity index based on human physiology and clothing science. *Journal of Applied Meteorology and Climatology* 18(7), 861–873.
- Stern, N. (2006). The Economics of Climate Change: The Stern Review. Cambridge University Press.
- Sunstein, C. (2004, November). Valuing Life: A Plea for Disaggregation. *Duke Law Journal* 54(2), 385–445.
- Sunstein, C. R. (2023, March). Inequality and the Value of a Statistical Life. *Journal of Benefit-Cost Analysis* 14(1), 1–7.
- Vanos, J., G. Guzman-Echavarria, J. W. Baldwin, C. Bongers, K. L. Ebi, and O. Jay (2023, November). A physiological approach for assessing human survivability and liveability to heat in a changing climate. *Nature Communications* 14(1), 7653.
- Vecellio, D. J., S. T. Wolf, R. M. Cottle, and W. L. Kenney (2022, February). Evaluating the 35°C wet-bulb temperature adaptability threshold for young, healthy subjects (PSU HEAT Project). *Journal of Applied Physiology* 132(2), 340–345. Publisher: American Physiological Society.
- Viscusi, W. K. and C. J. Masterman (2017). Income elasticities and global values of a statistical life. *Journal of Benefit-Cost Analysis* 8(2), 226–250. Publisher: Cambridge University Press.
- Watkiss, P. and C. Hope (2011). Using the social cost of carbon in regulatory deliberations. WIREs Climate Change 2(6), 886–901.

- Wilson*, A. J., R. D. Bressler*, C. Ivanovich, C. Raymond, R. M. Horton, A. Sobel, T. Cavazos, and J. G. Shrader (2024). Heat disproportionately kills young people: *Co-Lead Author. Accepted at Science Advances.
- Wong, T. E., A. M. R. Bakker, K. Ruckert, P. Applegate, A. B. A. Slangen, and K. Keller (2017, July). BRICK v0.2, a simple, accessible, and transparent model framework for climate and regional sea-level projections. *Geoscientific Model Development* 10(7), 2741–2760. Publisher: Copernicus GmbH.
- Wu, Y., S. Li, Q. Zhao, B. Wen, A. Gasparrini, S. Tong, A. Overcenco, A. Urban, A. Schneider, A. Entezari, A. M. Vicedo-Cabrera, A. Zanobetti, A. Analitis, A. Zeka, A. Tobias, B. Nunes, B. Alahmad, B. Armstrong, B. Forsberg, S.-C. Pan, C. Íñiguez, C. Ameling, C. De la Cruz Valencia, C. Åström, D. Houthuijs, D. Van Dung, D. Royé, E. Indermitte, E. Lavigne, F. Mayvaneh, F. Acquaotta, F. de'Donato, S. Rao, F. Sera, G. Carrasco-Escobar, H. Kan, H. Orru, H. Kim, I.-H. Holobaca, J. Kyselý, J. Madureira, J. Schwartz, J. J. K. Jaakkola, K. Katsouyanni, M. Hurtado Diaz, M. S. Ragettli, M. Hashizume, M. Pascal, M. de Sousa Zanotti Stagliorio Coélho, N. V. Ortega, N. Ryti, N. Scovronick, P. Michelozzi, P. M. Correa, P. Goodman, P. H. Nascimento Saldiva, R. Abrutzky, S. Osorio, T. N. Dang, V. Colistro, V. Huber, W. Lee, X. Seposo, Y. Honda, Y. L. Guo, M. L. Bell, and Y. Guo (2022, May). Global, regional, and national burden of mortality associated with short-term temperature variability from 2000–19: a three-stage modelling study. The Lancet Planetary Health 6(5), e410–e421.

A Appendix

A.1 Additional Distributional Mortality Cost of Carbon Results

Table A.1: The Distributional Mortality Cost of Carbon from a one tonne ${\bf CO}_2$ pulse in ${\bf 2025}$

		Heat-Vul	ting for Addition nerability Reduc Rising Incomes			Heat-Vulr	nting for Additi nerability Reduct Rising Incomes	
Region	Expected D-MCC	Share of Expected MCC	5th Percentile D-MCC	95th Percentile D-MCC	Expected D-MCC	Share of Expected MCC	5th Percentile D-MCC	95th Percentile D-MCC
India	2.95E-05	22%	-3.89E-06	7.62E-05	6.37E-05	16%	2.25E-05	1.25E-04
China	1.46E-05	11%	-6.44E-06	4.23E-05	3.27E-05	8%	1.27E-05	6.25E-05
Pakistan	9.55E-06	7%	-1.25E-06	2.67E-05	2.20E-05	6%	6.66E-06	4.88E-05
Nigeria	9.43E-06	7%	-8.09E-06	3.79E-05	3.11E-05	8%	6.27E-06	8.63E-05
Democratic Republic of Congo	5.57E-06	4%	-2.42E-06	2.06E-05	2.06E-05	5%	2.55E-06	5.98E-05
Niger	5.27E-06	4%	-9.32E-07	1.82E-05	1.56E-05	4%	2.24E-06	4.62E-05
Somalia	3.90E-06	3%	-1.49E-06	1.47E-05	1.33E-05	3%	1.36E-06	4.16E-05
Afghanistan	3.36E-06	2%	-1.64E-07	1.07E-05	8.63E-06	2%	1.29E-06	2.40E-05
Tanzania	2.75E-06	2%	-3.60E-06	1.25E-05	1.19E-05	3%	1.44E-06	3.39E-05
Sudan	2.64E-06	2%	-1.08E-06	8.49E-06	7.66E-06	2%	1.75E-06	1.88E-05
Ethiopia	2.63E-06	2%	-1.72E-06	9.55E-06	8.65E-06	2%	1.17E-06	2.17E-05
Mozambique	2.48E-06	2%	-4.68E-07	8.14E-06	7.03E-06	2%	9.73E-07	2.01E-05
Burkina Faso	2.25E-06	2%	-1.44E-07	6.62E-06	5.58E-06	1%	1.00E-06	1.48E-05
Egypt	2.17E-06	2%	-2.05E-06	8.09E-06	6.55E-06	2%	1.93E-06	1.48E-05
Bangladesh	2.17E-06 2.15E-06	2%	-3.73E-07	5.94E-06	5.21E-06	1%	1.35E-06	1.09E-05
Iraq	1.93E-06	1%	-9.85E-07	6.88E-06	4.59E-06	1%	1.10E-06	1.16E-05
Mali	1.92E-06	1%	-2.09E-07	6.17E-06	4.67E-06	1%	8.62E-07	1.27E-05
Angola	1.79E-06	1%	-2.69E-06	8.56E-06	8.24E-06	2%	9.04E-07	2.42E-05
Chad	1.73E-00 1.52E-06	1%	-2.38E-07	4.66E-06	4.04E-06	1%	8.14E-07	1.03E-05
Uganda	1.40E-06	1%	-2.38E-07 -8.79E-07	5.09E-06	4.79E-06	1%	7.69E-07	1.26E-05
Malawi	1.40E-00 1.36E-06	1%	-2.69E-07	4.43E-06	3.63E-06	1%	5.20E-07	1.00E-05
Indonesia	1.35E-06	1%	-2.85E-06	6.44E-06	5.49E-06	1%	1.69E-06	1.13E-05
		1%				1%		
Cote d'Ivoire	1.25E-06	1%	-7.11E-07	4.39E-06	4.02E-06	1%	7.44E-07	1.06E-05
Vietnam	1.18E-06	1%	-4.87E-07	3.41E-06	3.06E-06	1%	9.99E-07	6.06E-06
Iran	1.12E-06		-1.09E-06	4.23E-06	3.26E-06		1.04E-06	6.92E-06
Cameroon	1.09E-06	1%	-6.97E-07	3.89E-06	3.53E-06	1%	7.03E-07	9.08E-06
Madagascar	1.07E-06	1%	-7.25E-07	3.96E-06	3.92E-06	1%	5.75E-07	1.06E-05
Uzbekistan	1.00E-06	1%	-7.23E-09	2.61E-06	2.30E-06	1%	6.67E-07	4.93E-06
Zambia	9.39E-07	1%	-9.24E-07	3.70E-06	3.64E-06	1%	5.72E-07	1.00E-05
Philippines	8.46E-07	1%	-9.52E-07	3.07E-06	2.83E-06	1%	9.10E-07	5.85E-06
Myanmar	8.22E-07	1%	-1.81E-07	2.23E-06	1.92E-06	0%	6.23E-07	3.85E-06
Kenya	8.22E-07	1%	-7.75E-07	3.02E-06	3.06E-06	1%	5.42E-07	7.34E-06
Ghana	7.85E-07	1%	-5.85E-07	2.87E-06	2.53E-06	1%	5.96E-07	6.11E-06
Senegal	7.41E-07	1%	-4.71E-07	2.57E-06	2.49E-06	1%	5.10E-07	6.06E-06
Yemen	7.27E-07	1%	-2.10E-07	2.14E-06	2.08E-06	1%	5.27E-07	4.64E-06
Benin	7.08E-07	1%	-2.62E-07	2.34E-06	2.11E-06	1%	4.07E-07	5.35E-06
Brazil	6.76E-07	0%	-1.74E-06	3.52E-06	3.02E-06	1%	9.31E-07	6.22E-06
Russia	6.68E-07	0%	-1.39E-06	3.27E-06	2.23E-06	1%	3.05E-07	5.39E-06
Guinea	6.52E-07	0%	-2.18E-07	2.16E-06	1.91E-06	0%	3.54E-07	4.98E-06
Nepal	6.23E-07	0%	4.13E-08	1.56E-06	1.33E-06	0%	3.55E-07	2.90E-06
Syria	6.16E-07	0%	-1.33E-07	1.91E-06	1.83E-06	0%	3.52E-07	4.95E-06
Burundi	5.81E-07	0%	-1.90E-07	2.03E-06	1.81E-06	0%	1.90E-07	5.22E-06
Algeria	5.67E-07	0%	-5.93E-07	2.19E-06	1.82E-06	0%	5.81E-07	3.90E-06
Thailand	5.29E-07	0%	-3.92E-07	1.71E-06	1.21E-06	0%	4.26E-07	2.42E-06
Turkey	5.14E-07	0%	-1.09E-06	2.53E-06	1.74E-06	0%	4.73E-07	3.87E-06
Ukraine	4.83E-07	0%	-3.08E-08	1.30E-06	9.07E-07	0%	2.38E-07	1.89E-06
Togo	4.55E-07	0%	-8.87E-08	1.40E-06	1.27E-06	0%	2.37E-07	3.21E-06
Tajikistan	4.54E-07	0%	-1.31E-07	1.45E-06	1.39E-06	0%	2.56E-07	3.48E-06
South Africa	4.23E-07	0%	-1.01E-06	2.24E-06	2.01E-06	1%	4.64E-07	4.60E-06
Rwanda	3.90E-07	0%	-3.23E-07	1.56E-06	1.46E-06	0%	1.66E-07	4.11E-06
Morocco	3.73E-07	0%	-2.38E-07	1.21E-06	1.08E-06	0%	3.31E-07	2.29E-06
Zimbabwe	3.66E-07	0%	-8.01E-08	1.10E-06	9.97E-07	0%	1.92E-07	2.40E-06
Cambodia	3.36E-07	0%	-9.55E-08	9.56E-07	8.74E-07	0%	2.46E-07	1.89E-06
Saudi Arabia	3.14E-07	0%	-5.46E-07	1.64E-06	6.81E-07	0%	-2.26E-07	1.91E-06
Mauritania	2.96E-07	0%	-1.54E-07	1.03E-06	9.02E-07	0%	1.98E-07	2.28E-06
Sierra Leone	2.92E-07	0%	-7.44E-08	9.16E-07	8.47E-07	0%	1.67E-07	2.18E-06

xii

		Heat-Vul	ting for Addition nerability Reduc Rising Incomes			Heat-Vulr	unting for Additi nerability Reduct Rising Incomes	
Region	Expected D-MCC	Share of Expected MCC	5th Percentile D-MCC	95th Percentile D-MCC	Expected D-MCC	Share of Expected MCC	5th Percentile D-MCC	95th Percentile D-MCC
Liberia	2.82E-07	0%	-1.97E-07	1.11E-06	1.16E-06	0%	1.34E-07	3.37E-06
Mexico	2.47E-07	0%	-1.42E-06	2.22E-06	1.90E-06	0%	4.58E-07	4.34E-06
Central African Republic	2.41E-07	0%	2.63E-08	6.53E-07	5.59E-07	0%	9.82E-08	1.46E-06
United Arab Emirates	2.30E-07	0%	-5.04E-07	1.34E-06	8.34E-07	0%	1.26E-07	1.90E-06
Haiti	2.22E-07	0%	-1.99E-08	5.80E-07	5.51E-07	0%	1.41E-07	1.18E-06
Jordan	2.21E-07	0%	-2.80E-07	9.62E-07	8.45E-07	0%	1.62E-07	2.25E-06
Congo	2.13E-07	0%	-2.83E-07	8.61E-07	7.83E-07	0%	1.51E-07	2.00E-06
Eritrea	1.91E-07	0%	-1.89E-08	5.78E-07	4.85E-07	0%	8.10E-08	1.29E-06
Kazakhstan	1.90E-07	0%	-2.93E-07	8.92E-07	5.74E-07	0%	1.10E-07	1.49E-06
Kyrgyzstan	1.81E-07	0%	-3.73E-08	5.62E-07	4.76E-07	0%	6.50E-08	1.16E-06
Kuwait	1.70E-07	0%	-1.52E-07	6.84E-07	3.56E-07	0%	2.75E-08	8.35E-07
Guatemala	1.67E-07	0%	-2.63E-07	7.11E-07	6.84E-07	0%	1.60E-07	1.56E-06
Japan	1.66E-07	0%	-8.91E-07	1.55E-06	8.30E-07	0%	-3.94E-08	1.97E-06
Palestine	1.64E-07	0%	-9.68E-08	6.07E-07	4.94E-07	0%	8.80E-08	1.40E-06
Gambia	1.60E-07	0%	-4.47E-08	5.20E-07	4.57E-07	0%	7.60E-08	1.22E-06
Honduras	1.44E-07	0%	-7.24E-08	4.51E-07	4.20E-07	0%	1.12E-07	9.05E-07
Venezuela	1.35E-07	0%	-2.71E-07	6.55E-07	5.23E-07	0%	1.43E-07	1.22E-06
Tunisia	1.34E-07	0%	-7.77E-08	4.28E-07	3.66E-07	0%	1.26E-07	7.75E-07
Turkmenistan	1.32E-07	0%	-5.61E-08	4.11E-07	2.90E-07	0%	9.64E-08	6.23E-07
Canada	1.29E-07	0%	-6.64E-07	9.91E-07	5.83E-07	0%	-1.06E-07	1.77E-06
South Korea	1.14E-07	0%	-2.95E-07	6.15E-07	3.34E-07	0%	3.17E-08	7.57E-07
Sri Lanka	9.38E-08	0%	-1.40E-07	3.76E-07	3.23E-07	0%	1.13E-07	6.44E-07
Libya	9.06E-08	0%	-7.41E-08	3.25E-07	2.55E-07	0%	8.20E-08	5.52E-07
Laos	9.06E-08	0%	-5.02E-08	2.87E-07	2.42E-07	0%	7.21E-08	5.11E-07
Paraguay	8.58E-08	0%	-6.49E-08	2.95E-07	2.52E-07	0%	7.33E-08	5.50E-07
Nicaragua	8.55E-08	0% 0%	-4.79E-08	2.65E-07	2.45E-07	0% 0%	7.12E-08	5.14E-07
Azerbaijan	8.13E-08 7.91E-08	0%	-7.47E-08 -5.30E-07	2.85E-07	2.17E-07 7.10E-07	0%	7.33E-08 2.25E-07	4.55E-07
Argentina Malaysia	6.99E-08	0%	-5.50E-07 -4.46E-07	7.77E-07 6.65E-07	4.37E-07	0%	9.12E-08	1.52E-06 9.80E-07
Bolivia	6.71E-08	0%	-4.40E-07 -1.49E-07	3.51E-07	4.57E-07 3.23E-07	0%	2.61E-08	7.97E-07
Romania	6.59E-08	0%	-9.13E-08	2.59E-07	3.23E-07 1.90E-07	0%	5.62E-08	4.08E-07
Guinea-Bissau	6.25E-08	0%	-9.13E-08 -1.72E-08	2.01E-07	1.77E-07	0%	3.02E-08	4.66E-07
Qatar Qatar	5.76E-08	0%	-1.72E-08 -1.22E-07	3.45E-07	1.48E-07	0%	-4.41E-08	4.00E-07 4.15E-07
Italy	5.70E-08 5.70E-08	0%	-5.14E-07	7.66E-07	4.91E-07	0%	5.78E-08	1.17E-06
Belarus	5.48E-08	0%	-5.45E-08	2.15E-07	1.49E-07	0%	2.41E-08	3.47E-07
Papua New Guinea	5.46E-08	0%	-1.69E-07	3.20E-07	3.09E-07	0%	5.90E-08	7.27E-07
Colombia	5.44E-08	0%	-6.05E-07	7.75E-07	7.10E-07	0%	1.33E-07	1.66E-06
Oman	5.30E-08	0%	-1.50E-07	3.41E-07	1.54E-07	0%	-2.33E-08	4.32E-07
Dominican Republic	4.88E-08	0%	-9.91E-08	2.40E-07	1.91E-07	0%	6.21E-08	4.04E-07
Spain	4.83E-08	0%	-4.38E-07	6.22E-07	4.04E-07	0%	5.28E-08	9.91E-07
Serbia	4.81E-08	0%	-3.11E-08	1.55E-07	1.23E-07	0%	3.97E-08	2.58E-07
El Salvador	4.52E-08	0%	-4.25E-08	1.61E-07	1.46E-07	0%	3.87E-08	3.15E-07
Moldova	4.14E-08	0%	-5.42E-09	1.14E-07	7.91E-08	0%	2.33E-08	1.68E-07
Lebanon	4.04E-08	0%	-1.84E-07	3.21E-07	2.75E-07	0%	4.80E-08	7.70E-07
Greece	4.00E-08	0%	-5.73E-08	1.66E-07	1.28E-07	0%	4.20E-08	2.75E-07
Israel	3.67E-08	0%	-2.93E-07	4.55E-07	2.93E-07	0%	3.51E-08	8.15E-07
Mongolia	3.55E-08	0%	-4.00E-08	1.46E-07	1.12E-07	0%	1.08E-08	2.85E-07
Lesotho	3.54E-08	0%	-1.12E-08	1.13E-07	9.56E-08	0%	7.09E-09	2.43E-07
Georgia	3.50E-08	0%	-2.33E-08	1.21E-07	1.05E-07	0%	2.54E-08	2.57E-07
Djibouti	3.26E-08	0%	-4.06E-08	1.47E-07	1.15E-07	0%	2.32E-08	3.05E-07
Namibia	3.20E-08	0%	-5.00E-08	1.42E-07	1.25E-07	0%	3.17E-08	2.86E-07
Armenia	3.05E-08	0%	-1.72E-08	1.04E-07	8.74E-08	0%	2.04E-08	2.11E-07
Botswana	2.91E-08	0%	-5.17E-08	1.42E-07	1.17E-07	0%	3.06E-08	2.73E-07
Cuba	2.90E-08	0%	-5.56E-08	1.31E-07	1.03E-07	0%	3.76E-08	2.01E-07
Albania	2.88E-08	0%	-9.12E-09	8.89E-08	6.17E-08	0%	1.64E-08	1.49E-07
Bulgaria	2.76E-08	0%	-2.77E-08	9.77E-08	8.04E-08	0%	2.55E-08	1.69E-07
Hungary	2.44E-08	0%	-6.33E-08	1.32E-07	1.02E-07	0%	2.98E-08	2.22E-07
East Timor	2.07E-08	0%	-1.15E-08	6.92E-08	6.19E-08	0%	1.44E-08	1.44E-07
Bosnia and Herzegovina	1.80E-08	0%	-1.09E-08	6.27E-08	4.22E-08	0%	7.88E-09	1.06E-07
Ecuador	1.79E-08	0%	-2.36E-07	3.00E-07	2.89E-07	0%	4.50E-08	6.85E-07
Comoros	1.77E-08	0%	-1.04E-08	5.74E-08	5.78E-08	0%	1.34E-08	1.39E-07

		Heat-Vul	ting for Addition nerability Reduc Rising Incomes			Heat-Vulr	nting for Additi nerability Reduct Rising Incomes	
Region	Expected D-MCC	Share of Expected D-MCC	5th Percentile D-MCC	95th Percentile D-MCC	Expected D-MCC	Share of Expected MCC	5th Percentile D-MCC	95th Percentile MCC
Jamaica	1.74E-08	0%	-1.85E-08	6.27E-08	5.98E-08	0%	1.73E-08	1.36E-07
Taiwan	1.57E-08	0%	-1.87E-07	2.70E-07	1.09E-07	0%	-5.38E-08	3.06E-07
North Macedonia	1.46E-08	0%	-5.61E-09	4.52E-08	3.09E-08	0%	8.61E-09	6.78E-08
Bahrain	1.40E-08	0%	-3.25E-08	8.76E-08	3.29E-08	0%	-1.85E-08	1.01E-07
Croatia	1.32E-08	0%	-2.05E-08	5.49E-08	4.22E-08	0%	1.36E-08	8.89E-08
Solomon Islands	1.22E-08	0%	-1.90E-08	5.45E-08	4.69E-08	0%	1.05E-08	1.14E-07
Eswatini	1.06E-08	0%	-1.02E-08	3.90E-08	3.40E-08	0%	8.94E-09	7.48E-08
Bhutan	6.51E-09	0%	-5.08E-09	2.30E-08	1.99E-08	0%	3.12E-09	4.70E-08
Costa Rica	6.22E-09	0%	-5.39E-08	7.34E-08	6.78E-08	0%	1.67E-08	1.49E-07
Belize	4.78E-09	0% 0%	-4.51E-09	1.79E-08	1.59E-08	0% 0%	4.23E-09	3.88E-08
Uruguay Maldives	4.77E-09 4.49E-09	0%	-2.41E-08 -1.08E-08	3.92E-08 2.52E-08	3.06E-08 1.67E-08	0%	9.65E-09 3.84E-09	6.52E-08 4.23E-08
Slovakia	3.91E-09	0%	-3.72E-08	5.24E-08	4.16E-08	0%	5.34E-09	9.97E-08
Guyana	3.61E-09	0%	-1.10E-08	2.18E-08	1.73E-08	0%	4.83E-09	4.13E-08
Montenegro	3.31E-09	0%	-2.76E-09	1.18E-08	9.21E-09	0%	2.61E-09	2.02E-08
Suriname	3.00E-09	0%	-7.53E-09	1.68E-08	1.31E-08	0%	3.64E-09	3.14E-08
Gabon	2.97E-09	0%	-1.06E-07	1.26E-07	1.15E-07	0%	2.43E-08	2.86E-07
Sao Tome and Principe	2.68E-09	0%	-5.62E-09	1.46E-08	1.34E-08	0%	2.14E-09	3.76E-08
Cyprus	2.13E-09	0%	-1.31E-08	2.18E-08	1.31E-08	0%	1.74E-09	3.26E-08
Fiji	1.87E-09	0%	-7.42E-09	1.25E-08	1.06E-08	0%	3.17E-09	2.46E-08
Lithuania	1.60E-09	0%	-1.35E-08	1.91E-08	1.45E-08	0%	8.34E-10	3.76E-08
Cape Verde	1.30E-09	0%	-5.27E-09	8.61E-09	8.87E-09	0%	1.86E-09	2.24E-08
Bahamas	1.24E-09	0%	-5.08E-09	8.86E-09	5.71E-09	0%	1.23E-09	1.38E-08
Latvia	1.14E-09	0%	-1.14E-08	1.61E-08	1.22E-08	0%	3.30E-10	3.32E-08
Malta	9.83E-10	0%	-4.08E-09	7.82E-09	4.60E-09	0%	5.55E-10	1.07E-08
Mauritius	8.44E-10	0%	-7.33E-09	1.07E-08	8.64E-09	0%	2.74E-09	1.73E-08
Portugal	7.43E-10	0%	-6.87E-08	7.52E-08	5.69E-08	0%	1.22E-08	1.36E-07
Puerto Rico	7.35E-10	0%	-1.55E-08	1.78E-08	1.12E-08	0%	1.25E-09	2.76E-08
Samoa	7.16E-10	0%	-2.44E-09	4.65E-09	3.79E-09	0%	8.65E-10	1.02E-08
Slovenia	5.45E-10	0%	-1.92E-08	2.24E-08	1.54E-08	0%	8.13E-10	3.98E-08
Saint Vincent and the Grenadines	3.24E-10	0%	-8.48E-10	1.69E-09	1.42E-09	0%	4.48E-10	3.02E-09
Trinidad and Tobago	2.04E-10	0%	-1.09E-08	1.29E-08	8.05E-09	0%	7.58E-10	1.89E-08
Tonga	1.88E-10	0%	-2.82E-09	3.50E-09	2.97E-09	0%	5.09E-10	8.54E-09
Saint Lucia	1.08E-10	0%	-1.47E-09	1.86E-09	1.54E-09	0%	4.58E-10	3.44E-09
Aruba	1.48E-11	0%	-2.52E-09	2.83E-09	1.73E-09	0%	2.07E-10	4.90E-09
Barbados	-1.09E-10	0%	-2.38E-09	2.41E-09	1.55E-09	0%	1.44E-10	3.65E-09
New Caledonia	-1.63E-10	0% 0%	-4.43E-09	4.62E-09	2.84E-09	0% 0%	2.77E-10	7.03E-09
French Polynesia Estonia	-2.81E-10	0%	-2.96E-09 -1.22E-08	2.62E-09 1.23E-08	1.44E-09	0%	-1.79E-10	3.79E-09
Vanuatu	-4.69E-10 -8.70E-10	0%	-9.10E-09	7.33E-09	8.84E-09 7.36E-09	0%	-1.23E-09 -8.19E-10	2.62E-08 2.21E-08
Brunei	-9.43E-10	0%	-6.17E-09	7.55E-09 5.57E-09	7.30E-09 7.13E-10	0%	-8.19E-10 -4.35E-09	6.46E-09
Iceland	-1.64E-09	0%	-3.80E-09	4.50E-10	-1.22E-09	0%	-3.55E-09	1.40E-09
Czechia	-3.48E-09	0%	-9.56E-08	9.51E-08	7.45E-08	0%	3.03E-10	1.94E-07
Luxembourg	-4.91E-09	0%	-1.69E-08	4.87E-09	-2.33E-09	0%	-1.19E-08	5.75E-09
Equatorial Guinea	-4.98E-09	0%	-1.21E-07	1.13E-07	8.85E-08	0%	1.03E-08	2.67E-07
Macao	-6.57E-09	0%	-1.61E-08	7.01E-10	-6.00E-09	0%	-1.48E-08	5.94E-10
Poland	-7.14E-09	0%	-2.43E-07	2.55E-07	1.91E-07	0%	7.81E-09	4.69E-07
Panama	-9.27E-09	0%	-7.72E-08	6.14E-08	4.58E-08	0%	4.29E-09	1.15E-07
Peru	-1.19E-08	0%	-4.11E-07	4.45E-07	3.87E-07	0%	-3.05E-08	1.06E-06
Singapore	-1.41E-08	0%	-8.64E-08	6.37E-08	5.98E-09	0%	-5.41E-08	7.70E-08
Finland	-1.43E-08	0%	-6.07E-08	3.11E-08	9.11E-09	0%	-3.55E-08	7.00E-08
Austria	-2.07E-08	0%	-1.27E-07	8.33E-08	3.87E-08	0%	-3.55E-08	1.51E-07
New Zealand	-2.36E-08	0%	-6.74E-08	1.54E-08	5.78E-09	0%	-2.12E-08	4.03E-08
Denmark	-2.44E-08	0%	-6.96E-08	1.82E-08	-8.96E-10	0%	-3.62E-08	3.86E-08
Ireland	-2.55E-08	0%	-5.91E-08	-2.13E-09	-1.94E-08	0%	-4.88E-08	2.28E-09
Norway	-2.59E-08	0%	-1.02E-07	4.09E-08	-1.61E-08	0%	-8.35E-08	5.16E-08
Switzerland	-3.90E-08	0%	-1.35E-07	4.83E-08	-4.36E-09	0%	-8.02E-08	8.00E-08
Belgium	-4.05E-08	0%	-1.45E-07	5.92E-08	2.93E-08	0%	-3.84E-08	1.24E-07
Hong Kong	-4.16E-08	0%	-1.20E-07	2.43E-08	-1.90E-08	0%	-8.24E-08	4.28E-08
Sweden	-4.50E-08	0%	-1.61E-07	6.61E-08	1.03E-08	0%	-8.36E-08	1.32E-07
Chile	-4.85E-08	0%	-2.27E-07	1.31E-07	1.00E-07	0%	-2.28E-08	2.90E-07
Netherlands	-7.10E-08	0%	-1.88E-07	4.15E-08	-8.51E-09	0%	-1.02E-07	9.39E-08
United States	-8.89E-08	0%	-5.77E-06	7.30E-06	3.23E-06	1%	-1.75E-06	1.01E-05
France	-1.38E-07	0%	-8.38E-07	6.00E-07	3.42E-07	0%	-1.25E-07	1.06E-06
Australia	-1.43E-07	0%	-5.25E-07	1.95E-07	5.48E-08	0%	-1.71E-07	3.40E-07
Germany United Kingdom	-2.32E-07	0%	-1.01E-06 8.45F-07	5.63E-07	1.66E-07	0% 0%	-3.76E-07	8.68E-07
Aggregated Gloablly	-3.14E-07 1.37E-04	0% 100%	-8.45E-07 -8.21E-05	1.58E-07 4.69E-04	8.26E-09 3.93E-04	100%	-3.81E-07 8.81E-05	4.59E-07 9.61E-04
	1.01E-04	100/0	-0.4111-00	T.UJLFU4	0.30E-04	10070	0.011-00	J.UIL-04

A.2 Additional SCC Results

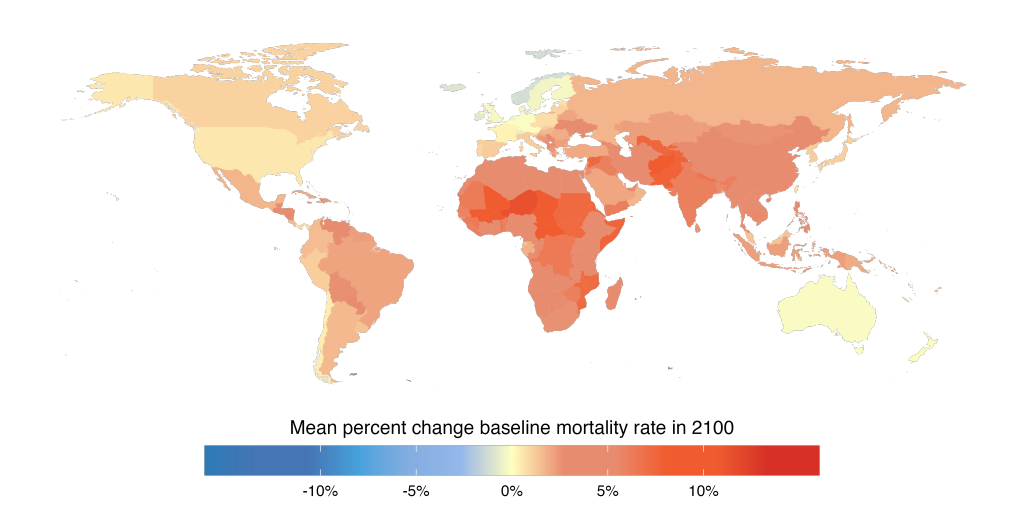
Table A.2: Social Cost of Carbon Sensitivity to Choices Around Valuing Lives and Livelihoods - Including Global Average Income Reference Point

Quasi-Kaldor Hicks		Income Weighting (Global)	Income Weighting (U.S.)	Prioritarian Weighting (Global)	Prioritarian Weighting (U.S.)	
2025 SCC [2.5th-97.5th Percentile]	\$237 [-\$93, \$861]	\$380 [-\$8, \$1,302]	\$574 [\$28, \$1,872]	\$3,567 [\$172, \$11,640]	\$2,095 [-\$216, \$2,985]	\$11,839 [-\$1,220, \$16,870]
SCC Breakdown by Impact Category						
Mortality	\$145	\$287	\$438	\$2,723	\$1,963	\$10,880
Agriculture	\$81	\$81	\$118	\$736	\$123	\$754
Energy	\$8	\$8	\$14	\$85	\$32	\$181
Sea Level Rise	\$4	\$4	\$4	\$23	\$4	\$25

A.3 The Total Mortality Impact of Climate Change

As mentioned above, in addition to determining the impact of a marginal pulse of emissions, SCC models can also be used to estimate the total mortality impacts caused by climate change. Figures A.1 and A.2 project the total mortality impact of climate change compared to the current climate. Figure A.1 shows the expected percentage change in the baseline mortality rate due to climate change in the year 2100, which is averaged across 10,000 Monte Carlo simulations as described in the figure caption.

(a) Not accounting for additional heat-vulnerability reduction from rising incomes



(b) Accounting for additional heat-vulnerability reduction from rising incomes

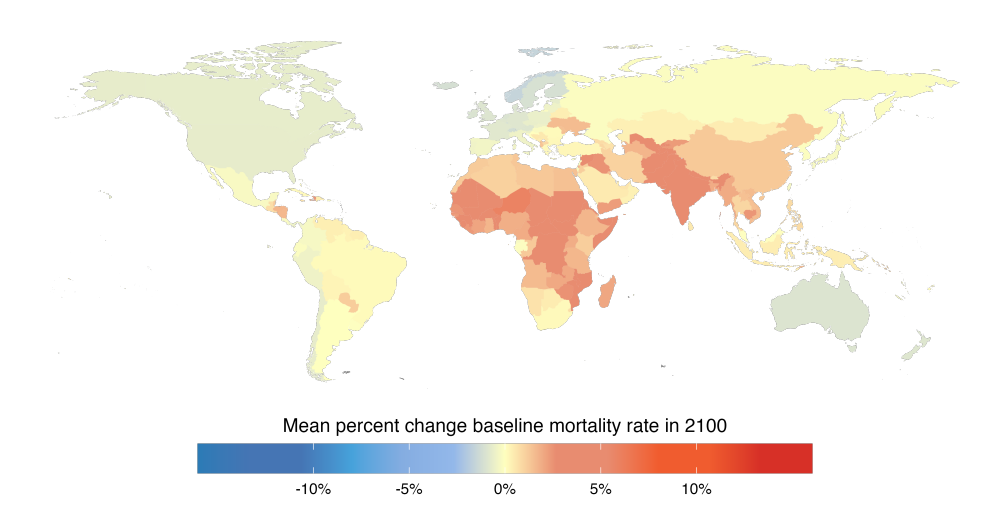


Figure A.1 | The spatial distribution of the total impact of climate change on temperature-related mortality impacts in 2100. Maps show the mean estimated percent increase in all-cause mortality due to the impact of climate change on temperature-related mortality in 2100. I take averages across the 10,000 draws in a Monte Carlo simulation, which captures uncertainty in socioeconomic and emissions scenarios (RFF-SPs), uncertainty in climate (FaIR v1.6.2), and damage function parameters (see Methods section for details). (a) Shows results without accounting for income-based adaptation.

Figure A.2 aggregates premature deaths across all countries to project the net global mortality impact from climate change. The increase in premature deaths in hotter and poorer locations significantly exceeds the decrease in premature deaths in colder and richer locations. Climate change causes a significant number of premature deaths even after accounting for heat-vulnerability reduction from rising incomes. Without accounting for the benefits of future income growth, and instead assuming that currently observed temperature-mortality relationships hold into the future, climate change causes 4.8 million premature deaths per year in 2100 (1.2M–10.4M: 5%-95% range). When accounting for income-based adaptation, climate change causes 1.6 million temperature-related deaths per year in 2100 (-1.5M–5.6M: 5%–95% range).

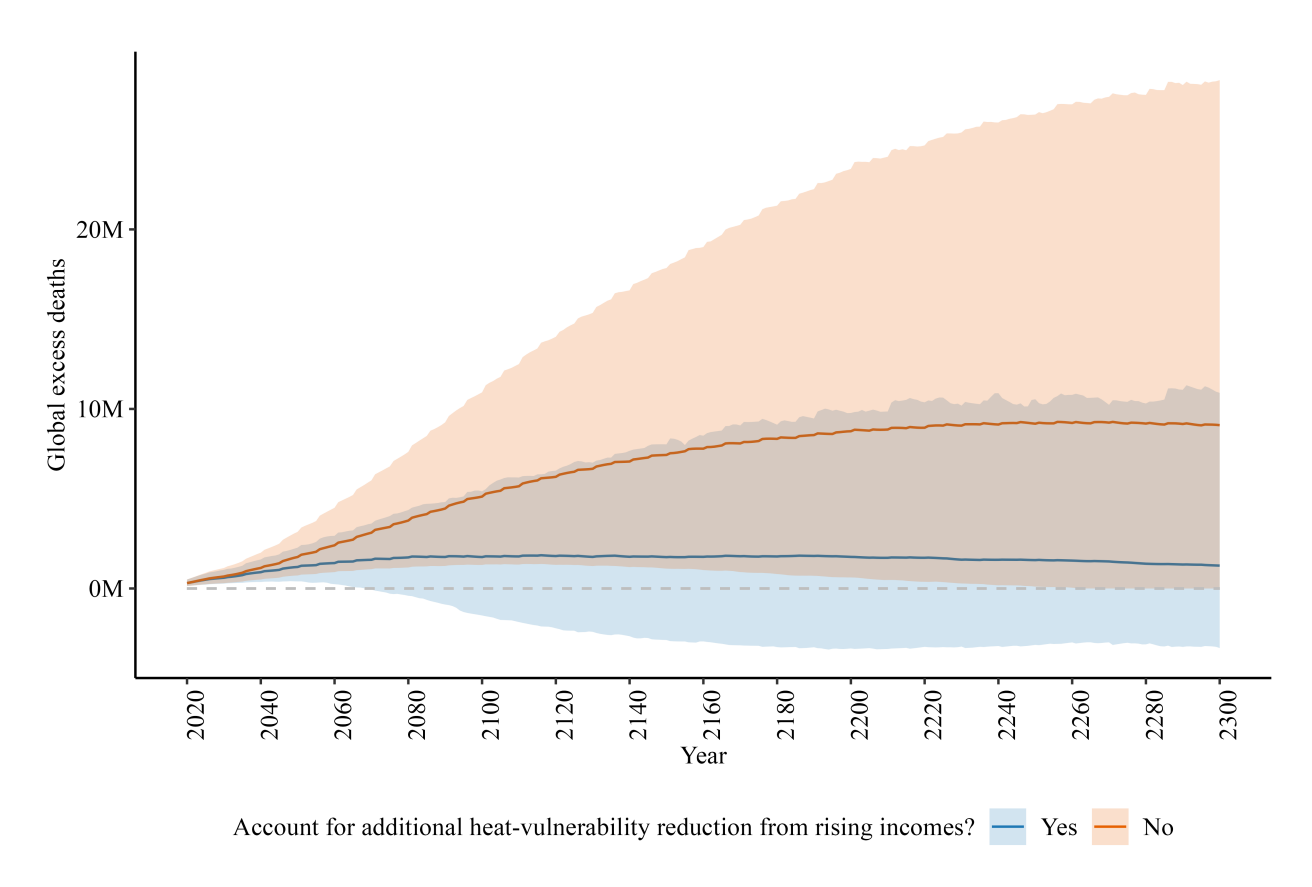


Figure A.2 | Total Yearly Global Premature Deaths From Climate Change, 2023–2300. Lines represent mean projections, and shaded regions represent the 5th-95th percentile projections. Projections that assume that currently observed vulnerability to temperature holds into the future are shown in orange. Projections that account for income-based heat-vulnerability reduction are shown in blue.

A.4 Temperature Pattern Scaling in the Climate-Economy-Mortality Integrated Assessment Model

The temperature-related mortality damage function Bressler et al. (2021) used in this study requires country-level mean surface temperature (CMST) as an input, but the climate model we use provides only projections of global mean surface temperature (GMST). To downscale GMST to CMST, we rely on the spatial patterns from high-resolution, spatially resolved surface temperatures from the sixth phase of the Coupled Model Intercomparison Project (CMIP6) general circulation and earth system models (Eyring et al., 2016). These models project climate futures at fine spatial and temporal resolutions but are computationally expensive, prohibiting their use in many probabilistic settings such as those underlying this study. One solution to this problem is to approximate local temperatures using a pattern scaling approach (EPA, 2023b; Lynch et al., 2017).

For each of the 21 available models underlying CMIP6, we regress the local mean surface temperature LMST in grid cell i in year t on the corresponding GMST:

$$LMST_{it} = \sum_{i} \beta_{i} GMST_{it} [gridcell = i] + \varepsilon_{it}$$
(46)

This results in a time-invariant vector of β 's that dictate the relationship between GMST and LMST in each grid cell at the spatial resolution of the GCM, with ε_{it} being the remaining variation in LMST not explained by the regression. We then calculate a weighted average of the β 's across all grid cells within each country to estimate the relationship between GMST and CMST. Because temperature-related climate impacts affect people and not land, we weight the aggregation of the β 's using spatially-explicit, sub-national population centers observed in the year 2000 (Murakami and Yamagata, 2019) to recover a vector of population-weighted, country-level $\widetilde{\beta}$'s.

The steps taken above result in 21 unique country-level patterns, one for each CMIP6 model. From the available set of 21 patterns, we randomly select one pattern to use in each Monte Carlo simulation of the model, providing another source of climate module uncertainty. We recover CMST in each simulation s for each country c in model year t by scaling GMST with the population-weighted country-level $\widetilde{\beta}$'s such that

$$CMST_{sct} = \widetilde{\beta}_{sc} \times GMST_{st} \tag{47}$$

The $CMST_{sct}$'s described here correspond to the T's in equations 48 and 50.

A.5 Mortality Damage Function Implementation in the Climate-Economy-Mortality Integrated Assessment Model

I use the preferred models from Bressler et al. 2021 for both heat (model 4) and cold (model 3).

Formally, the model for heat-related mortality is:

$$Y_{c,t}^{\text{Heat}} = \beta_1 T_{c,t} + \beta_2 T_{c,t}^2 + \beta_3 (\text{Hottest Month Avg Temp}_c) + \beta_4 T_{c,t} (\text{Hottest Month Avg Temp}_c) (\log(y_{c,t}))$$
(48)

where $Y_{c,t}^{\text{Heat}}$ is the percentage increase in the all-cause mortality rate due to heat in country c at time t, $T_{c,t}$ is the increase in yearly average temperature relative to the 2001-2020 period in country c at time t, Hottest Month Avg Temp_c is the population-weighted average temperature in the hottest month in country c between 1984 and 2015, and $y_{c,t}$ is the PPP adjusted per capita GDP.³⁶ See Bressler et al. (2021) for further details. For the projection results that do not account for additional income-based adaptation, I hold $y_{c,t}$ constant at current levels. For the projection results that do account for income-based adaptation, I use the model's projections of future country-level income in each year for $y_{c,t}$.

The model for cold-related mortality is:

$$Y_{c,t}^{\text{Cold}} = \beta_1 T_{c,t} + \beta_2 T_{c,t}^2 + \beta_3 (\text{Coldest Month Avg Temp}_c)$$
 (49)

To represent damage function uncertainty in Monte Carlo runs, a vector of coefficients for the heat and cold models is sampled from a multivariate normal distribution centered on the point estimate and standard deviation equal to the reported standard error in Bressler et al. (2021). The net percentage increase in mortality rate, $Y_{c,t}$, is the sum of $Y_{c,t}^{\text{Heat}}$ and $Y_{c,t}^{\text{Cold}}$.

$$Y_{c,t} = Y_{c,t}^{\text{Heat}} + Y_{c,t}^{\text{Cold}} \tag{50}$$

After the calculation of $Y_{c,t}$, the net percentage increase in mortality rate is converted

³⁶Population-weighted average temperatures are not available for seven countries, although population-weighted average temperatures are needed to calculate the hottest and coldest month for each country. We assign these seven countries the values of their neighbor as follows: Aruba is assigned Venezuela, Bahrain is assigned Saudi Arabia, Barbados and St. Lucia are assigned Puerto Rico, the Maldives are assigned Sri Lanka, Malta is assigned Tunisia, Singapore is assigned Malaysia, and Tonga is assigned Fiji.

into net additional deaths:

Excess deaths_{c,t} = (Population_{c,t}) × (Baseline mortality rate_{c,t}) ×
$$\left(\frac{Y_{c,t}}{100}\right)$$
 (51)

where baseline mortality is defined as the country population level times its baseline mortality rate from the RFF-SPs. Since I run 10,000 Monte Carlo simulations, which captures uncertainty in emissions, population, economic growth, the response of the climate system, and damage functions, I estimate equation 51 for each country in each time period 10,000 times.

In Bressler et al. 2021, damage functions were tested in making temperature-related mortality projections out to 2100 using deterministic SSP-RCP socioeconomic projections Bressler et al. (2021). In that study, heat-related mortality was always increasing and cold-related mortality was always decreasing under increasing temperatures, which is consistent with Gasparrini et al. 2017 Gasparrini et al. (2017). This study, however, makes projections out to 2300 using stochastic socioeconomic projections across 10,000 Monte Carlo draws. To ensure that the model does not produce theoretically inconsistent behavior simply due to the nonlinear functional form in the most extreme Monte Carlo runs, I impose additional functional form restriction that ensures that holding all else equal, including income, heat-related mortality does not rise under higher temperatures (i.e., ensuring that the partial derivative of heat-related mortality with respect to temperature does not decrease under higher temperatures) and cold-related mortality does not fall under higher temperatures (i.e., ensuring that the partial derivative of cold-related mortality with respect to temperature decreases under higher temperatures). Imposing this restriction only has a small impact on results: it raises the 2020 SC-CO₂ by 2.8%.

A.6 Temperature-Related Mortality in Mexico

In this section, I explore the distribution of temperature-related mortality across demographic groups. As opposed to previous sections that look at the mortality burden of climate change across the whole world, this section takes a deep dive into a single country that has sufficiently rich data to explore which parts of society are most vulnerable to temperature. This enables a deeper exploration of the distributional impacts of climate change than was possible in the previous sections.

Note that this appendix section represents work in progress. At the moment, these results cannot be considered fully identified because there is an issue with selection bias: people endogenously choose their occupations, perhaps in part based on their expectations about how much they may be exposed to heat and cold in these occupations. Currently, the results

suggest that manual workers are particularly vulnerable to heat and represent around half of the overall heat-related mortality burden in Mexico. There are reasons to think that this selection bias may result in an understatement of these findings. Ceteris Paribus, it seems that individuals who are more vulnerable to heat would go into professions where they tend to be less exposed to heat (i.e., non-manual professions). In any case, due to the selection bias issue, the current work cannot be considered fully identified, so I leave this work here in the appendix as a work in progress. Suggestions on how to achieve clean identification in this setting are most welcome.

Here, I leverage rich national weather and demographic microdata in Mexico spanning 22 years and covering 13.4 million deaths divided into 2,402 Mexican municipalities assembled in previous coauthored work (Wilson* et al., 2024). That study found that heat-related mortality is concentrated in the younger population: 75% of heat-related deaths were among those under 35 years old. Whereas cold-related mortality is overwhelmingly concentrated in the older population: 96% of cold-related deaths are concentrated among those over 50 years old. The age-specific findings on heat-related deaths in that study were in contrast to some previous studies in the literature, which found that the elderly were the most vulnerable to heat (Carleton et al., 2022; Gallo et al., 2024; Hajat et al., 2014; Kim et al., 2016; Lee and Kim, 2016; Li et al., 2016). One crucial reason why that study may have found these age-specific findings where other studies had not is that, thanks to the rich data available in Mexico that included the exact age at death, it was able to assess heterogeneity across age groups at a finer scale than previous empirical work, which usually focused on mortality irrespective of age (Gasparrini et al., 2015; Cromar et al., 2022; Wu et al., 2022), across broader age groups (Carleton et al., 2022; Gallo et al., 2024; Hajat et al., 2014; Lee and Kim, 2016; Li et al., 2016), or only on the elderly (Hales et al., 2014; Honda et al., 2014). Importantly, the findings in Wilson* et al. (2024) underscore the importance of exploring age-specific mortality impacts in other countries, although data availability remains a significant limiting factor in this endeavor.³⁷

While we analyzed age-specific heterogeneity in temperature-related mortality in Wilson* et al. (2024), we left the analysis of occupational-specific heterogeneity to future work. In the discussion section of that paper, we hypothesized that occupational exposure to heat could be a major mechanism behind our results: although younger adults may be more physiologically robust to heat, they also likely experience more exposure to extreme heat in outdoor occupations with minimal flexibility for precautionary action. Here, I analyze occupational heterogeneity, and I indeed find that occupational heat exposure appears to be a major driver of premature mortality in Mexico.

³⁷I am currently working on similar coauthored projects in Brazil and the United States.

A.6.1 Data

I leverage precise historical data on both mortality and temperature exposure. Mortality microdata comes from the Subsistema de Información Demográfica y Social of Mexico's Instituto Nacional de Estadística y Geografía (INEGI), which is the same data leveraged in my previous coauthored work (Wilson* et al., 2024). This data includes a record of each death in the country since 1998. Importantly, it contains information on age and occupation at death, as well as day and municipality of occurrence. Municipality is Mexico's second-order administrative unit (ADM2), numbering 2,402 across the country. The study period ends in 2019, before the COVID-19 pandemic. Over the 22 years from 1998 to 2019, the data contains a record of 13.4 million deaths over more than 21 million municipality—days. More information on this data is provided below in section A.6.4.

As in Wilson* et al. (2024), these records are combined with station-level measurements of temperature, humidity, and pressure, which is used to develop estimates of local daily mean wet-bulb temperature Davies-Jones (2008) (see section 2.2.1 for a description of wet-bulb temperature and an explanation as to why its an important metric in understanding the impact of ambient conditions on temperature-related mortality) This is important because recent literature has suggested that the spatial and temporal smoothing involved in the creation of reanalysis products often leads to underestimations of the intensity of extreme humid heat events compared to observational datasets Raymond et al. (2020). Indeed, in this setting, the ERA5-Land weather reanalysis data does a poor job of reproducing high humid heat events observed in Mexico's station network (see (Wilson* et al., 2024) for further details). The observational weather dataset is collected from the UK Met Office Hadley Centre's Integrated Surface Dataset, which consolidates observations from a global network of weather stations but performs various quality control adjustments to ensure the consistency of observations over time. Precipitation data is collected from the European Centre for Medium-range Weather Forecasting Reanalysis 5 - Land (ERA5-Land) dataset (and included as a control to avoid confounding effects). Using Google Earth Engine, a daily total precipitation measure is calculated by taking a sum over the hourly values across each day at each grid cell and then taking a spatial average over each administrative unit, weighting by a gridded estimate of the time-varying distribution of population (Gridded Population of the World v4, revision 11). See section A.6.4 for further details.

A.6.2 Statistical Model

I estimate an occupation-specific exposure relationship between excess mortality and daily average wet and dry-bulb temperature. The empirical model leverages current best practices

to isolate causal impacts of temperature on excess mortality (Carleton et al., 2022; Gasparrini et al., 2015). I investigate effects over a set of distributed lags to capture the dynamic effects of temperature on health, including the time-delayed mortality response to hot and cold temperatures as well as harvesting—when those who would have otherwise died in the near future die slightly earlier due to hot or cold temperature exposure (Schwartz, 2000). The model flexibly captures differences in impacts from cold, moderate, and hot temperature exposures and includes control variables to account for potential confounders, including seasonality and time trends. I identify effects based on otherwise random changes in weather across days within a given municipality, such that a municipality experiencing mild weather acts as the "control group" for itself during more extreme weather, eliminating confounding spatial variation. Lastly, I flexibly adjust for daily precipitation to ensure that the effects of temperature are not operating via rainfall. Importantly, the statistical model allows the minimum mortality temperature (MMT) to vary by age group. I find that different occupational groups experience minimum mortality at substantially different temperatures. For instance, manual workers experience minimum mortality at 13°C wet-bulb temperature and 21°C dry-bulb temperature. Non-manual workers experience minimum mortality at 12°C wet-bulb temperature and 20°C dry-bulb temperature. Whereas those not working experience minimum mortality at much higher temperatures: 22°C wet-bulb temperature and 28°C dry-bulb temperature. As is standard in this literature, deaths from heat and deaths from cold are identified relative to the subgroup-specific minimum mortality temperature (MMT).

Estimates of the effect of temperature on mortality come from fitting a mortality response function following Gasparrini et al. (2015). The outcome variables—daily, location-specific mortality rates for each age group—are modeled as dynamic functions of temperature and precipitation, with additional controls for location-specific, time-varying, and seasonal confounders. Formally,

$$y_{ait} = f_a(x_{it}, \dots, x_{it-30}; \mathbf{B}_a) + g_a(p_{it}, \dots, p_{it-30}; \mathbf{\Gamma}_a) + \rho_{at} + \delta_{ai} \times \text{year}_t + \theta_{as} \times \text{week}_t + \varepsilon_{ait}$$
(52)

where y_{ait} is the mortality rate (deaths per 100,000 people) in municipality i on date t and occupational group a. Separate models are fit for each occupational group.

The main right-hand-side variable is daily average temperature—either dry-bulb or wetbulb depending on the specification—generically denoted x_{it} in the above equation. The relationship between temperature and mortality is allowed to be nonlinear and dynamic, as captured by the function $f_a(x_{it}, \ldots, x_{it-30}; \mathbf{B}_a)$, with \mathbf{B}_a denoting the matrix of unknown coefficients to be estimated. This function transforms temperature observations along two dimensions. In the temperature dimension, the function is a natural cubic spline over daily temperature with knots at the 10^{th} , 50^{th} , and 90^{th} percentiles (Harrell, 2015). Across 31 days of distributed lags, the function is a b-spline with knots spaced equally, in log terms, across the lag period. Putting these elements together, fitting the model generates estimates of the effect of temperature on mortality at each point across the distribution of temperatures and for each of 31 days starting with the initial day of the temperature realization. These estimates yield the 30-day cumulative effect of temperature on mortality, as depicted in Figures A.3 and A.4.

The other elements of the estimating equation are controls. Daily total precipitation, p_{it} is included in a similar way to temperature, with the cumulative effect estimated using a b-spline distributed lag. The effect of precipitation is modeled flexibly using 0^{th} -order splines (i.e., bins) for precipitation below the 80^{th} percentile (roughly zero precipitation), between the 80^{th} and 90^{th} percentiles, between the 90^{th} and 95^{th} percentiles, between the 95^{th} and 98^{th} percentiles, between the 98^{th} and 99.5^{th} percentiles, and above the 99.5^{th} percentile. Other confounders are accounted for using fixed effects, in some cases interacted with continuous controls. These controls are: date of sample fixed effects, ρ_{at} , to account for national temporal patterns, holidays, day-of-week effects, and other time-series confounders; a municipality-by-year fixed effect, $\delta_{ai} \times \text{year}_t$, to account for location-specific fixed factors such as topography, governance, and differences in access to healthcare or mortality reporting as well as secular changes in mortality rates and climate; and a state-level fixed effect, θ_{as} , interacted with the week of the year, week, to account for state-level seasonal patterns. The term ϵ_{ait} is the remaining error term. The regression is weighted by the daily municipality population (linearly interpolated from annual population counts). Standard errors are clustered at the state level to account for spatial autocovariances at the subnational level while maintaining robustness to arbitrary temporal correlation patterns. Models are fit using R software version 4.2.2 and the dlnm package version 2.4.7 (Gasparrini, 2011).

A.6.3 Results

Figure A.3 shows the effect of exposure to a single day at the indicated wet-bulb temperature on mortality risk for different occupational groups. For instance, the manual worker exposure-response function implies that when a manual worker experiences one day with an average wet-bulb temperature of 28°C, their risk of mortality increases by 20% relative to if they had experienced one day with an average wet-bulb temperature of 13°C. The bottom part of the figure below each exposure-response function is a histogram that shows the distribution of wet-bulb temperatures as experienced by people in Mexico over the sample period (gray bars)

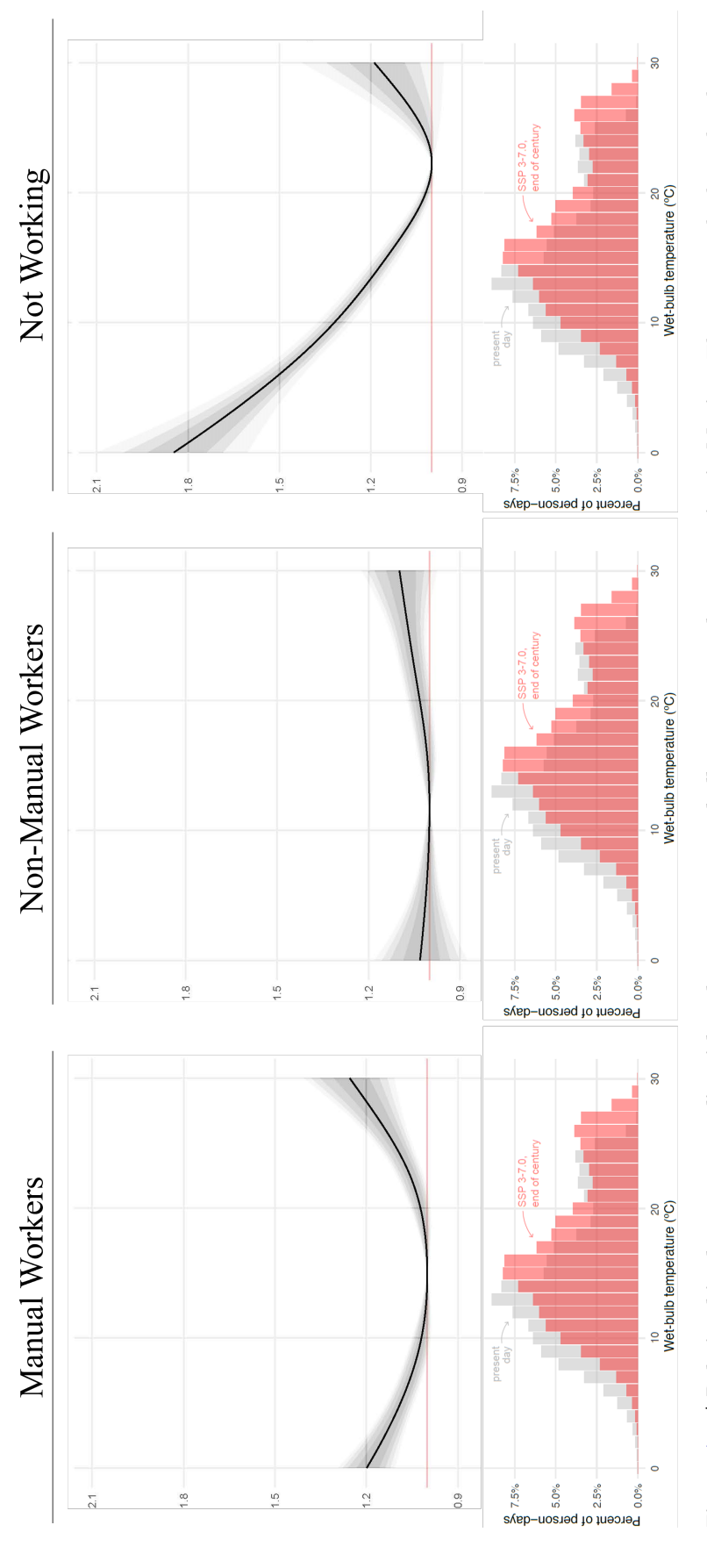


Figure A.3 | Relationships between mortality risk and exposure to wet-bulb temperature by occupation in Mexico. The top panels show the change in temperature distribution at the end of the century (2083–2099) under the SSP 3-7.0 emission scenario. Note that the bottom histograms represent the relative mortality risk (y-axis) caused by exposure to one day of the indicated average daily wet-bulb temperatures (x-axis) by occupation. The bottom panels show the distribution of daily average wet-bulb temperatures in Mexico throughout the sample period as well as the ensemble mean of projected distribution of temperatures across the whole Mexican population, so each of the three histograms are exactly the same. Shaded bands around the functions in the top panels indicate 95, 90, 80, and 50% confidence intervals. Absolute changes in mortality are shown in Figure xx.

as well as the distribution of wet-bulb temperatures that they are expected to experience at the end of the century (red bars). This communicates how often people are exposed to wet-bulb temperatures at different levels. For instance, 8% of the days as experienced by people in Mexico over the sample period had a wet bulb temperature of 13°C, while temperatures rarely exceeded 26°C. Taken together, this figure communicates both how deadly a marginal day at a certain wet-bulb temperature is for each occupational group (exposure response functions in the top part of the figure), along with the frequency with which those days occur now and how often they are expected to occur in the future (histograms in the bottom part of the figure). As the figure shows, non-workers face the highest mortality risk from cold while manual workers face the highest mortality risk from heat.

Figure A.4 is the same as Figure A.3 except that it uses dry bulb temperature as the main treatment variable. Similar to Wilson* et al. (2024)—which found that results on the age-specific temperature-related mortality burden were robust whether we use wet-bulb or dry-bulb temperature as our metric of exposure—I find here that the occupation-specific results are also robust whether we use wet-bulb or dry-bulb temperature as the metric of exposure (also see further results below). As in Wilson* et al. (2024), I also find that the exposure-response function over wet-bulb temperature is estimated a bit more precisely than the exposure-response function over dry-bulb temperature.

As the exposure-response functions in figures A.3 and A.4 show, the hottest temperatures—e.g., 30°C wet-bulb temperature and 40°C dry-bulb temperature—are the most damaging temperatures in terms of their impact on heat-related deaths. However, as the bottom temperature-distribution histograms in those figures show, heat waves that reach those temperatures actually occur very rarely. This leads to the question: what is the overall temperature-related mortality burden associated with exposure to temperatures over the course of the whole year, from the coldest days to the hottest days?

This question is addressed in figure A.5. The overall temperature-related mortality burden is a function of both (1) the damage caused by exposure to a certain temperature (i.e., figures A.3 and A.4 top panels) as well as (2) how often people are exposed to those temperatures (i.e., figures A.3 and A.4 bottom panels). Figure A.5 combines these two factors to show the temperature-related mortality burden associated with exposure to each degree of temperature. The left hump of this figure represents cold-related deaths. The right hump of this figure represents heat-related deaths. The peak of the right hump—which represents the temperature exposure that causes the most heat-related deaths in the sample period—is at 25°C wet-bulb temperature and 29°C dry-bulb temperature. Whereas the peak of the left hump of the figure—the temperature exposure that causes the most cold-related deaths in the sample period— is at 9°C wet-bulb temperature and 17°C dry-bulb temperature.

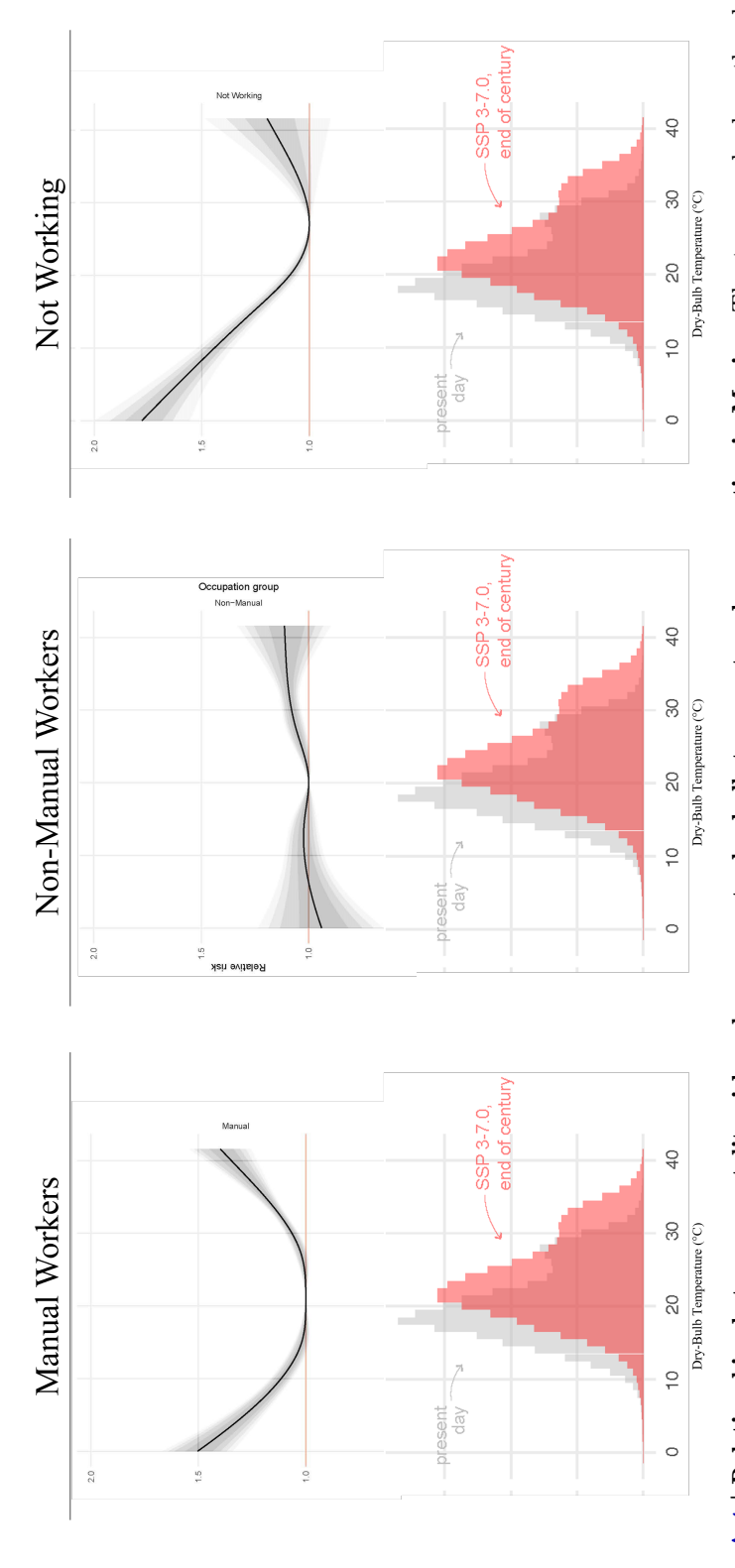


Figure A.4 | Relationships between mortality risk and exposure to dry-bulb temperature by occupation in Mexico. The top panels show the change in relative mortality risk (y-axis) caused by exposure to one day of the indicated average daily dry-bulb temperatures (x-axis) by occupation. The bottom temperature distribution at the end of the century (2083–2099) under the SSP 3-7.0 emission scenario. Shaded bands around the functions in the top panels show the distribution of daily average dry-bulb temperatures in Mexico throughout the sample period as well as the ensemble mean of projected panels indicate 95, 90, 80, and 50% confidence intervals. Absolute changes in mortality are shown in Figure xx.

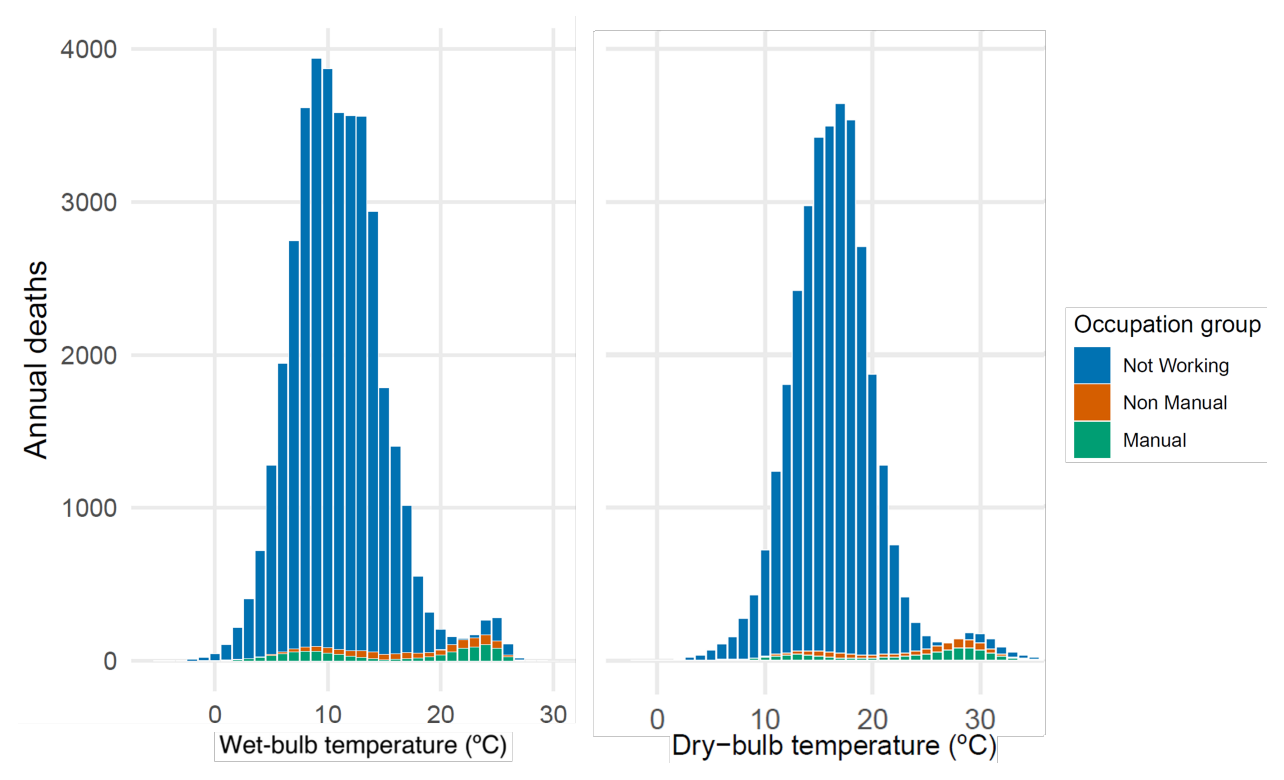


Figure A.5 | Historical temperature-related deaths in Mexico. The panels show average annual temperature-related deaths resulting from exposure to days with the average temperatures shown on the x-axis during the historical period across occupation in Mexico. The left panel shows deaths resulting from exposure to wet-bulb temperature. The right panel shows deaths resulting from exposure to dry-bulb temperature.

Consistent with past literature on temperature-related mortality in Mexico (Cohen and Dechezleprêtre, 2022; Jáuregui-Díaz et al., 2020), I find that cold is historically associated with many more deaths than heat across the whole population. However, this masks substantial heterogeneity on the differential impacts of heat and cold on different demographic groups within the population. I break out premature deaths from both cold and heat in table A.3 below.

Table A.3

	Cold-Rela	ted Deaths	Heat Relat	ed Deaths
	Wet-Bulb Temperature	Dry-Bulb Temperature	Wet-Bulb Temperature	Dry-Bulb Temperature
Manual Workers	477 (1%)	341 (1%)	684 (47%)	766 (55%)
[2.5th-97.5th Percentile] Non-Manual Workers	$[193, 760] \\ 267 (1\%)$	$\begin{bmatrix} -13, 695 \end{bmatrix}$ $240 \ (1\%)$	$[122, 1,256] \\ 408 (28\%)$	$[153, 1,380] \\ 301 (22\%)$
[2.5th-97.5th Percentile] Not Working [2.5th-97.5th Percentile]	[-403, 937] 36,849 (98%) [29,994, 43,703]	[-79, 560] 30,926 (98%) [22,291, 39,561]	[-11, 827] 359 (25%) [-342, 1,060]	[87, 515] 318 (23%) [-474, 1,110]

Table A.3 | Annual Historical Cold-Related and Heat-Related Deaths in Mexico by Occupation. Table shows the average number of yearly cold and heat-related deaths broken down by occupation, using both wet-bulb and dry-bulb temperature as the metric of temperature exposure. The parentheses indicate the percentage of the total heat or cold deaths that are occurring in that occupational category. E.g., for heat-related deaths using wet-bulb temperature as the metric of temperature exposure, 47% of heat-related deaths are occurring among manual workers, 28% are occurring among non-manual workers, and 25% are occurring among non-workers.

For both wet-bulb temperature and dry-bulb temperature, cold-related mortality is overwhelmingly and disproportionally concentrated among non-workers, with 98% of coldrelated deaths occurring among non-workers, who make up 85% of overall deaths in the population. Heat-related mortality, however, is quite a different story. Heat-related deaths are especially and disproportionally concentrated among manual workers: 47% of deaths occur among manual workers, who comprise just 9% of deaths in the overall population. While only 25% of deaths are among non-workers. When dry-bulb temperature is used as the exposure metric, manual workers make up 55% of heat-related deaths while non-workers make up just 23% of heat-related deaths. Non-manual workers are also disproportionally impacted by heat-related mortality, although not to the extent of manual workers. Non-manual workers comprise 28% of heat-related deaths when using wet-bulb temperature as the measure of exposure and 22% of heat-related deaths when using dry-bulb temperature despite comprising just 6% of the deaths in the overall population. This suggests that occupational exposure to heat appears to be an important mechanism in driving heat-related mortality, but it may not be the whole story given that non-manual workers are also disproportionally impacted by heat-related mortality, although to a lesser extent than manual workers.

A.6.4 Extended Description of Data

The data period for this study begins in 1998, when INGEGI's mortality microdata first began to carry information about the day and municipality of each mortality event. The data period ends in 2019 before the COVID-19 pandemic. Between 1998 and 2019, the data contains 13,426,931 deaths. The World Bank estimates that Mexico's all-cause crude mortality rate is around 6 deaths per 1000 people per year. Relative to a population of around 110 million during this period, this would imply total deaths of 14.5 million during our data period, giving confidence that these mortality records are relatively complete. Death records that are missing information on the day of death, the individual's age at death, or the death location are dropped, as are those that occurred outside of Mexico. These dropped records represent less than 0.92% of the data.

Data on administrative unit population, which is used to determine mortality rates and regression weights, is collected from IPUMS International, which consolidates and harmonizes census data for Mexico. The study uses data from the 1990, 2000, and 2010 Mexican censuses, as well as the 2015 Intercensal Survey. Population for each administrative unit is assumed to grow at a constant rate between observations, and population growth between the 2010 Census and 2015 Intercensal Survey is assumed to remain constant through the end of our data in 2019. Across both mortality and population data, 67 municipal boundary changes occurring between 1998 and 2019 are accounted for by assigning values reported for modified units to an aggregate set of 2,402 municipal units that is stable across all years of our study.

The weather dataset leveraged here contains a set of weather metrics recorded at a sub-daily frequency (some stations report weather at an hourly frequency, but many report at three- or six-hour intervals). The method described in Davies-Jones (2008) is used to approximate wetbulb temperature from dry-bulb temperature, surface pressure, and dew point temperature at each station location. As the method requires matching station temperature records to administrative units, missing hourly dry-bulb and wet-bulb temperature observations are filled in by leveraging distributional information from nearby non-missing stations. To avoid filling missing data for stations that report infrequently or for which the historical record is not sufficiently diverse, data from all stations that report fewer than 10,000 observations during the period from 1990 to 2019 (roughly 3\% of hours) are dropped, as well as stations that do not report more than 1000 observations across at least 10 years. For each of the remaining stations, an empirical cumulative distribution function is determined for all non-missing observations. Next, if the data does not contain an observation for a given station at a particular hour, a likely quantile for this observation is determined using an inverse squared geodesic distance-weighted mean of all stations in Mexico that are reporting values at that hour. Then, missing values are filled using the temperature at that quantile for that station. Said differently, if a station is missing data at a particular hour and nearby non-missing temperatures are on average at their 90^{th} percentile, the missing value is set to the 90^{th} percentile of the historical readings for that station. This method is deployed in the dataset here.

Daily mean dry-bulb and wet-bulb temperatures are obtained by calculating the average of the daily minima and maxima of each metric at each station. Next, geodesic distances between each station and the population-weighted centroid of each administrative unit are determined. Temperature observations are mapped to administrative units by taking the inverse squared distance-weighted mean of each temperature metric for the five nearest stations. This method is similar to other papers studying temperature effects on mortality using weather station data Barreca et al. (2016). Meta's High-Resolution Population Density Maps Lab and for International Earth Science Information Network – CIESIN – Columbia University (2016) are used to determine the population-weighted centroid of each administrative unit. To ensure that representative weather station data is used to estimate exposure, municipalities whose population center of mass is more than 50 kilometers from the nearest weather station are omitted; these municipalities represent 24.83% of Mexico's population as of the date of the 2010 Census.